Mechanism of host cell death interference by fungal RALPH effector in cereal powdery mildew infection

Michal Przydacz

Imperial College London

Department of Life Sciences

Thesis submitted for the degree of Doctor of Philosophy

Declaration of originality:

I declare that this thesis is a result of author's own work. All the data and conclusions have been analysed and formulated by the author. Any external contributions are indicated and acknowledged appropriately. This study has been conducted at Imperial College London, between October 2015 and March 2019, and it has not been submitted for any other degree.

Copyright Declaration:

The copyright of this thesis rests with the author. Unless otherwise indicated, its contents are licensed under a Creative Commons Attribution-Non Commercial 4.0 International Licence (CC BY-NC). Under this licence, you may copy and redistribute the material in any medium or format. You may also create and distribute modified versions of the work. This is on the condition that: you credit the author and do not use it, or any derivative works, for a commercial purpose. When reusing or sharing this work, ensure you make the licence terms clear to others by naming the licence and linking to the licence text. Where a work has been adapted, you should indicate that the work has been changed and describe those changes. Please seek permission from the copyright holder for uses of this work that are not included in this licence or permitted under UK Copyright Law.

Abstract

Global food security is threatened by impending climate change, limited agricultural land and resources, and by an increase in human population disproportional to the increase in food production. One way to increase food production is to decrease crop yields lost to pathogens. *Blumeria graminis* is an obligate biotrophic fungal pathogen that causes powdery mildew in wheat and barley. It is an economically important phytopathogen that employs over 500 effectors to facilitate infection by subduing the plant immune system. In particular, RNase-like effector proteins associated with haustoria (RALPHs), such as BEC1054/CSEP0064, are thought to play a crucial role in *Blumeria* infection. I hypothesised that BEC1054 facilitates infection by inhibiting host cell death via host ribosome binding. This study focuses on the relationship between RALPH effector BEC1054 and the barley Jasmonate-induced protein 60 (JIP60), whose N-terminal domain acts as a ribosome-inactivating protein (RIP). JIP60 probably induces host cell death by depurination of the SRL site on the 28S rRNA subunit, leading to ribosome inactivation and translation inhibition. In plants exposed to methyl-jasmonate, a phytohormone that induces expression of JIPs and results in senescence, host rRNA degradation was inhibited in transgenic wheat expressing BEC1054. Transient expression of active recombinant JIP60, via agroinfiltration, mediates host cell death in non-native *Nicotiana benthamiana*. Conversely, co-expression of BEC1054 with JIP60 in *N. benthamiana* inhibits the JIP60 RIP-mediated necrosis. So far, no specific residues have been identified that are involved in BEC1054 function. Therefore, I propose BEC1054 effector employs a mode of action based on non-specific factors, such as structural compatibility with its targets and hydrophobic interactions, rather than complementary hydrophilic residues. The main function of BEC1054 is to bind host ribosomes and occlude the SRL site. This then inhibits host RIPs from performing rRNA cleavage, which would lead to ribosome inactivation, host cell death and prevent establishment of infection.

Contents

List of Figures **7**

List of Tables **9**

Abbreviations **10**

Acknowledgements **11**

1 Introduction **12**

1.1 Food security 12

1.2 Importance of wheat and barley 13

1.3 Phytopathogens – the pathogens of plants 15

1.4 Pathogen control 16

1.5 Powdery mildews 18

1.6 *Blumeria graminis* 19

1.7 CSEPs, RALPHs and BEC1054 22

1.8 Plant immunity 23

1.8.1 PTI and ETI zig-zag model 23

1.8.2 Caveats of the zig-zag model 24

1.8.3 Molecular basis of plant immunity pathways 26

1.8.4 SA/JA phytohormone crosstalk 29

1.8.5 Hypersensitive response and programmed cell death 30

1.8.6 PTI-induced programmed cell death 30

1.9 Hypothesis, aims and objectives of this thesis 32

2 Materials and methods **34**

2.1 Materials 34

2.2 Buffers & media recipes 34

2.3 Plants . . . 34
2.3.1 *Nicotiana benthamiana* . . . 34
2.3.2 *Triticum aestivum* . . . 34
2.4 *Blumeria graminis* cultivation . . . 36
2.5 Bacteria . . . 36
2.6 Constructs . . . 36
2.7 Agroinfiltrations of *N. benthamiana* . . . 37
2.8 Co-agroinfiltration with P19 to increase expression . . . 38
2.9 Site-directed mutagenesis of BEC1054 . . . 40
2.10 Site-directed mutagenesis of JIP60ml . . . 40
2.11 Transformation of chemically competent *E. coli* . . . 43
2.12 Electroporation of electro-competent Agrobacterium . . . 43
2.13 Analysis of aniline-treated total RNA profiles obtained from MeJA-treated wheat 43
2.14 Protein extraction from plants . . . 44
2.15 SDS-PAGE . . . 44
2.16 Western blotting . . . 45
2.17 *In vitro* Transcription/Translation assay . . . 45
2.18 Statistical analysis . . . 45

3 Properties of N-terminal RIP domain of JIP60 47

3.1 Introduction . . . 47
3.1.1 Ribosome-inactivating proteins (RIPs) . . . 47
3.1.2 RIP structure & mode of action . . . 48
3.1.3 Versatility of RIPs . . . 49
3.1.4 Classification of RIPs . . . 51
3.1.5 RIPs in cereals . . . 52
3.1.6 Barley RIP jasmonate-induced protein 60 (JIP60) . . . 54
3.1.7 Aims . . . 55

3.2 Results . . . 57
3.2.1 JIP60 as member of the ribosome inactivating protein family . . . 57
3.2.2 Mode of action of JIP60 . . . 58
3.2.3 The recombinant JIP60 N-terminal domain causes necrosis *in planta* . . . 61
3.2.4 Essential residues of JIP60 active site . . . 62
3.2.5 Presence of transiently expressed JIP60 *in planta* . . . 64
3.2.6 Recombinant JIP60ml leads to translation inhibition *in vitro* . . . 70
3.3 Discussion . . . 72
3.3.1 JIP60 as a part of PTI response . . . 72
3.3.2 JIP60 as a barley RIP . . . 72
3.3.3 JIP60 mode of action . . . 74

4 *Blumeria* effector BEC1054 interferes with JIP60-mediated host cell death 79

4.1 Introduction . . . 79
4.1.1 CSEPs in *Blumeria* . . . 79
4.1.2 Host-pathogen interface . . . 79
4.1.3 RNase-like effector proteins expressed in haustoria (RALPHs) . . . 80
4.1.4 Family 21 – crucial effectors in *B. graminis* infection . . . 81
4.1.5 BEC1054 as a potential pseudoenzyme . . . 82
4.1.6 Aims . . . 83
4.2 Results . . . 84
4.2.1 MeJA treatment leads to emergence of novel RNA species in wheat rRNA 84
4.2.2 Effector BEC1054 alone is not sufficient to interfere with MeJA-induced host RNA degradation . . . 85
4.2.3 Effector BEC1054 inhibits JIP60-mediated necrosis *in planta* . . . 89
4.2.4 Effect of BEC1054 effector on JIP60 RIP domain and *in vitro* translation 95
4.3 Discussion: . . . 99
4.3.1 BEC1054 inhibits MeJA-mediated host rRNA degradation . . . 99
4.3.2 BEC1054 interferes with JIP60 . . . 101

5 Mode of action of RALPH effector BEC1054 **104**

5.1 Introduction . . . 104

5.1.1 *Blumeria* effectors . . . 104

5.1.2 BEC1054 - RALPH effector crucial for powdery mildew infection . . . 104

5.1.3 Basis of molecular interaction . . . 105

5.1.4 BEC1054 molecular interaction potential . . . 106

5.1.5 Aims . . . 107

5.2 Results . . . 108

5.2.1 Properties of BEC1054 molecular interaction . . . 108

5.2.2 Mutagenesis of suspected active residues of BEC1054 . . . 111

5.2.3 BEC1054 double mutant and JIP60ml competition *in planta* . . . 113

5.2.4 The effect of BEC1054$_{FYA}$ on *in vitro* translation . . . 117

5.3 Discussion . . . 120

5.3.1 Unoccluded surface is necessary for BEC1054 function . . . 120

5.3.2 Role of structure and hydrophobic interactions in BEC1054 function . . . 121

6 General Discussion **124**

6.1 Successful plant-microbe interaction depends on effectors . . . 124

6.2 Impact of *Blumeria* RALPH effector BEC1054 . . . 125

6.3 BEC1054 contributes to inhibition of the host rRNA degradation . . . 126

6.4 BEC1054 affects RIP-mediated host cell death . . . 127

6.5 BEC1054 – a molecular Swiss penknife of *Blumeria* . . . 129

6.6 Conclusions . . . 132

References **133**

List of Figures

1.1 Appearance of cereal powdery mildew and *Blumeria graminis* 20

1.2 Life cycle of *Blumeria graminis* 21

1.3 Cartoon of zig-zag model of plant immune response to fungal infection 25

2.1 Schematic representation of constructs used for agroinfiltrations 37

2.2 Increased expression of BEC1054 by addition of P19 39

3.1 Molecular structure of RIP domain of ricin and mechanism of action 50

3.2 Molecular model of wheat ribosome and of the α-sarcin/ricin loop (SRL) 53

3.3 Cartoon representation of JIP60 processing and function in barley 56

3.4 Alignment of amino acid sequences and HMM logo representation of RIP domain family 59

3.5 Predicted molecular model of the N-terminal RIP domain of JIP60 60

3.6 Hypothetical mode of action of hydrolytic depurination of adenine by the JIP60 RIP domain 61

3.7 Time course of transient expression of active JIP60 via agroinifiltration of *Nicotiana benthamiana* 63

3.8 Time course of transient expression of JIP60 mutants with alanine substitution . 65

3.9 Time course of transient expression of isostructural or isofunctional JIP60 mutants in *N. benthamiana* 66

3.10 Fluorescent micrograph of transiently express JIP60 variants in *N. benthamiana* 68

3.11 Western blot of protein extract from agroinfiltrated *N. bethamiana* leaves 69

3.12 *In vitro* translation assay using JIP60 variants in wheat germ extract 71

4.1 Comparison between structures of Ribonuclease T1 and BEC1054 81

4.2 Emergence of putative peak in total RNA extracts from MeJA-treated wheat . . 84

4.3 Size estimation of the putative peak using standard RNA markers 85

4.4 Total RNA profiles obtained from MeJA-treated transgenic wheat 87

4.5 Relative abundance of putative RNA peak in total RNA extracts from MeJA-treated transgenic wheat primary leaves in response to presence or absence of *B. graminis* . . . 88

4.6 Observation of JIP60 RIP domain-mediated necrosis in agroinfiltrated *N. benthamiana* . . . 90

4.7 Comparison of necrotic phenotypes resulting from agroinfiltration with JIP60 RIP domain . . . 91

4.8 Time course of co-agroinfiltration of *N. benthamiana* with JIP60 contested with either BEC1054 or GFP . . . 93

4.9 Flow chart of measuring grey scale intensity/luminosity of agroinfiltrated zones . 94

4.10 Time course of JIP60ml and BEC1054 competition in *N. benthamiana* leaves . . 96

4.11 Effect of BEC1054 and JIP60ml competition on ribosome inhibition *in vitro* . . 98

5.1 Time course of co-agroinfiltration of *N. benthamiana* with JIP60 contested with BEC1054 fused with either N-terminal or C-terminal GFP . . . 109

5.2 The effect of the localisation of the GFP tag on the function of BEC1054 110

5.3 Hydrophobic pockets on BEC1054 surface . . . 111

5.4 Mutagenesis of BEC1054 potential active site residues . . . 112

5.5 Transient expression of BEC1054 variants in *N. benthamiana* . . . 114

5.6 Time course of co-agroinfiltration of *N. benthamiana* with JIP60 contested with either BEC1054$_{FYA}$ or GFP . . . 115

5.7 The effect of BEC1054$_{FYA}$ double mutant on JIP60ml-mediated host cell death *in planta* . . . 116

5.8 Effect of BEC1054 variants on JIP60ml-mediated ribosome inhibition *in vitro* . . 119

6.1 Mechanism of inhibition of RIP-mediated host cell death by *Blumeria* RALPH effectors . . . 134

List of Tables

2.1 List of buffers used in the study and their recipes 35

2.2 List of plasmids used in the study 37

2.3 List of constructs used in agroinfiltrations 38

2.4 List of primers used in site-directed mutagenesis of BEC1054 40

2.5 List of JIP60ml mutations and their properties 41

2.6 List of primers used in mutagenesis of JIP60 42

2.7 List of primers for amplification of genes of interest with T7 promoter 46

4.1 List of transcription/translation (TnT) reactions for JIP60ml and BEC1054 competition *in vitro* experiment 97

5.1 List of transcription/translation (TnT) reactions for JIP60ml and BEC1054$_{FYA}$ competition *in vitro* experiment 118

Abbreviations

avr avirulent factor

BEC *Blumeria* effector candidate

BiFC Bimolecular fluorescence complementation

CC Coiled-coil

COI1 Coronatine insensitive 1

CPK Calcium-dependant protein kinase

CSEP Candidate secreted effector protein

CSIR Cell surface immune receptor

DAMP Danger-associated molecular pattern

EDS1 Enhanced Disease Susceptibility 1

eEF eukaryotic elongation factor

eIF eukaryotic initiation factor

ETI Effector-triggered immunity

ETS Effector-triggered susceptibility

GST Glutathione-S-Transferase

HIGS Host-induced gene silencing

HMM Hidden Markov model

HR Hypersensitive response

IIR Intracellular immune receptor

IP Invasion pattern

IPR Invasion pattern receptor

IPTR IP-triggered response

JA Jasmonates

JAZ Jasmonate-Zim domain

JIP Jasmonate-induced protein

LRR Leucine-rich repeat

MAMP Microbe-associated molecular pattern

MAPK Mitogen-activated protein kinase

MDH Malate dehydrogenase

MeJA Methyl-jasmonate

MST Microscale thermophoresis

NLP Nep-1-like protein

NLR Nucleotide-binding site leucine-rich receptor

NMR Nuclear magnetic resonance

NPR1 Non Expresser of Pathogenesis Related 1

PAD4 Phytoalexin deficient 4

PAMP Pathogen-associated molecular pattern

PAP Pokeweed antiviral protein

PR Pathogenesis related

PRR Pattern recognition receptor

PTI PAMP-triggered immunity

QTL Quantitative trait locus

R gene Resistance gene

RALPH RNase-like effector protein expressed in haustorium

RIP Ribosome inactivating protein

RLCK Receptor-like cytoplasmic kinase

RLK Receptor-like kinase

RLP Receptor-like protein

ROS Reactive oxygen species

SA Salicylic acid

TBSV Tomato bush stunt virus

TIR Toll-interleukin 1-like receptor

Acknowledgements

Firstly, I would like to thank my supervisor, Professor Pietro Spanu. His conceptualisation and continuous support and advice throughout the entire project were indispensable, and I especially appreciate the help and sympathy he gave during my last year when I was trying to balance finishing my PhD and beating cancer.

I would also like to thank my secondary supervisor, Dr Ernesto Cota, for help and advice on the structural aspects of the project.

I would like to acknowledge substantial contributions to this project, especially to past and current PhD students within the group. These include Dr Helen Pennington for her cloning of JIP60 domain and previous work on BEC1054 interactions, as well as Dr Rhian Jones for her creation of JIP60ml recombinant construct and structural work on BEC1054. Their work made a great foundation for this project. Moreover, I would like to thank Dr Linhan Li for her help with quantification of the necrosis score, and Summer Zhang for her help with *N. benthamiana* cultivation and optimisation of yeast-three-hybrid system. I would also like to thank Dr Josh Hodge for his help in assessing and devising the appropriate statistical analysis approach.

I want to acknowledge other students who also contributed to this project. Seomun Kwon for the first concept of the hypothesis; Maya Bruderer, Rachel Greenhill and Peter Wellham for the creation and work on the JIP60ml mutants; Gerard Belmans and Tia Salter for their optimisation and work on the *in vitro* model of JIP60ml.

Last but not least, I would like to thank my wife, Helen, for her enormous support throughout this process and especially while writing this thesis. I could not have done it without you.

Chapter 1: Introduction

1.1 Food security

Food security is one of the most pressing matters for our civilisation. Food security refers to the state where "all people, at all times have physical and economic access to sufficient, safe and nutritious food to meet their dietary needs and food preferences for a healthy and active life" (Pinstrup-Andersen 2009). Even though the global hunger and malnourishment is on a slow but consistent decline, food security is still threatened. Recent data suggests that at least one in seven people today still have no access to a sufficient diet (FAO et al. 2015).

Food production is going to face new challenges in coming years. The continuously growing global population, with predicted nine billion people by the year 2050, is outpacing the growth achieved in food production (Evans 2009; Brown 2012; Godfray et al. 2010; Challinor et al. 2016). Moreover, increased wealth in rapidly developing countries leads to changes in dietary preferences, increasing the demand on food groups with higher energy requirements, such as meat and processed food, putting additional strain on those industries (Tilman et al. 2001; Godfray et al. 2010). Furthermore, dedicating more land to grow food is increasingly difficult. More and more land is being made unusable for food production due to desertification, salinisation and soil degradation. Finally, the looming climate change is very likely to lead to even further losses of usable land (Nellemann et al. 2009; Wheeler and Braun 2013). Hence various food industries these days face greater competition for land, water and energy, as well as enforcement to curb environmental impact (Tilman et al. 2001; Godfray et al. 2010). As a result of this, lack of space for new fields and the threat of the progressing climate change are dramatically limiting our ability to produce more food (Wheeler and Braun 2013; Challinor et al. 2016). In spite of this, the issue is not completely hopeless: even though, the utilised land increased only by 9% in the last 50 years, the grain production more than doubled in this time (Pretty 2008). That means there are other ways, such as protecting current crops from environmental and pathogen threats, to increase yield of the crop

production. However, the constantly evolving pathogens and fast changing environment will always threaten crop yields. Consequently, in order to achieve the global food security, a collective and continuous input of effort and innovation is required.

1.2 Importance of wheat and barley

This study focuses on wheat (*Triticum aestivum*) and barley (*Hordeum vulgare*). Both wheat and barley are historically crucial to human civilisation. Evidence suggest they are ancient crops that were domesticated around 10 000 BC during the Neolithic revolution, facilitating the switch from hunter-gathering to settlement and agriculture (Grando and Macpherson 2005; Shewry 2009; Riehl et al. 2013). Selective breeding allowed development of favourable traits and increased yields, however essentially they are the same crops that are cultivated today and they remain the most used cereals worldwide (Ullrich 2010; Friedt et al. 2011).

Their exceptional nutritional value and adaptability to diverse environments led to wheat and barley holding 3rd and 5th place, respectively, among all cultivated crops by globally produced dry mass (Baik and Ullrich 2008; Dubcovsky and Dvorak 2007). According to data from FAO (2017), more than 744 Mt of wheat were produced worldwide in 2017 alone, with an outlook for 755 Mt in 2018 and over 804 Mt in 2024. Moreover, both wheat and barley are also used for other purposes than food for human consumption. Due to the growing demand wheat starch is more and more considered for use in production of biofuels, whereas barley is predominantly used as animal feed and in industries such as breweries and whisky production (European Commission Directorate-General for Agriculture and Rural Development 2011; Baik and Ullrich 2008; Faltermaier et al. 2014; Waterschoot et al. 2015). Hence, both crops are extremely economically important. Wheat was estimated to have contributed $20.6 billion in 2005 to the US economy while production and sales of Scotch whiskies contribute more than £5 billion annually to the UK economy (Richardson et al. 2006; The Scotch Whisky Association 2015).

Only up to 2% of barley that is produced is used directly in human food products (Baik and Ullrich 2008). It is due to lower palatability and appearance of barley products in compar-

ison with wheat flour products (Andersson et al. 2004). However, the interest in barley has increased in the last decade or so, as its health benefits become apparent (Zhou 2009). Barley seeds contain essential amino acids such as valine, lysine, threonine and arginine (Sullivan et al. 2013). Moreover, they contain between 8% and 20% of β-glucan, depending on cultivar, which is associated with lowering blood cholesterol, thus leading to lower chances of chronic heart disease (Baik 2016). Furthermore, β-glucans were associated with lower chances of developing type 2 diabetes due to increased insulin response (Sullivan et al. 2013). Finally, barley has high content of both soluble and insoluble fibre, leading to healthier colon function and favourable gut microbiota, thus contributing to tackling obesity and lowering chances of colonic cancer (Sullivan et al. 2013; Conway and Behall 2006).

Despite the fact that barley and wheat have been with humanity since the dawn of agriculture and remain some of the most important staple foods to this day, their respective genomes have only been fully sequenced and annotated in 2017 and 2018, though not for the lack of trying (Mascher et al. 2017; International Wheat Genome Sequencing Consortium 2018). The barley genome proved to be difficult to sequence not only due to its size, estimated at 5.3 Gbps (haploid), thus one of the largest diploid genomes sequenced to date, but also due to presence of large amount of repetitive sequences which made the assembly much more problematic.

The wheat genome was even more troublesome. The modern bread wheat, *T. aestivum*, is a hexaploid, meaning that over the course of its cultivation, two separate hybridisation events of closely related grasses occurred, where three separate species amalgamated their genomes into one. The first hybridisation event is believed to have occurred between *T. urartu* (AA) and *Aegilops speltoides* (BB), giving rise to a tetraploid *T. turgidum* (AA BB). Subsequently, *T. turgidum* hybridised with *Ae. tauschii* (DD), leading to emergence of the breed (AA BB DD) (Feldman and Levy 2005; Shewry 2009). That added "extra" complexity to the task of assembling the genome, not only due to additional sheer size, estimated to be 15.4 Gbps long, but also because of how many genes are duplicated (International Wheat Genome Sequencing Consortium 2018).

Completely sequenced and annotated genomes of wheat and barley bring a lot of potential to

the agriculture and research of these important crops. For example, access to the sequence-level information on the genes used will allow easier and deeper understanding of the molecular processes involved and may lead to targeted breeding technologies in the future, to create crop varieties that are able to better cope with specific abiotic stresses, such as drought or salinity. Moreover, this information will help making varieties that are inherently resistant to certain pests or pathogens by introduction of resistance genes, or conversely by silencing genes responsible for susceptibility to those pathogens. Selective breeding has already been used for hundreds of years to obtain desirable traits and resistance, for example for decades the barley *mlo* mutants are known to be resistant to powdery mildews (Lyngkjaer et al. 2000). The detailed reference genome might now allow a targeted breeding or gene editing approach to achieve optimal results faster. Varieties naturally resistant to pests lead to lower pesticides usage, which is better for the farmer (economically), for the consumer (healthier as less of potentially harmful residual chemicals in food) and for the environment (less harm to "bystander" insects) (Langner et al. 2018). Finally, with the knowledge of genome regulatory regions, it might be easier to design varieties that are healthier and more nutritious by containing more desirable molecules (International Wheat Genome Sequencing Consortium 2018). It might even be possible to create wheat strains safe for people that are currently sensitive or allergic to it.

However, just the knowledge of complete genomes itself is not enough. In order to get the most out of that knowledge and achieve a long-lasting resistance, a detailed understanding of plant immunity and host-pathogen interaction is also necessary.

1.3 Phytopathogens – the pathogens of plants

Plant pathogens (phytopathogens) lead to crop losses by causing disease in plants. Most common phytopathogens are fungi (e.g. *Magnaporthe oryzae* or *Botrytis cinerea*), nematodes (e.g. *Meloidogyne spp.* or *Globodera spp.*), bacteria (e.g. *Pseudomonas syringae* or *Ralstonia solanacearum*) and viruses (e.g. Tomato Mosaic Virus or Cassava Mosaic Virus), which lead to a whole range of diseases in plants (Dean et al. 2012; Scholthof et al. 2011; Mansfield et al.

2012; Jones et al. 2013).

Phytopathogens are often grouped into biotrophs, necrotrophs and hemibiotrophs depending on the trophic interactions with their host (Moore et al. 2011a). Biotrophs are characterised by the requirement of a living host cell in order to live. Many biotrophs use feeding body or interface, e.g. appressorium or haustorium, to extracts nutrients and resources from a living host cell. A biotroph infection in a compatible interaction does not lead to host cell death. In an incompatible interaction, for example with a non-host, a common outcome is host cell death through hypersensitive response (see 1.8.5). Some biotrophs exhibit only a very narrow range of compatible hosts, for example *Ustilago maydis* and *Puccinia graminis* (Dean et al. 2012), which cause maize smut and black stem rust in cereals, respectively. There are examples of biotrophs with wider range of host, such as *Podosphaera leucotricha* which predominantly infects apples, however it can also affect other fruit trees such as pears and peaches (Ellis et al. 1981).

In contrast to biotrophs, necrotrophs derive the nutrients from dead cells of their hosts. They release many lytic enzymes and toxins to induce rapid death of plant tissue and then feed saprophytically on the remains and unlike biotrophs, they rarely produce feeding bodies such as haustoria. Examples of necrotrophs include *Botrytis cinerea* and *Ophiostoma novo-ulmi*, which cause grey mould and Dutch elm disease, respectively. Finally, there are hemibiotrophs, characterised by the initial stage of biotrophic, asymptomatic interaction, followed by necrotrophic stage. A noteworthy example of this group is *Phytophthora infestans* which causes potato late blight (Kamoun et al. 2015). Interestingly, Spanu and Pastruga (2017) argue that many of the necrotrophs start with an asymptomatic stage, thus can in a way be considered hemibiotrophs.

1.4 Pathogen control

Methods of pathogen control can be divided into exclusion, eradication and protection. Exclusion is achieved by use of pathogen-free soil, seeds, grafts, etc. This way the growers try to ensure that the potential pathogens are never introduced into the environment in the first place. However, in most cases it is not feasible to maintain such a state, e.g. on an open

field. A current example of attempted exclusion through quarantine and using pesticides against the vector insects is the issue of bacterial infection of olive groves in Italian region of Puglia by *Xylella fastidiosa* (Abbott 2018). The bacterium causes olive quick decline syndrome and leads to extensive damage to the trees and huge fruit yield losses. The disease is currently considered incurable once present, thus exclusion may be the only possible way of tackling the problem.

In the instance a pathogen was introduced to the environment or has been already present there, the growers might attempt eradication. Eradication can sometimes be achieved by proper use of appropriate pesticides or by crop rotation, i.e. growing plants on which the particular pathogen cannot thrive. However, many pathogens can remain dormant for a very long time or they can develop resistance to pesticides, and often complete eradication is not possible. When neither exclusion nor eradication is possible, various methods of crop protection can still be applied to ensure sufficient control.

Employment of crop protection is absolutely essential for agriculture as otherwise crop losses would be overwhelming and could make their cultivation unprofitable. For example, it is estimated that worldwide total potential losses to wheat due to pests in period 2001-03 would reach 49.8%, if no pest control was used (Oerke 2006). Of that, 15.6% are attributed to pathogens (fungi and bacteria). However, the pest control is not perfect. Despite the current controls, the actual worldwide losses to wheat production in that period reached 28.2% due to all pests, of which, 10.2% were attributed to pathogens (Oerke 2006). Interestingly, absolute value of crop losses seemed to have increased in the last 40 years, despite the increased use of pesticides (Oerke 2006).

Climate change will lead to further increase in crop losses caused by pests or pathogens (Gregory et al. 2009). Higher ambient temperatures will increase metabolic rates of insects, thus their food consumption will increase accordingly (Deutsch et al. 2018). Change in temperature will also affect the numbers of insects. Higher temperatures may lead to a decrease in their numbers in tropical climates but to an increase everywhere else (Deutsch et al. 2018). The effects of climate change are not limited to insects. For example, already outbreaks of potato late-blight are more frequent and occur earlier on in the season due increased median

temperatures in Finland (Hannukkala et al. 2007). Moreover, some pathogens, such as oilseed rape stem canker, are predicted to increase in severity and spread to currently unaffected areas within the next two decades, as the climate becomes more favourable for them (Evans et al. 2008).

Under this premise, the most feasible way to increase the food production is to breach the yield gap. Yield gap is the difference between realised harvest yield and the one actually achieved. Yield gap is created by deficiencies in infrastructure, lack of access to expertise, fertilisers, and optimal crop varieties, as well as by pathogens and pests. Pests and pathogens negatively affect crop yields every year: understanding of the processes involved in plant-pathogen interaction may prevent harvest yield losses (Fisher et al. 2012; Dean et al. 2012). Increase in crop productivity needs to go hand in hand with increased crop protection, as increased output often causes increased vulnerability, hence the attainable yields won't increase (Oerke 2006).

1.5 Powdery mildews

Powdery mildew is a disease that affects many plants caused by various ascomycete fungi from the order *Erysiphales* (Moore et al. 2011a). For instance, grape powdery mildew is caused by *Erysiphe necator*, whereas apples and pears are affected by *Podosphaera leucotricha*. The common name is derived from its characteristic appearance: the infected plants show white flour-like patches on the foliage and stems (Figure 1.1a), caused by the external growth of the fungi on the plant surface (Figure 1.1b). Powdery mildews are obligate biotrophic parasites and they do not usually lead to plant death, however, the disease can cause significant damage and decrease in plant vigour and can lead to distortion or stunting of the host or its parts, especially in young plants. Most importantly, the presence of the disease decreases crop yields. Powdery mildews tend to grow well in environments with high humidity and moderate temperatures, often making greenhouses a perfect place for the disease to spread. The fact that powdery mildews affect many crops leading to significant yield losses, make it an economically important disease. Moreover, powdery mildews are not only important in

crops but also in areas such as forestry. For example, *Microsphaera alphitoides* led to devastating epidemic of juvenile pedunculate oak in Europe in early 20th century (Pap et al. 2012).

1.6 *Blumeria graminis*

Blumeria graminis, phylum *Ascomycota*, is a fungal phytopathogen that causes powdery mildew disease in cereal crops (Both and Spanu 2004; Dean et al. 2012). It is a strict biotroph, i.e. it requires a living host plant cell in order to survive (Wicker et al. 2013). *B. graminis* also exhibits extreme host specificity, which divides the species into several subspecies, called *formae speciales* (ff.spp.), and each is capable of infecting only a single plant host (Oberhaensli et al. 2011; Troch et al. 2014). For example, *B. graminis* f.sp. *hordei* and f.sp. *tritici* can only infect barley and wheat, respectively, but not *vice versa*. *B. graminis* is economically a very important pathogen due to its efficacious infection capabilities which lead to substantial losses in harvest yields in wheat and barley (Dean et al. 2012). It is estimated that *B. graminis* causes losses of up to $39 million annually in Australia alone (Murray and Brennan 2010).

B. graminis propagates from plant to plant very quickly due to its short life cycle. Throughout the season, the pathogen mostly reproduces asexually via conidia (Both 2005). Conidia are released from conidiophores of *B. graminis* colony and as it lands on a susceptible host, it germinates within 30 min. Within the next 24 hours it develops an intracellular feeding body, known as an haustorium (Figure 1.1c), which marks a successful infection (Both 2005). The now established colony continues to grow and develops conidiophores. The entire cycle, from conidium germination to release of new conidia, takes about five days (Figure 1.2).

The genome of *B. graminis* is very unusual for an *Ascomycete* fungus. For instance, genome of *B. graminis* is circa 120 Mbp in length, considerably longer than any of their non-parasitic relatives (Spanu et al. 2010; Frantzeskakis et al. 2018). Moreover, more than 64% of the genome is comprised of retrotransposons, believed to be advantageous in rapid adaptation to the plant-pathogen interaction, due to increased rate of gene multiplication and mutation (Spanu

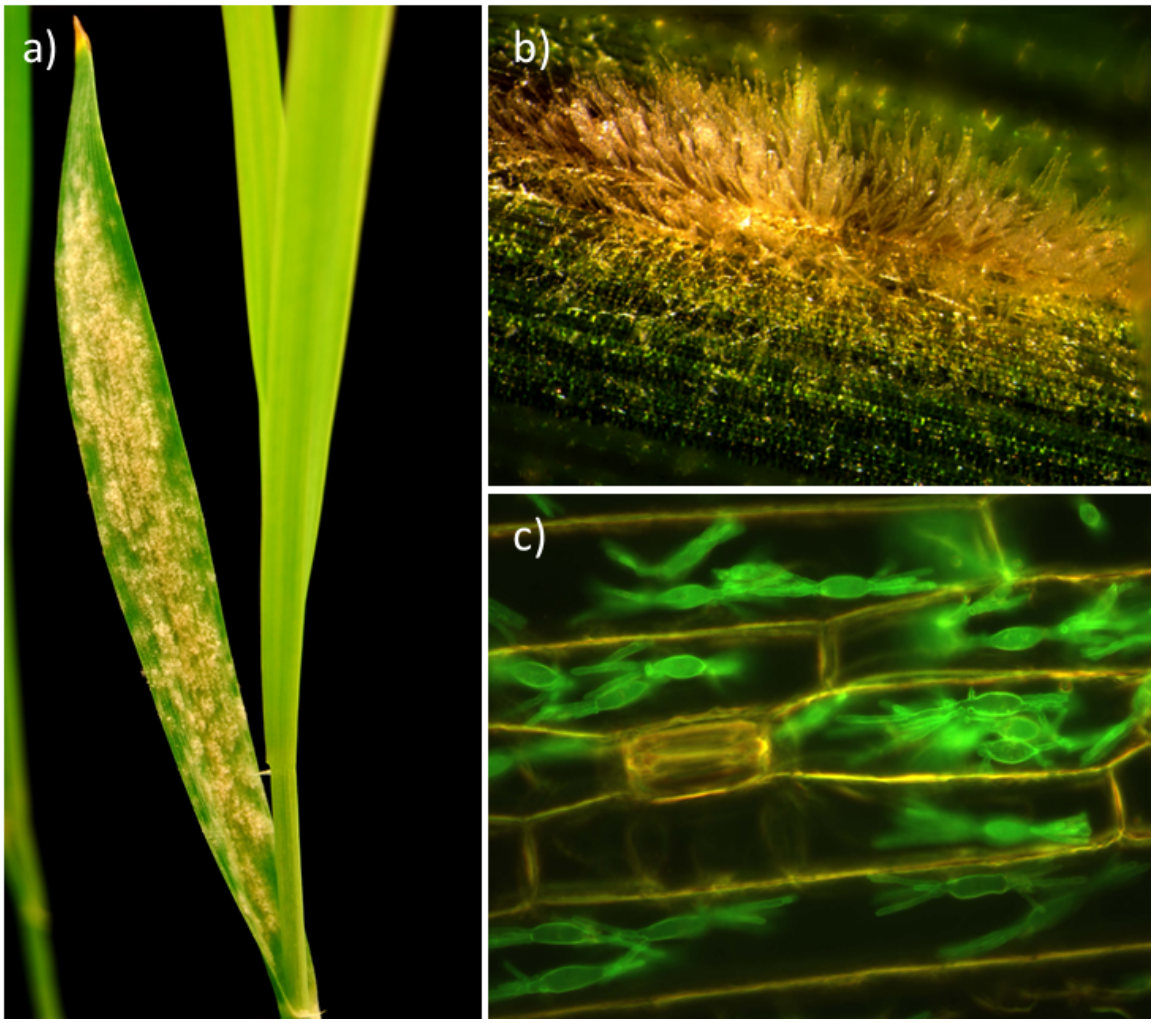


Figure 1.1: Appearance of cereal powdery mildew and *Blumeria graminis*
a) A leaf of barley infected with *Blumeria graminis*. The characteristic powder-like appearance gave name to powdery mildew. b) Close-up on *Blumeria graminis* colony. Hyphae and conidiophores can be seen protruding from the surface of the leaf. c) Micrograph of infected leaf cells. Haustoria, the feeding bodies of *Blumeria*, can be seen inside the host cells. (images courtesy of Pietro Spanu)

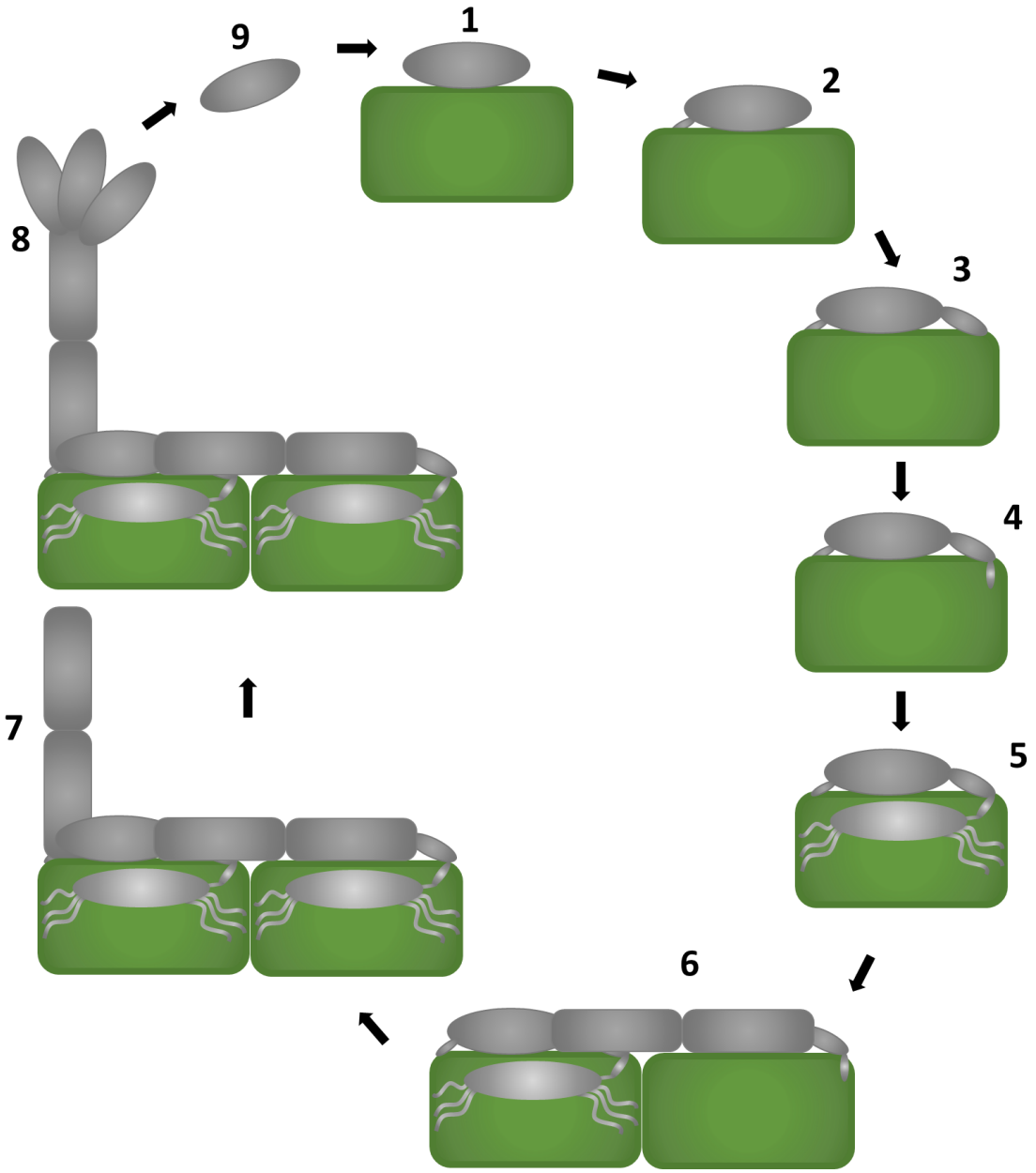


Figure 1.2: Life cycle of *Blumeria graminis*
1. A conidium lands on a susceptible host. 2. Within 30 min conidum germinates and develops primary germ tube. 3. The conidum develops secondary germ tube withing the next few hours which then develops into appresorium. 4. Appresorium 'drills' through the cell wall into the host cell, allowing access to the cell interior. 5. Within 24 hr from initial landing, haustorium develops, marking a successful infection. 6. *Blumeria* grows hyphae and spreads to nearby cells. 7. *Blumeria* keeps growing and spreading the colony, developing more haustoria in nearby host cells. It also starts growing conidiophores. 8. The colony grows larger. Conidiophores develop and start producing new conidia. 9. Within 5 days from initial germination new conidia are ready to colonise other leaves and plants.

et al. 2010).

1.7 CSEPs, RALPHs and BEC1054

The never-ending evolutionary arms race between host and pathogen has led to the emergence of hundreds of effectors (Thordal-Christensen et al. 2018). Effectors are small proteins secreted by virulent bacteria and fungi into host cell to facilitate infection (Boller and He 2009; Spanu et al. 2010; Bozkurt et al. 2012; Selin et al. 2016). *Blumeria* effectors play an important role in manipulating plant defences and facilitating establishment of infection. Analysis of the *B. graminis* genome sequence revealed that there are over 500 candidate secreted effector proteins (CSEPs) with no known homology outside of *Blumeria* (Pedersen et al. 2012, Pastruga, R., pers.comm.). CSEP amino acid sequences suggest large structural and functional diversity within the effector group (Pedersen et al. 2012). This diversity may be important in subduing an equally intricate arsenal of plant immune responses. Interestingly, over 120 of the effectors are predicted to adopt a ribonuclease-like fold (Pedersen et al. 2012). The majority of CSEPs are more highly expressed in the haustoria. Haustoria act as a pathogen-plant interaction interface, facilitating secretion of effectors from *Blumeria* into the plant and uptake of host nutrients into *Blumeria* (Bindschedler et al. 2009). The number of RNase-like effector proteins expressed in haustorium (collectively known as RALPHs), compared to other effectors, suggests RALPHs could be very important during the infection process and are therefore worth further study. Interestingly, analysis of RALPH sequences suggest they evolved from a single common ancestral gene as they all contain an intron at an identical location (Spanu 2017). An extensive proteogenomics study identified a group of *B. graminis* effector candidates (BECs) (Bindschedler et al. 2009; Bindschedler et al. 2011). BECs are small, secreted proteins that are closely associated with haustoria and highly likely to be secreted into the plant cell (Pliego et al. 2013). The majority of BECs have also been identified as CSEPs, including effector BEC1054 (syn. CSEP0064) (Bindschedler et al. 2016). The importance of BEC1054 was highlighted, using host-induced gene silencing (HIGS), as an effector facilitating *B. graminis* infection (Pliego et al. 2013). Pliego et al. (2013) showed with molecular bombardment in barley that RNAi constructs suppress-

ing BEC1054 led to a 60% decrease in haustorial index, i.e. successfully established haustoria in host cell, in comparison to the control. A structural study of the effector confirmed that it assumes an RNase-like fold, however, it lacks the conserved catalytic residues responsible for cleavage of RNA (Pennington et al. 2019). RNases have very robust structures and the fold suggests a possible interaction with RNA but not an enzymatic function (Pace et al. 1988). Since the *Blumeria* effector BEC1054 is crucial in the infection process, it is important to understand its function. That understanding can be then used to create a targeted treatment against this pathogen.

1.8 Plant immunity

1.8.1 PTI and ETI zig-zag model

The plant immune system can be divided into two major branches: pathogen associated molecular pattern (PAMP)-triggered immunity (PTI) and effector-triggered immunity (ETI) (Jones and Dangl 2006; Boller and He 2009; Miller et al. 2017). The former, similarly to the animal innate immune system, is based on the recognition of highly conserved, generic PAMPs found on/in pathogens by plant pattern recognition receptors (PRRs) (Dodds and Rathjen 2010). This recognition elicits an immune response. PTI is also involved in mounting an appropriate response to microbe-associated molecular patterns (MAMPs) that come from non-pathogenic microbes, and endogenous defence signals danger-associated molecular patters (DAMPs) (Eckardt 2017). Plants do not possess adaptive immunity or any mobile immune cells the way animals do (Staskawicz et al. 2001; Nürnberger et al. 2004; Zipfel and Felix 2005; Dodds and Rathjen 2010; Spoel and Dong 2012; Eckardt 2017). Instead, the second category of plant innate immune system, the ETI, is seen only in plants and due to its pathogen specificity it acts as plants' 'adaptive' immunity, however, it is adaptive on an evolutionary scale, and not within the lifespan of a single organism (Dodds and Rathjen 2010; Nürnberger et al. 2004). ETI is a hereditary resistance against specific pathogens based on resistance genes (R genes) that evolved to recognise particular pathogen effectors and then signal to mount an appropriate response (Chisholm et al. 2006).

R genes have been used for decades to breed pathogen resistant crop varieties. An effector with a cognate R gene in a host plant cell is known as an avirulent factor (*avr*) and this avirulence factor-resistance (*avr*-R) protein interaction is the basis of avirulence, where a defence response is initiated by the resistant plant due to presence of appropriate R gene and no disease develops (Surico 2013). ETI was thought to work on a gene-for-gene concept, when each R gene product was cognate to a singular pathogen effector, however recent studies suggest that the interactions are much more complex (Bourras et al. 2015; Bourras et al. 2016). For instance, a single avirulence effectors, such as AVR-Pik/km/kp from *Magnaporthe oryzae* or AvrL567 from *Melampsora lini*, are recognised by multiple R genes (Yoshida et al. 2009; Barrett et al. 2009).

Currently, the most supported simplification of plant immune system that puts together PTI and ETI is the so-called zig-zag model (Jones and Dangl 2006; Eckardt 2017; Miller et al. 2017). This model states that the plants detect the invader directly via PAMPs or MAMPs, or indirectly via DAMPs, and attempts to elicit PTI. However, some pathogens or symbionts manage to stop that response by secreting specific effectors, causing effector-triggered susceptibility (ETS). At this stage, plants that possess the cognate R gene to said effector, mount ETI. Subsequently, the microbe can evolve to avoid the recognition by either loss/mutation of the recognised effector or by using a novel effector (Figure 1.3).

1.8.2 Caveats of the zig-zag model

PTI and ETI are not always that easy to distinguish nor do they always follow the separation stating that PAMPs/MAMPs are generic, ubiquitously preserved patterns with little change over time, whereas effectors and R genes are rapidly evolving and always pathogen-host specific (Boller and Felix 2009; Cook et al. 2015). In fact, more and more discoveries are made that lead to blurring of the clear division between PTI and ETI that the zig-zag model proposes. For example, flagellin, whose peptide are generally regarded as classical PAMP, purified from two strains of *Pseudomonas avenae* have a differential response in rice, showing strain specificity, behaviour more commonly seen in ETI (Che et al. 2000). Similarly, bacterial elongation factor EF-Tu, recognised as a common PAMP, is recognised by various plants

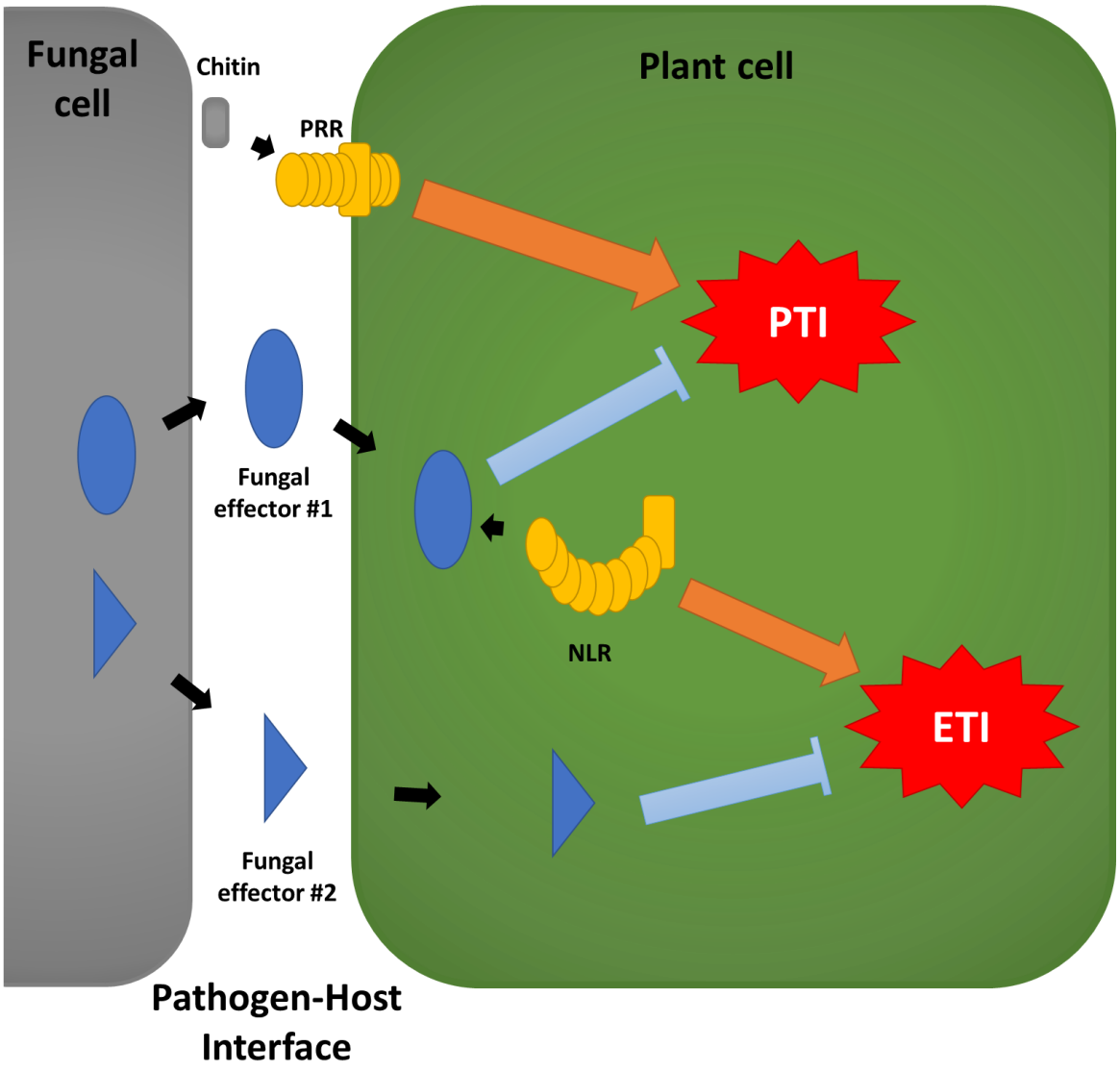


Figure 1.3: Cartoon of zig-zag model of plant immune response to fungal infection
The cartoon represents a simplified plant immune response to infection using zig-zag model, here using an example of fungal infection. Plant cell recognises pathogen associated molecular patterns (PAMPs), such as chitin particles, with pattern recognition receptors (PRRs). That recognition usually occurs at the pathogen-host interface, e.g. at the intersection of haustorial and plant cell lipid membranes. Successful recognition of a PAMP by a corresponding PRR leads to PAMP-triggered immunity (PTI) response. However, an adapted invader can down regulate or stop host PTI by secretion of a specialised effector (here represented by oval fungal effector #1). The fungal effector #1 can in turn be 'countered' by the cognate nucleotide-binding site leucine-rich receptor (NLR), an R gene product that evolved specifically to recognise fungal receptor #1. Upon recognition, which occurs intracellularly in the host, the host cell mounts effector-triggered immunity (ETI), often causing the hypersensitive response (HR). However, a well-adapted invader can mutate the effector #1 so it is no longer recognised by the NLR or evolve another effector, here the triangular effector #2, which in turn stops the ETI response elicited by recognition of effector #1. Many bacterial and fungal pathogens would have hundreds of various effectors at their disposal. (Cartoon is an own work designed based on model described by Jones and Dangl 2006)

via different epitopes, braking the concept of well preserved and generic PAMPs and falling more into the category of specific host-pathogen interactions (Cook et al. 2015). By contrast, a conserved region of 20-24 amino acids was found in Nep-1-like protein (NLP) effectors encoded by many bacteria, oomycetes and fungi, which is sufficient to induce a strong immune response, thus acting more like PAMP (Oome et al. 2014). In fact, these discrepancies led Boller and Felix (2009) to propose merged danger signals model and for Cook et al. (2015) to advocate to abandon the zig-zag model in favour of the invasion model for plant immunity. The invasion model abandons the dichotomy into PTI and ETI, and instead integrates it into a single system where all microbe-derived signals, such as PAMPs, MAMPs and DAMPs, as well as the effectors are called collectively invasion patterns (IPs). These IPs are then recognised by IP receptors (IPRs), and upon successful recognition lead to IP-triggered response (IPTR). Cook et al. (2015) argue that the invasion model allows research to be more focused on the outcome and eliminates the discrepancies by abandoning the seemingly only artificial separation between the PTI and ETI. The invasion model was further refined and Kanyuka and Rudd (2019) proposed "spacial invasion model", where the perception of the invader by the plant is classified based on the localisation of the receptors involved, i.e. intracellular immune receptors (IIRs) and cell surface immune receptors (CSIRs).

Each plant immunity model has its advantages and disadvantages. Therefore, as majority of the literature cited within this thesis still uses the terminology of the zig-zag model, i.e. PTI and ETI responses, I am going to conform with it, despite the caveats of the model, to maintain the continuity and clarity with previous research. It can be later translated into the spactial invasion model by assuming the PTI response comes from apoplastic CSIRs and the ETI response is driven by cytoplasmic IIRs.

1.8.3 Molecular basis of plant immunity pathways

From a purely molecular perspective, there seems to be some basis for the separation between the PTI and ETI responses. Many PRRs have been identified that respond to various PAMPs derived from bacteria and fungi (Tang et al. 2017). All known PRRs to date belong to either receptor-like kinase or protein (RLK or RLP) families (Yu et al. 2017). Upon

recognition of a PAMPs, in many PRR cases, the signal is transduced downstream by recruitment and activation of two leucine-rich repeat (LRR)-RLKs, BAK1 and SOBIR1 that act as an adapter and a signalling kinase, respectively (Liebrand et al. 2014). BAK1 seems to be more generic by interacting with membrane-bound receptors of both RLK and RLP families, whereas SOBIR1 seems to be specific to RLKs only, though it still needs the presence of BAK1.

The ETI receptors, i.e. the R gene products, are more diverse than PRRs. Some of them belong to the RLK or RLP families, however, the majority of them are nucleotide-binding site-leucine-rich repeat receptors (NLRs). NLRs are commonly divided into two subgroups based on the nature of their N-terminal domain: either a Toll-interleukin 1-like receptor (TIR) or a coiled-coil (CC) (Peng et al. 2018).

Both PTI and ETI have a common signalling pathway which they seem to utilise differently (Tsuda and Katagiri 2010; Boller and Felix 2009; Peng et al. 2018). Research suggests that in both cases the initial trigger (detection of a PAMP or an effector protein) is followed by rapid flux of ions, mostly Ca^{2+}, across the plasma membrane, followed by oxidative bursts of reactive oxygen species (ROS) and induction of the mitogen-activated protein kinase (MAPK) cascade as well as production of plant hormones, such as jasmonates (JA) and salicylic acid (SA) (Jones and Dangl 2006; Tsuda and Katagiri 2010; Dodds and Rathjen 2010; Du et al. 2009). In turn, the hormones lead to up- or down-regulation of expression of appropriate defence-related genes (Reymond and Farmer 1998).

Even though PTI and ETI use a common signalling pathway, they trigger responses that differ in amplitude and resulting effect by varying composition and timing of shared messenger molecules and signals (Peng et al. 2018). For example, although both PTI and ETI lead to Ca^{2+} influx and ROS production, different calcium-dependant protein kinases (CPKs) seem to be involved in triggering the downstream ROS activation; PTI response to a PAMP such as flg22 seems to be dependent on CPK4, CPK5, CPK6 and CPK11, whereas an ETI response to RPM1 seems to also involve CPK5 and CPK6, but then relies on CPK1 and CPK2 instead (Boudsocq et al. 2010; Gao et al. 2013). Furthermore, PTI seems to favour short burst of signals, whereas ETI induces prolonged signal, which in turn leads to differ-

ent responses downstream the pathway (Tsuda and Katagiri 2010). For instance, the MAPK cascade pathway seems to be active for about 1 hour when triggered by PTI, whereas it is active for several hours in response to CC-NLR activation in ETI (Tsuda et al. 2013). One of the most divergent points between PTI and ETI responses seems to lie in receptor-like cytoplasmic kinases (RLCKs). These molecules are, similarly to RLKs, Ser-Thr-special cytoplasmic kinases but they lack the extracellular and transmembrane domains (Shiu and Bleecker 2001). The RLCKs are direct targets of RLKs and they are signal transducers for the downstream responses, however, they seem to be solely involved in PTI response (Lin et al. 2013).

Ultimately, the plant immune response can result in many outcomes, ranging from expression of toxins and fungicidal or bactericidal molecules, to programmed cell death (Miller et al. 2017; Tsuda and Somssich 2015; Jones and Dangl 2006). Some plants, in response to attack by herbivorous insects, are even capable of secreting molecules that can attract the attackers' natural predators (Wu and Baldwin 2010). The outcome of the plant immune response is dependent on many factors. One of the most important factors is the nature of the invader. A plant will mount a different response depending if it is invaded by a biotroph, a necrotroph, an herbivore or a mutualistic organism (Jones and Dangl 2006; Pieterse et al. 2012; Glazebrook 2005; Zamioudis and Pieterse 2012). There are also secondary factors that can influence the outcome. For example, there is evidence that chloroplasts are also involved in plant defence. There is a possibility that light quantity and quality gives information on the energy state of the plant cell and 'helps decide' on appropriate response (Stael et al. 2015). Interestingly, both PTI and ETI can lead to host-induced programmed cell death, however ETI is much more likely to induce it than PTI (Jones and Dangl 2006). In *Arabidopsis thaliana* dosing with different *Pseudomonas* strains showed that it was gene dosage, rather than switching gene expression on/off that led to the intensity of immune response, host cell death or less drastic method (Tao et al. 2003).

1.8.4 SA/JA phytohormone crosstalk

The outcome of the plant immune response is controlled by two major plant hormones involved in plant defences: salicylic acid (SA) and jasmonates (JA) (Jaillais and Chory 2010). Studies in *A. thaliana* show that SA signalling pathway is mostly associated with the defence against biotrophs, whereas JA signalling pathway against necrotrophs and herbivorous insects (Verhage et al. 2010; Pieterse et al. 2012). However, that is not always true as JA was also shown to respond to biotrophic attack (Spoel et al. 2003; Ellis et al. 2002; Duan et al. 2014). The cross-communication of these two phytohormones, often referred to as SA/JA crosstalk, allows fine tuning of plant transcriptional programs, immune responses and developmental trade-offs (Caarls et al. 2015). Apart from the two major plant hormones, there are other ones that can influence the outcome. For instance abscisic acid (ABA) and ethylene act synergistically towards JA signalling while antagonising SA pathway (Pieterse et al. 2012). It is believed that the crosstalk allows to prioritise the pathway which will induce the best response in an event of simultaneous attacks by multiple pathogens in nature (Spoel et al. 2007). Moreover, SA/JA crosstalk is also implicated in abiotic stresses, such as thermotolerance (Clarke et al. 2009). Interestingly, the results of SA/JA crosstalk have been reported to be heritable epigenetically and the defences remain primed and active even in the next generation due to chromatin remodelling and DNA methylation (Luna et al. 2012).

Most of the crosstalk takes place at the level of transcription (Pieterse et al. 2012). SA and JA pathways are antagonistic towards each other and the final outcome depends on relative concentrations of these hormones (Mur et al. 2006). Biosynthesis of SA is mediated by Enhanced Disease Susceptibility 1 (EDS1) and Phytoalexin Deficient 4 (PAD4) in both ETI and PTI (Wiermer et al. 2005). SA overrides the JA signalling using many strategies. SA-mediated post-translational modification of JA-induced transcription factors affect their activity and localisation. For instance, SA-induced thioredoxin and glutaredoxin-mediated redox changes can modify transcriptional regulators dependant on JA. Moreover, SA induces negative regulators of JA-signalling, such as WRKY transcription factors. Finally, SA-dependant histone modifications can influence JA-responsive genes expression (Caarls et al. 2015; Van der Does et al. 2013). Downstream signalling of SA is predominantly mediated by redox-

sensitive Non Expresser of Pathogenesis Related 1 (NPR1) transcription factor (Moore et al. 2011b). NPR1 plays an essential role in SA/JA crosstalk, as it changes conformation in result to redox changes, translocates to the nucleus and subsequently leads to downregulation of JA signalling pathway (Caarls et al. 2015). Downstream signalling of JA is mediated by Coronatine Insensitive 1 (COI1) and Jasmonate-Zim domain (JAZ) (Sheard et al. 2010). Activation of COI1 leads to release of the JA pathway by ubiquitylation and subsequent degradation of JAZ which acts as repressor of JA signalling (Memelink 2009). Studies show SA antagonism of JA signalling occurs downstream of the COI1-mediated ubiquitylation of JAZ, at the level of transcriptional activation of JA-responsive genes (Van der Does et al. 2013). JA-mediated suppression of SA signalling was also observed, however the details of the molecular mechanisms behind this process are not yet known (Brooks et al. 2005; Nomura et al. 2005).

1.8.5 Hypersensitive response and programmed cell death

The Hypersensitive response (HR) is the weapon of last resort in plant defences and refers to a localised form of programmed host cell death (Lam et al. 2001). Although, it differs from animal cell apoptosis, it is still an intrinsically controlled process that requires active transcription and translation apparatus, unlike some forms of necrosis (He et al. 1994). HR can be triggered by various stresses but mostly by infection (Morel and Dangl 1997; Young and Gallie 2000). Its main purpose is to sacrifice the infected cell in order to stop pathogens, especially biotrophs, from spreading to adjacent tissue by removing the source of nutrients (Coll et al. 2011). HR can also be triggered by a wide range of other stresses, including abiotic ones (Mur et al. 2008; Rao et al. 2000). In this thesis, I will be referring to HR exclusively as the phenomenon of programmed cell death caused by ETI response.

1.8.6 PTI-induced programmed cell death

PTI is also capable of triggering host cell death, however it is thought that the cell death pathway used differs from that in the standard HR. PTI leads to strong expression of methyl

jasmonate (MeJA), one of the phytohormones belonging to JA. MeJA proved to be a potent hormone involved in reprogramming the plant towards defence against pathogens. Repka et al. (2001) reported that MeJA alone was sufficient to induce HR-like response in grapevine in the absence of pathogen. Upon induction, MeJA led to downregulation of genes involved in photosynthesis, such as small subunit of RuBisCo and LHCP (Reinbothe et al. 1993; Reinbothe et al. 1997). At the same time, MeJA induces a broad range of proteins including jasmonate-induced proteins (JIPs) which seem to be heavily involved in plant defences. There is a range of currently identified JIPs, such as JIP54 and JIP24, which are allene oxidase synthase and cyclase, respectively, or a lipoxygenase JIP100 (Maucher et al. 2000; Maucher et al. 2004; Voros et al. 1998). JIP23 is only expressed in cereals and it plays a role in response to abiotic stresses and downregulation of photosynthesis (Hause et al. 1994; Hause et al. 1999). Heavily expressed JIP37 localises to cytoplasm, nucleus and vacuole but its function remains unknown (Leopold et al. 1996). MeJA also induces JIP15, a precursor of the thionin JIP6, a fungitoxic molecule localised in plant cell wall and vacuole (Reinbothe et al. 1997; Bohlmann et al. 1988; Andresen et al. 1992). MeJA seems to be particularly important in cereals. For example, it leads to increased resistance to *B. graminis* in wheat via induction of a range of pathogenesis related (PR) proteins (Duan et al. 2014).

In this thesis, I focus on JIP60, due to its relationship with BEC1054 (see Chapter 4). JIP60 is found in barley and it acts as a ribosome inactivating protein (RIP) (Wasternack 2007; Reinbothe et al. 1994b). Interestingly, JIP60 is induced only in response to PTI and not to ETI stimulus (Chang et al. 2016). JIP60 possesses N-glycosidase activity, however relatively little is known about precise mode of action of JIP60. Although the sequence of JIP60 possesses the conserved RIP domain motif, the molecular structure and the location of the active site has not been resolved. Therefore, I hypothesise that RIP domain of JIP60 acts similarly to that of ricin and I set out to test it experimentally (see Chapter 3).

1.9 Hypothesis, aims and objectives of this thesis

I hypothesise that *B. graminis* RALPH effectors associate with the large ribosomal subunit of the host plant cell and obstructs it from interacting with RIPs, hence preventing ribosome inactivation and subsequent host cell death. Thus, RALPH effectors allow the biotrophic pathogen to successfully establish the infection and continue drawing on nutrients from the host cell in order to spread to neighbouring cells and plants.

Aim: To test the JIP60 function and mode of action

Objective 1: To investigate JIP60-mediated necrosis *in vivo* in *Nicotiana benthamiana* via *Agrobacterium*-mediated transient expression

Objective 2: To generate JIP60 mutants to identify the active site residues

Objective 3: To investigate the effects of JIP60 and its mutants on ribosomes using *in vitro* translation system

Aim: To investigate the relationship between JIP60 and BEC1054

Objective 1: To use Bioanalyzer to investigate effects of BEC1054 on total rRNA from MeJA-treated wheat leaves

Objective 2: To investigate the effects of BEC1054 on JIP60-mediated necrosis in *N. benthamiana* using *Agrobacterium*-mediated transient expression

Objective 3: To investigate the effects of BEC1054 on JIP60 in *in vitro* translation system

Aim: To identify the mode of action of BEC1054

Objective 1: To generate BEC1054 mutants to investigate the active site residues

Objective 2: To investigate the effect of BEC1054 mutants on JIP60-mediated necrosis in *N. benthamiana*

Objective 3: To investigate the effects of BEC1054 mutants on JIP60 in *in vitro* translation system

Disclaimer

This PhD thesis contains my work as well as work of undergraduate and postgraduate students under my guidance. Their work and contribution, for which I am grateful, is clearly indicated where appropriate. All of the raw data used but not directly generated by me was reevaluated and analysed by me and all of the figures presented in this thesis were created and assembled by me.

Chapter 2: Materials and methods

2.1 Materials

All materials and chemicals were purchased from Sigma-Aldrich, unless otherwise stated. All water used in the study was obtained through reverse osmosis and autoclaved at 121°C for 15 min, unless otherwise stated.

2.2 Buffers & media recipes

Table 2.1 lists recipes of buffers and media used routinely throughout this study.

2.3 Plants

2.3.1 *Nicotiana benthamiana*

Nicotiana benthamiana plants were cultivated in growth chamber under long-day conditions (16 hrs light, 8 hrs dark) at 24°C and 19°C during day time and night time, respectively. Initially, *N. benthamiana* seeds were grown in compost in a single pot under transparent cover to create a high humidity condition. One-week old seedlings were then transferred to individual pots and grown for three weeks.

2.3.2 *Triticum aestivum*

Triticum aestivum (bread wheat) cultivar 'Cerco' was grown. There were termed the "wild type" plants. Additionally, two transgenic varieties of *T. aestivum* (cv. Fielder) were grown: a homozygote which stably and constitutively expresses *B. graminis* effector BEC1054 as well

Procedure	Name	Recipe
Media	Lysogeny Broth (LB) *Agar	1% (w/v) Tryptone 0.05% (w/v) Yeast extract 1% (w/v) NaCl *1.5% (w/v) agar
Agroinfiltration buffer	MMA	10 mM $MgCl_2$ 10 mM MES (pH 5.6)
Protein extraction buffers	Non-denaturing extraction buffer	0.01% (v/v) Tween-20 50 mM sodium phosphate (pH 8) 300 mM NaCl 1 mM $MgCl_2$ 1% (w/v) PVPP
	Denaturing extraction buffer	7 M Urea 2 M Thiourea 10 mM DTT 0.1% (w/v) CHAPS 1x protease inhibitor
SDS-PAGE buffers	5% Stacking gel	0.1% (w/v) SDS 125 mM Tris-HCl (pH 6.8) 16% (v/v) Polyacrylamide 30% solution 0.1% (w/v) Ammonium Persulphate 0.1% (v/v) TEMED
	12% Separating gel	0.1% (w/v) SDS 400 mM Tris-HCl (pH 8.8) 40% (v/v) Polyacrylamide 30% solution 0.1% (w/v) Ammonium Persulphate 0.04% (v/v) TEMED
	4x Loading buffer	200 mM Tris-Cl (pH 6.8) 8% (w/v) SDS 0.04% (w/v) Bromophenol blue 40% (v/v) Glycerol 2% (v/v) β-Mercaptoethanol
	Running buffer	25 mM Tris-HCl 250 mM Glycine 0.1% SDS
	Coomassie Blue staining	10% (w/v) Ammonium sulphate 0.12% (w/v) Coomassie Brilliant Blue R-250 10% (v/v) Phosphoric acid 20% (v/v) Methanol
Western blotting buffers	Transfer buffer	50 mM Tris-HCl 400 mM Glycine 20% (v/v) Methanol
	TBS-T	50 mM Tris-HCl (pH 7.6) 150 mM NaCl 0.1% (v/v) Tween-20

Table 2.1: List of buffers used in the study and their recipes

as an azygote used as a negative control. The azygote was bred from the same heterozygous parental line as the homozygote but with the purpose to lack the BEC1054 transgene. The transgenic wheat lines were developed as described by Pennington et al. (2019). All bread wheat varieties were grown in plant growth chambers (Fitotron) set to long day light cycle at 20°C and 55% humidity at all time.

2.4 *Blumeria graminis* cultivation

Blumeria graminis f.sp. *tritici* was propagated and maintained on wildtype wheat plants. Seven day old plants were inoculated by 'dusting' with heavily infected plants to spread conidia. In order to achieve and maintain a high density of *B. graminis* infection plants were re-inoculated daily for three consecutive days.

2.5 Bacteria

During this study the following bacterial strains were used: *Agrobacterium tumefaciens* GV3-101 (henceforth Agrobacteria) and *E. coli* Dh5α. The Agrobacteria strain used has an innate resistance to rifampicin and carries a helper plasmid conferring gentamycin resistance.

2.6 Constructs

In this study a number of constructs were used in the *in planta* co-agroinfiltration system. Figure 2.1 shows simplified visualisation of these constructs, whereas Table 2.2 explains the features of the plasmid backbones used in the study. Table 2.3 shows constructs/backbone combinations used in the agroinfiltration study. The constructs used in agroinfiltration study fuse eGFP to the gene of interest in order to allow testing for expression of the construct following the infiltration with either fluorescent microscopy or anti-GFP antibodies in western blotting.



Figure 2.1: Schematic representation of constructs used for agroinfiltrations
The schematics represents what various constructs are being expressed in *N. benthamiana* following an agroinfiltration. There are two constructs containing the BEC1054 effector fused to eGFP either at its N or C terminus, a) and b) respectively. c) represents the construct containing the N-terminal domain of JIP60 responsible for the ribosome inactivating function. The red band represents a deletion within JIP60 of inactivating sequence and its replacement with Met-Leu linker. The construct is also expressed fused with eGFP at its C-terminus. d) represents a construct inducting expression of only eGFP, used as a negative control

Plasmid	Size	Resistance	Features
pCR8	3.8 kbp	spectinomycin	GATEWAY® entry vector
pDONR201	4.5 kbp	kanamycin	GATEWAY® entry vector
pK7WGF2	11.8 kbp	spectinomycin	GATEWAY® destination vector Adds promoter 35S Fuses eGFP at N-terminus of an insert T-DNA brackets for agroinfiltration
pK7FWG2	11.8 kbp	spectinomycin	GATEWAY® destination vector Adds promoter 35S Fuses eGFP at C-terminus of an insert T-DNA brackets for agroinfiltration

Table 2.2: List of plasmids used in the study
The list states the plasmid backbones used in the study including their size, conferred resistance and additional feature

2.7 Agroinfiltrations of *N. benthamiana*

Agrobacteria carrying required plasmid constructs were maintained on LB agar plates with the appropriate antibiotics at concentration of 100 μg/ml (see Table 2.1 & 2.2) and grown at 28°C for up to two days. Afterwards, the bacteria were collected by scooping the cells with a sterile loop into a 1.5 ml tube, washed in 1 ml of H_2O and centrifuged at 14,000 rcf for 1 min. The supernatants were removed and the pellets were resuspended in 1 ml of H_2O, then re-pelleted, the supernatants removed by aspiration. The pellets were then suspended in 1 ml of MMA buffer (10 mM MES, pH 5.7, 10 mM $MgCl_2$) and the optical density at 600 nm

Construct	Transient expression in *N. benthamiana*
pK7WGF2/BEC1054	BEC1054 with N-terminal eGFP
pK7FWG2/BEC1054	BEC1054 with C-terminal eGFP
pK7FWG2/JIP60	JIP60 with C-terminal eGFP
pK7FWG2/GFP	n/a (eGFP only)

Table 2.3: List of constructs used in agroinfiltrations
The list shows the constructs used in the study. It indicates the plasmid backbone and the insert of each construct. It also states what transient expression each of the construct elucidates in *N. benthamiana*

(OD_{600}) was measured. Finally, the Agrobacteria suspensions were diluted with an appropriate amount of MMA buffer to achieve 2 ml suspension of required concentrations prior to infiltrations. The Agrobacteria strains were mixed in order to achieve a uniform co-infiltration. *N. benthamiana* (approximately four-week old) plants were used for agroinfiltrations. Each experiment was repeated at least three to five times, each spaced a week apart. Each biological repeat consisted of three plants. From each plant two leaves (technical repeats), the third and the fourth youngest leaves, were selected for agroinfiltration as they were the most suitable in size and age for the assays, showing the most consistent expression of constructs (Bozkurt T., pers. comm.). Due to individual differences between leaves, each leaf contained the fully independent set of required controls. Each leaf is considered a stand alone repeat.

2.8 Co-agroinfiltration with P19 to increase expression

BEC1054 exhibited relatively poor expression following agroinfiltration into *N. benthamiana*. In order to ensure stronger and more consisted expression, infiltrates were combined with Agrobacterium containing plasmid with P19 (OD_{600}=0.1). P19 is a virally encoded suppressor of gene silencing from tomato bush stunt virus (TBSV) (Voinnet et al. 2003). Addition of P19 substantially increased the expression of other constructs, including BEC1054 (Figure 2.2).

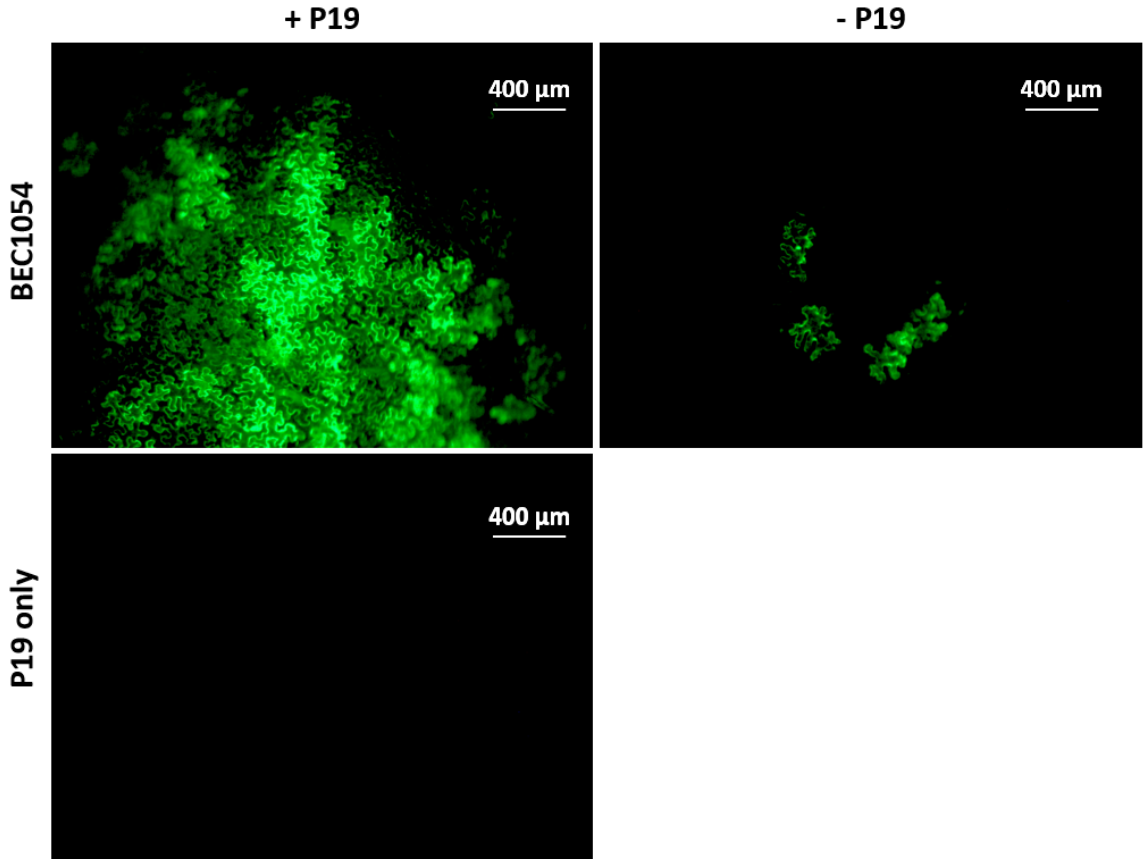


Figure 2.2: Increased expression of BEC1054 by addition of P19
N. benthamiana was agroinfiltrated with either BEC1054-only or along with P19 (OD_{600}=1.0 and OD_{600}=0.1, respectively). At 3 dpi leaf discs were collected from the infiltrated zones and inspected under epifluorescent microscope

2.9 Site-directed mutagenesis of BEC1054

Mutants of BEC1054 effector were created by site-directed mutagenesis. The construct carrying BEC1054 clone on pCR8 vector was mutated via PCR amplification with the mismatched primers (Table 2.4) using *Pfu* polymerase (Thermo-Fisher). The PCR program used was as follows: 95°C for 2 min, followed by 20 cycles of 95°C for 30 sec, 50°C for 30 sec and 72°C for 7 min, finished with 10 min at 72°C. The parental plasmid was digested with *Dpn*I (NEB) restriction enzyme at 37°C for 3 hrs and the product was then ligated with T4 ligase (Promega) at 25°C overnight. The ligation reactions were subsequently used directly to transform chemically competent *E. coli* via standard transformation protocol.

The residue numbering considers the 19-amino acid-long peptide signal that is not included in the recombinant protein. Therefore, the Phe59 and Tyr100 in the mature protein correspond to Phe40 and Tyr81, respectively, in recombinant protein used in the study.

Primer	**Sequence (5' – 3')**	**Tm (°C)**
BEC1054$_{F59A}$ For	C AGA AAA TGT AGA TCC TAT AAT AGC AGT TGC GGG	52
BEC1054$_{F59L}$ For	C AGA AAA TGT AGA TCC TAT AAT TAA AGT TGC GGG	
BEC1054$_{F59}$ Rev	PHO-GAG TAG GGG AAG TAC GAC AGT TTC CAG	
BEC1054$_{Y100A}$ For	C AAC TGA TGA AAA AAC TTC GAG AGC AGA CCC C	52
BEC1054$_{Y100L}$ For	C AAC TGA TGA AAA AAC TTC GAG TAG AGA CCC C	
BEC1054$_{Y100}$ Rev	PHO-GAT CTG GCA ATA AGT GTA CAT TTG TTG AGG G	

Table 2.4: List of primers used in site-directed mutagenesis of BEC1054
The list shows sequences of oligonucleotides used in site-directed mutagenesis of BEC1054. The codons in red represent the site of mutagenesis. Tm indicates the annealing temperature used in thermocycler program. PHO represents a phosphate group

2.10 Site-directed mutagenesis of JIP60ml

Literature search revealed highly conserved residues among ribosome-inactivating protein domain which were also present in alignment with the JIP60 amino acid sequence. Four residues were picked for mutagenesis as potential active site: Tyr96, Glu202, Arg205, and Trp235.

Residue location	Residue before mutation	Residue after mutation	Type of mutation	Predicted effect
96	Tyrosine (Y)	Alanine (A)	Loss-of-function	Loss of function
		Phenylalanine (F)	Isostructural	Loss of function
		Serine (S)	Isofunctional	Partial retention of function
202	Glutamate (E)	Alanine (A)	Loss-of-function	Loss of function
		Aspartate (D)	Isofunctional	Partial retention of function
205	Arginine (R)	Alanine (A)	Loss-of-function	Loss of function
		Lysine (K)	Isofunctional	Partial retention of function
235	Tryptophan (W)	Alanine (A)	Loss-of-function	Loss of function
		Phenylalanine (F)	Isostructural	Partial retention of function
		Proline (P)	Structure disruption	Disruption of structure

Table 2.5: List of JIP60ml mutations and their properties
The list of mutants of JIP60ml create, stating the target residue location, the resulting residue and the predicted effect

These residues were then mutated to investigate their involvement and nature in the ribosome inactivating function, according to the Table 2.5. Primers were designed to perform mutagenesis on JIP60ml clone located on entry vector pDONR201 according to QuikChange I protocol for JIP60ml$_{Y96A}$ and QuikChange II protocol for the remaining mutations (Table 2.6).

QuikChange I mutagenesis was performed by first amplifying the JIP60ml clone in a thermocycler. The template was digested with *Dpn*I restriction enzyme (NEB) at 37°C for 3 hrs and the product was ligated with T4 ligase (Promega) at 25°C overnight. The ligated product was then transformed into chemically competent *E. coli*. The colonies were sequenced to confirm successful mutagenesis.

QuikChange II mutagenesis was performed by amplifying the JIP60ml clone in a thermocycler. The template was digested with *Dpn*I restriction enzyme (NEB) at 37°C for 3 hrs and then the product was directly transformed into chemically competent *E. coli*. The colonies were sequenced to confirm successful mutagenesis.

Name	Sequence (5'- 3')	Tm (°C)
JIP60ml$_{Y96A}$ For	PHO-CGACGACGCCGCAATCATGGG	52
JIP60ml$_{Y96A}$ Rev	CTTCGGATGGCCACCTTGGGATTAGG	
JIP60ml$_{E202A}$ For	GCCTTCTGCGCGGCCGCGAGATTCATCC	55
JIP60ml$_{E202A}$ Rev	GGATGAATCTCGCGGCCGCGCAGAAGGC	
JIP60ml$_{R205A}$ For	GCGAGGCCGCGGCATTCATCCCTGTCTCC	
JIP60ml$_{R205A}$ Rev	GGAGACAGGGATGAATGCCGCGGCCTCGC	
JIP60ml$_{W235A}$ For	GGTCAACTACATCAGGGAGGCGGGTGACTTGTCCACCGC	
JIP60ml$_{W235A}$ Rev	GCGGTGGACAAGTCACCCGCCTCCCTGATGTAGTTGACC	
JIP60ml$_{Y96F}$ For	GAAGCGACGACGCCTTCATCATGGGTTTCAC	
JIP60ml$_{Y96F}$ Rev	GGTGAAACCCATGATGAAGGCGTCGTCGCTTCGG	
JIP60ml$_{Y96S}$ For	CCGAAGCGACGACGCCAGCATCATGGGTTTCACC	
JIP60ml$_{Y96S}$ Rev	GGTGAAACCCATGATGCTGGCGTCGTCGCTTCGG	
JIP60ml$_{E202D}$ For	CGTCGCCTTCTGCGATGCCGCGAG	
JIP60ml$_{E202D}$ Rev	CTCGCGGCATCGCAGAAGGCGACG	
JIP60ml$_{R205K}$ For	CTGCGAGGCCGCGAAATTCATCCCTGTCTC	
JIP60ml$_{R205K}$ Rev	GAGACAGGGATGAATTTCGCGGCCTCGCAG	
JIP60ml$_{W235F}$ For	CGAGGTCAACTACATCAGGGAGTTCGGTGACTTGTCC	
JIP60ml$_{W235F}$ Rev	GGACAAGTCACCGAACTCCCTGATGTAGTTGACCTCG	
JIP60ml$_{W235P}$ For	CAACTACATCAGGGAGCCGGGTGACTTGTCCACC	
JIP60ml$_{W235P}$ Rev	GGTGGACAAGTCACCCGGCTCCCTGATGTAGTTG	

Table 2.6: List of primers used in mutagenesis of JIP60
The list shows sequences of oligonucleotides used in site-directed mutagenesis of JIP60. The codons in red represent the site of mutagenesis. PHO represents a phosphate group at the 5' end

2.11 Transformation of chemically competent *E. coli*

All transformation of *E. coli* in this study were performed on chemically competent bacteria. The bacteria were prepared in house according to the calcium chloride method (Swords 2003). Initially, a 25 μl aliquot of cell suspension was inoculated with 100 ng of required plasmid and was incubated on ice for 30 min. Afterwards, the bacteria were heat shocked at 42°C for 30-45 sec and were allowed to recover on ice for 2 min before 150 μl of LB medium was added and the bacteria were incubated at 37°C for 1 hr. Finally, the bacteria were plated on LB agar plates with the appropriate antibiotic for selection and grown at 37°C till distinct colonies were visible.

2.12 Electroporation of electro-competent Agrobacterium

The electro-competent Agrobacterium was prepared in house according to the protocol by Wise et al. (2006). The bacteria in 50 μl aliquots were inoculated with 100 ng of desired plasmid and electroporated with MicroPulser (BioRad) using the Agrobacterium specific program. The bacteria were allowed to recover on ice for 15 min before 250 μl of LB medium were added and the bacteria were incubated at 28°C while shaking for 1 hr. Afterwards, the Agrobacterium were plated on an appropriate selective LB agar plates.

2.13 Analysis of aniline-treated total RNA profiles obtained from MeJA-treated wheat

One-week old seedlings of either BEC1054 azygous or homozygous transgenic wheat were inoculated with *B. graminis* daily for three days to achieve high density of infection. Corresponding pots of uninfected seedlings were grown alongside in a separate translucent enclosure as control plants. Afterwards, the first leaves were collected from the plants and treated for four days in 15 cm diameter Petri dishes containing 100 ml of H_2O with 40 μM of methyl-

jasmonate (MeJA; Sigma-Aldrich) and 0.1% (v/v) DMSO (Sigma-Aldrich). The leaves were ground in liquid nitrogen with mortar and pestle, and total RNA was extracted from the samples with the RNeasy mini extraction kit (Qiagen). The RNA samples were then treated with 12% (v/v) aniline at 60°C for 3 min. The reaction was terminated with Stop solution (5 M ammonium acetate, 100 mM EDTA, made with DEPC-treated H_2O). The RNA was recovered via ethanol precipitation and analysed with RNA Nano II chips (Agilent) using Agilent 2100 Bioanalyzer.

2.14 Protein extraction from plants

About 150 mg of plant material, or up to eight 10 mm in diameter leaf disks, were ground with mortar and pestle in liquid nitrogen to fine powder and then collected in 1.5 ml centrifuge tube. 150 μL of either native or denaturing protein extraction buffer was added along with glass beads. The tube was vortexed for 10 sec, then allowed to settle on ice for 7 min, and then vortexed again for 10 sec. Subsequently, the tube was centrifuged at 4°C at 20,800 rcf for 30 min. The supernatant was carefully transferred into a fresh, pre-chilled 1.5 ml centrifuge tube, and then centrifuged again at 4°C at 20,800 rcf for 30 min. The resulting supernatant constituted the protein extract.

2.15 SDS-PAGE

SDS-Polyacrylamide gels were cast using Mini-PROTEAN Tetra Vetical Handcast system (Bio-Rad) according to recipes in Table 2.1. The protein samples were mixed with 4x Loading buffer and denatured at 95°C for 10 min and subsequently loaded on the gel. The gels were resolved using Mini-PROTEAN Tetra Vertical system (Bio-Rad) at 100 V for approximately 90 min in 1x Running buffer.

2.16 Western blotting

Protein transfers onto a PDVF membrane (Amersham) were performed in a Mini Trans-Blot cell (Bio-Rad) at 100 V for 60 min in a 1x Transfer buffer. Subsequently, the membrane was blocked in 5% (w/v) dry milk in TBS-T shaking for 60 min at room temperature. Then the membrane was incubated in 5% (w/v) dry milk in TBS-T with the primary antibody overnight shaking at 4°C. The membrane is then washed in four washes with TBS-T shaking at room temperature for 10 min and then it is incubated with secondary antibody in 5% (w/v) dry milk in TBS-T at room temperature for 60 min. The membrane is then washed in four washes with TBS-T at room temperature shaking for 10 min. The detection is performed using SuperSignal West Dura Substrate (ThermoFisher) according to manufacturer's description. The chemiluminescence is visualised using LAS-3000 imager (FujiFilm).

2.17 *In vitro* Transcription/Translation assay

The *in vitro* transcription/translation assays were performed using TnT Coupled Reticulocyte Lysate Systems (Promega). The constructs for the study were amplified as linear PCR products with T7 promoter attached to the 5' end (Table 2.7). The 5 μl reactions were incubated at 30°C for 90 min. Subsequently, the 5 μl of the reactions were added to 50 μl of Luciferase Assay Reagent (Promega) in a flat bottom 96-well black plate and then the luminescence was immediately measured with Tecan illuminometer. Five consecutive measurements with 1000 msec attenuation were taken with a 10 sec break in between each one.

2.18 Statistical analysis

All statistical analysis was performed using R scripting language (R Core Team 2013). The precise approach of each statistical analysis is outlined in the relevant result sections. Three levels of statistical significance were distinguished: * for $p<0.05$, ** for $p<0.01$ and *** for $p<0.001$.

Primer	Sequence (5'-3')	Tm (°C)
T7_BEC1054 Forward	TAATACGACTCACTATAGGGATGGCAGCTTATTGGGATTGTGATGG	52
T7_BEC1054 Reverse	CTAGCCCTCAACAAAAGTACACTTATTG	
T7_JIP60 Forward	TAATACGACTCACTATAGGGATGGCTTTAGACAAAGTTGCTCCCATCG	52
T7_JIP60 Reverse	TTTTTTTCTAGTCCGCCATGTTGCTTCGGATGACT	
T7_rRNA Forward	TAATACGACTCACTATAGGGACCAAGGAGTCTGACATGCGTGC	
T7_rRNA Reverse	CGTCTCCGGACTTCCTAACGTCG	

Table 2.7: List of primers for amplification of genes of interest with T7 promoter
This table shows a list of primers used to amplify genes of interest with T7 promoter attached. The sequences in green represent the added T7 promoter. The sequences in orange represent added START codon whereas sequences in red STOP codons. Sequences in blue show addition of poly-A tail

Chapter 3: Properties of N-terminal RIP domain of JIP60

3.1 Introduction

3.1.1 Ribosome-inactivating proteins (RIPs)

Ribosome-inactivating proteins (RIPs) have been studied for a long time. Use of castor beans for medicinal purposes has already been documented in ancient Egypt and Greece (Olsnes 2004). First identification of the active ingredients and description of ricin and abrin as proteins by Paul Ehrlich dates back to late 19th century (Ehrlich 1891a; Ehrlich 1891b) cited in Bolognesi et al. (2016). The interest in RIPs resurfaced when it was demonstrated that their cytotoxic properties make them potential antitumor agents and they could be used in cancer treatment (Lin et al. 1970). They were more recently suggested for clinical use as immunotoxins by conjugation with targeted antibodies (Pastan et al. 1992). The most studied RIP by far is ricin, derived from *Ricinus communis L.* (castor bean), which is often used as a model RIP, while other proteins of this family remain mostly neglected. The vast variety in RIPs and the emergence of unconventional types call for more in-depth studies of other examples than ricin. Especially, since studies showed distinct interactions of RIPs with ribosomal proteins, leading to changes in both their function and specificity (Hudak et al. 1999; McCluskey et al. 2008; Chan et al. 2007).

The evolutionary origin of RIPs is debated. It was suggested they evolved very early on from a common ancestor, however lack of any identified RIPs in Archaea puts this hypothesis in doubt (Lapadula et al. 2013). More recent theory is that RIPs actually first emerged in plants and only then spread to other kingdoms via horizontal gene transfer (Zaeytijd and Damme 2017). This hypothesis is supported by the fact that even though RIPs can be found in bacteria, fungi and even some animal groups like insects, the vast majority of identified

RIPs are in plants (Schrot et al. 2015). RIPs are found in both monocots and dicots but are far from being ubiquitous. For instance, there are no identified RIPs in *Arabidopsis thaliana* (Zaeytijd and Damme 2017). Interestingly, there are far more RIPs in monocots than in dicots, and they seem to be particularly favoured by cereals, where they are proportionally the most prevalent.

3.1.2 RIP structure & mode of action

RIPs seem to be poorly conserved both at the gene and protein sequence level. Their primary sequence alignment similarity varies from 80% to as little as 15% (Bolognesi et al. 2016). Despite the lack of sequence conservation, they all share a common fold that can be roughly divided into two subdomains: the larger N-terminal subdomain consisting of six α-helices and a six-stranded mixed β-sheet (Figure 3.1a: blue ellipsis), and the smaller C-terminal subdomain with an anti-parallel β-sheet and a single α-helix (Figure 3.1a: orange ellipsis) (Shi et al. 2016; Virgilio et al. 2010).

Based on studies on ricin, RIPs are proposed to act as N-glycosidases. The ribosome inactivation is achieved by depurination of a ubiquitously conserved adenine within a GAGA motif on the large ribosomal subunit RNA (Schrot et al. 2015). The target adenine of the GAGA motif is located on a part of rRNA often referred to as α-sarcin/ricin loop (SRL) (Figure 3.2) (Stirpe et al. 1992; Endo and Tsurugi 1987; Dunaeva et al. 1999). The depurination of the adenine prevents elongation factors from binding to the ribosome, hence arrests the translation at the elongation step (Lancaster et al. 2008). This leads to irreversible ribosome degradation, protein translation inhibition and the subsequent cell death (Narayanan et al. 2005). Although RIPs target predominantly SRL, they are often capable of depurination of multiple sites on a ribosome (Barbieri et al. 1992). RIP-ribosome interaction seems to be facilitated by presence of ribosomal proteins (Hudak et al. 1999; McCluskey et al. 2008; Chan et al. 2007). That is supported by the fact that depurination of naked rRNA was shown to be much slower than that of a complete ribosome (Endo and Tsurugi 1987). Moreover, majority of RIPs show capability to depurinate not only RNA but also DNA and poly(A) tails (Barbieri 1997). Some studies showed that some RIPs may also possess other functions, such

as DNase, RNase or even phosphatase and chitinase activity; however many of those results were later attributed to impurities (Zaeytijd and Damme 2017).

Based on research done on ricin, a RIP mechanism of action was proposed (Figure 3.1b) (Virgilio et al. 2010; Ho et al. 2009; Wong et al. 1994; Kim and Robertus 1992). In order to hydrolyse the glycosidic bond between the purine and the ribose ring of the target adenine on SRL, a negatively charged residue (an electron donor) and a positively charged residue (an electron acceptor) are required (Chen et al. 2000; Monzingo and Robertus 1992). Cytoplasm of plants usually has a slightly alkali pH, around 7.4-7.5 (Gout et al. 1992). Under these condition, arginine is most likely to be positively charged, whereas a glutamate is negatively charged (Fitch et al. 2015; Henchoz et al. 2007). Both of these residues are found conserved in majority of known RIPs (Lapadula et al. 2013). RIPs tend to be extremely effective. According to Eiklid et al. (1980) a single ricin molecule is sufficient to cause cell death when it reaches the intracellular target.

3.1.3 Versatility of RIPs

Despite the simple structure and usually a singular enzymatic activity, RIPs tend to be utilised by plants in many ways. Various functions can be, for instance, achieved by expression with a temporal and special distinction (Nielsen and Boston 2001). For example, RIP30 in barley is expressed in the seed germ but not in a grown plant whereas JIP60 is expressed in the tissue of the mature plant (Leah et al. 1991). Moreover, RIP30 seems not to be able to affect conspecific ribosomes. One of the RIPs' main role is defence against infection and attack. Many plants express and store RIPs in seeds to act as antifungal proteins. For example, barley seed germ RIPs overexpressed in wheat led to increased protection against *B. graminis* infection (Bieri et al. 2003). Overexpression of barley RIP also conferred increased protection in transgenic tobacco against fungal infection (Logemann et al. 1992). In case of fungal infections, a RIP can either be a secreted antifungal protein or it can lead to host cell death, this way collapsing the infected plant cell, hence preventing the infection from spreading (Stirpe 2013; Vigers 1991). Moreover, other RIPs have also antiviral properties. For instance, pokeweed antiviral protein (PAP) was found to confer both antiviral and antifungal resistance in

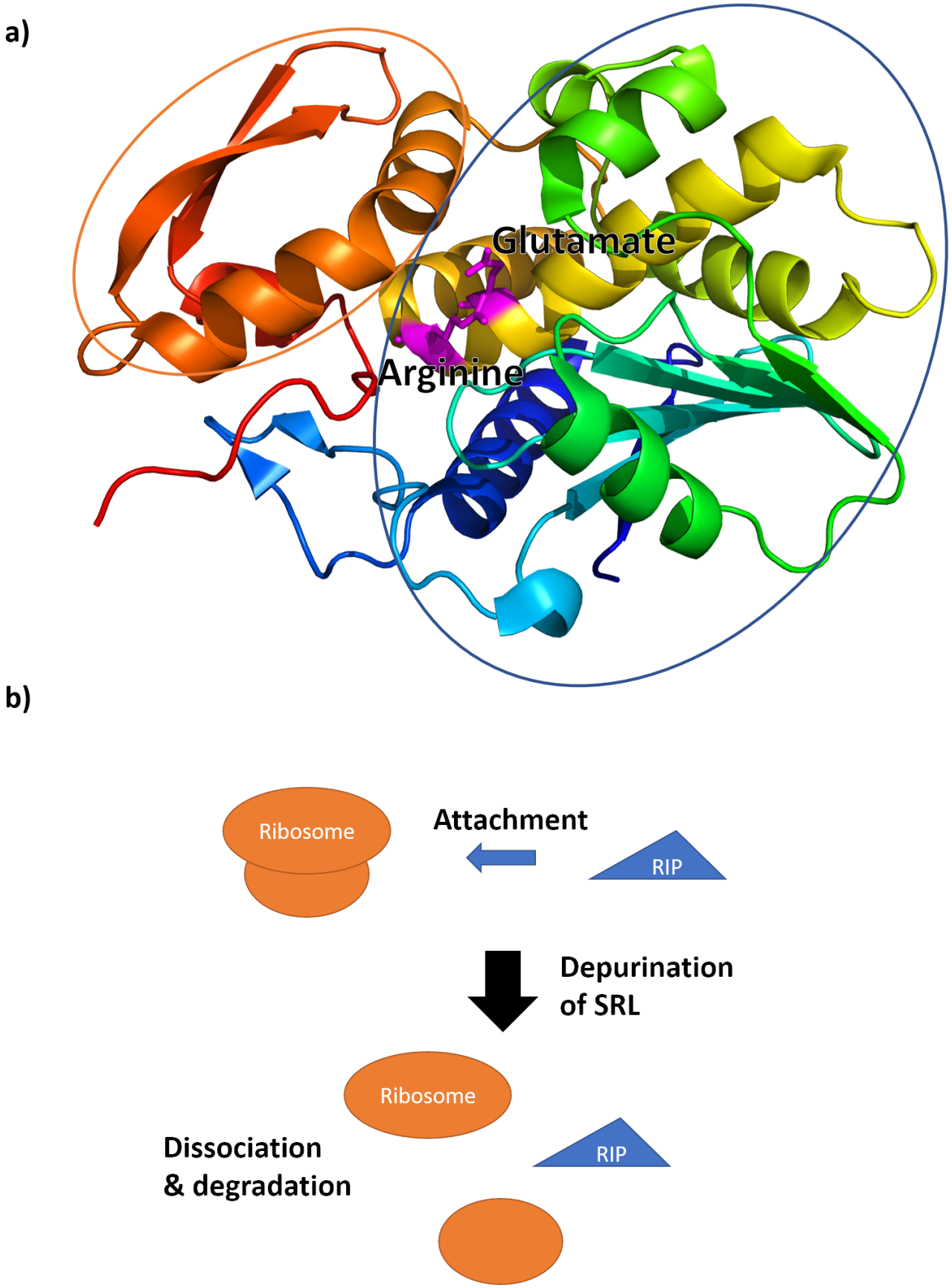


Figure 3.1: Molecular structure of RIP domain of ricin and mechanism of action
a) Molecular structure of the RIP domain of ricin (PDB ID: 2P8N). Blue ellipsis marks the N-terminal subdomain, whereas the orange ellipsis shows the C-terminal subdomain. Magenta residues highlight the two catalytic residues: Glutamate and Arginine. b) Schematic of the mode of action. RIP associates itself with ribosome, where it targets and depurinates the conserved adenine within the SRL sequence. This leads to dissociation of the ribosomal subunits and to their subsequent disintegration. That causes inhibition of translation which leads to cell death

transgenic plants (Hudak et al. 1999; Krivdova et al. 2014; Di and Tumer 2015). Their ability to interact and cleave RNA can be utilised by plants to directly defend themselves from viral infection by cleaving viral RNA (Krivdova et al. 2014). Some RIPs are even involved in defence against herbivorous insects. For example, inactivation loop of proRIP2 in maize can be excised by proteinases found in midgut of a caterpillar, leading to maturation of RIP2 and extensive damage to caterpillar gut epithelium (Chuang et al. 2014).

There are, however, other functions that plant RIPs are involved in. Tritin, a RIP from wheat, plays role in natural senescence in development of plant coleoptiles (Sawasaki et al. 2008). Other studies showed that some RIPs, such as OsRIP18 from *Oryza sativa*, are involved in reprogramming of translational machinery to respond to abiotic stresses like drought and salinity (Jiang et al. 2008; Jiang et al. 2012). Barley and maize seed germ RIPs have also been suggested to act as a potential methionine and lysine storage protein, as they have either evolved not to affect conspecific ribosomes or are expressed and stored in their inactive form, respectively (Leah et al. 1991; Habben et al. 1993).

3.1.4 Classification of RIPs

Classification of RIPs is a contentious issue. One view is that there are two distinct canonical RIP types. RIPs of type I, also known as type A, consist solely of a single chain peptide with N-glycosidase activity, for example RIP30 from barely or tritin from wheat (Schrot et al. 2015). The type IIs (syn. type AB) have two distinct domains: the N-terminal N-glycosidase, responsible for ribosome inactivation and the C-terminal lectin domain, necessary for transmembrane trafficking. The prime example of type II is ricin.

Conversely, some interesting RIPs do not fit into either of these two types. These aberrant RIPs have been so far solely identified in cereals and there is a growing consensus these RIPs, with examples such as maize RIP1 (syn. b-32) and JIP60 from barley, should have a division of their own, that is type III (Schrot et al. 2015; Zaeytijd and Damme 2017). What makes them stand out from the other RIPs, is their unusual architecture. RIP1 from maize is synthesised as an inactive proenzyme which needs proteolytic processing for activation, hence

it is sometimes classified as a "peculiar type I" (Schrot et al. 2015). Barley JIP60 also needs proteolytic processing to be activated but it also possesses a C-terminal domain that is not a lectin, so it cannot be classified as type II (Reinbothe et al. 1994b). RIPs such as maize RIP1 and JIP60 developed a unique "safety feature" in the form of an inactivating loop which needs to be proteolytically excised for the protein to be activated, so far seen only in RIPs found in cereals (Zaeytijd and Damme 2017). The emergence of the inactivation loop is most likely due to the fact that cereals possess many different RIPs, often expressed in various organs or at different developmental stages, so control of their activity is crucial (Nielsen and Boston 2001; Stirpe 2013). Moreover, a presence of an inactivation loop makes sense in proteins involved in immune response, as it allows the production and storage of a "ready-to-go" protein which can then be rapidly activated when faced by a threat, rather than go through the entire process of expression and translation.

As more RIPs with unusual origin of C-terminal domain are discovered, it is necessary to rethink the current classification. Zaeytijd and Damme (2017) propose designation of type AN where "N" stands for variable domains. For instance, RIPs from AX lineage differ from AB lineage. The AB tend to be secreted, whereas AX are synthesised on free ribosomes and lack the signal peptide, so the protein stays in the cytosol. That suggests a different function from the AB type (Shang et al. 2014; Peumans et al. 2014).

3.1.5 RIPs in cereals

RIPs seem to be particularly important in cereals, as cereals have the highest proportion of RIPs in plant kingdom (Stirpe 2013). Cereal RIPs exhibit an enhanced rate of evolution, resulting in a large and heterogeneous family, with chimeric forms not seen outside the clade (Zaeytijd and Damme 2017). *Oryza sativa* boasts more than 30 paralogs of RIPs in its genome (Jiang et al. 2008). As mentioned before, type III RIPs have only been found in cereals and many RIP domain genes, the "A" component of the proteins, in *Poaceae* family are of unknown origins, suggesting independent evolution (Peumans et al. 2014). Moreover, that family exhibits some unique lineages of C-terminal domain emerging from AX lineage, designated AC, AP and AD (Zaeytijd and Damme 2017). Cereal RIPs also show more versatile mode of

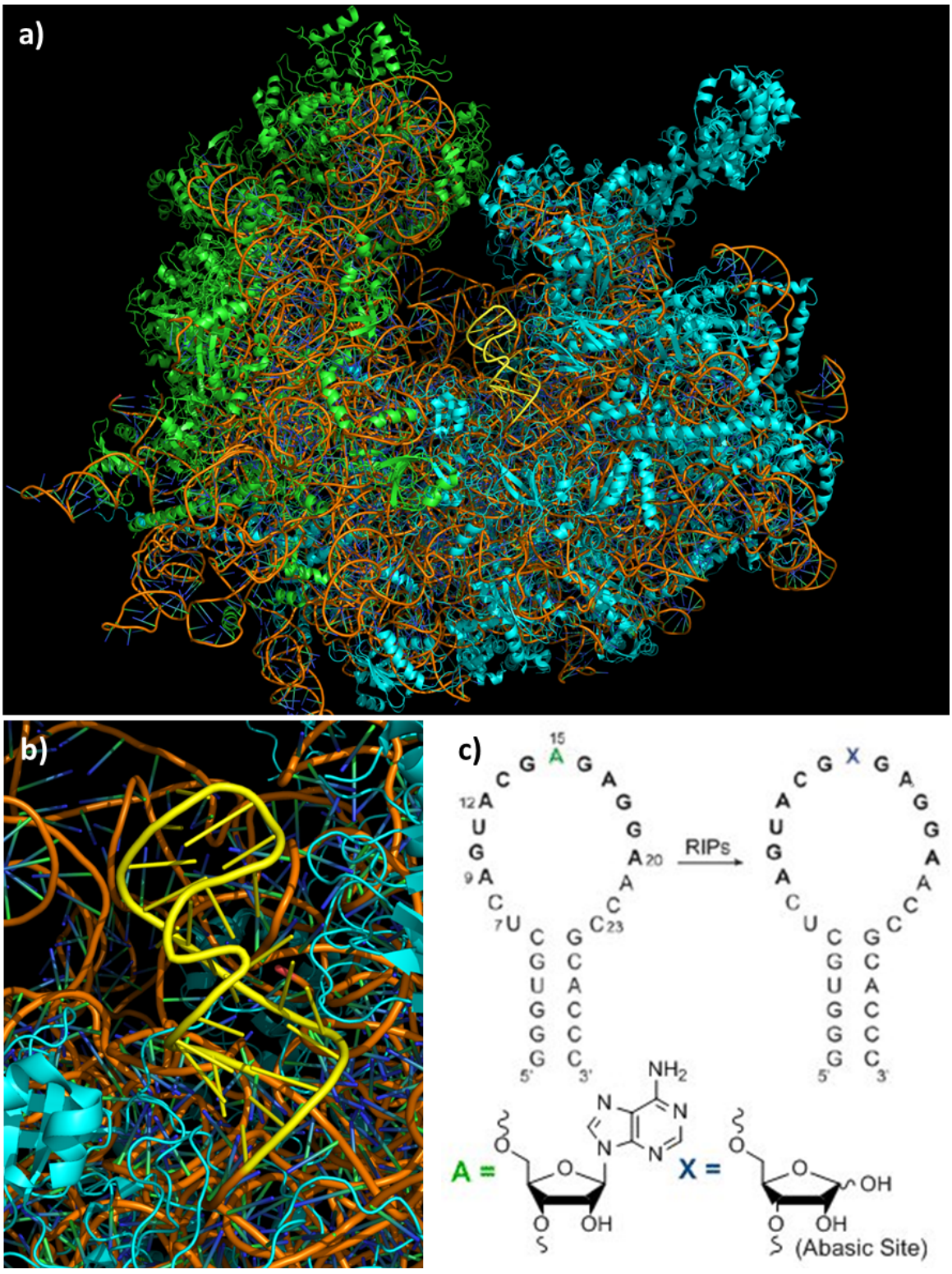


Figure 3.2: Molecular model of wheat ribosome and of the α-sarcin/ricin loop
a) The molecular model of complete wheat ribosome. The green and cyan molecules represent ribosomal proteins of the small and the large ribosomal subunits, respectively. The orange molecules represent the ribosomal RNA constituents of a ribosome. The yellow element shows the α-sarcin/ricin loop (SRL). b) Close-up on the molecular representation of SRL. c) Diagram of the consensus on sequence of SRL. The conserved within SRL GAGA motif contains the adenine base that is targeted by RIPs; depurination of this base leads to instability of the rRNA. (Molecular structure of the wheat ribosome resolved by Armache et al. (2010); the images for a) and b) were generated using PyMol software (Schrodinger LLC 2010); the cartoon of SRL depurination adapted from Srivatsan et al. (2008))

actions. For example, in addition to the inactivation loop featured in type III RIPs, some cereal RIPs evolved another unique control mechanisms. For example, bRIP1 possesses a "switch region" i.e. a stretch of amino acids within the gene, with its location corresponding to the inactivation loop seen in maize RIP1. However, for the protein to become enzymatically active, the "switch region", instead of being proteolytically cleaved off, undergoes a conformational change from a helix to a loop structure, depending on whether it is bound to AMP or an adenine, respectively (Lee et al. 2012). Moreover, while classic RIP interact with ribosomes due to hydrophobic forces, the maize RIP1 functions based on electrostatic forces created by the KKKK motif which was not identified in any other RIP (Wong et al. 2012). The more unusual RIP functions, such as use of the proteins as lysine storage in seeds, are so far encountered only in cereals.

3.1.6 Barley RIP jasmonate-induced protein 60 (JIP60)

This study focuses on JIP60 found exclusively in barley. Two paralogous genes of JIP60 were reported in barley: JIP60 and JIP60-like. The two genes are located in barley genome nearby to QTLs such as powdery mildew resistance, boron sensitivity and resistance to spot blotch (Rustgi et al. 2014). The expression of JIP60 is initiated by MeJA, a plant defence hormone 'master switch', which responds to stress, predominantly fungal infection (Chaudhry et al. 1994). This peculiar RIP is classified as a type III. Its N-terminal domain is an N-glycosidase which contains the tell-tale 17 amino acid long shigatoxin motif of a RIP, whereas its C-terminal domain resembles eukaryotic initiation factor IV (eIFIV) with a currently unknown function (Chaudhry et al. 1994). More recent studies suggest that C-terminal domain of JIP60 increases abundance of other JIPs by causing preferential translation of JIP transcripts (Rustgi et al. 2014). The JIP60 protein lacks a signal peptide hence upon translation it is predicted to be localised in cytoplasm (Hause et al. 1994). JIP60 was also confirmed to exhibit N-glycosidase activity *in vivo* (Dunaeva et al. 1999). Studies showed that JIP60 has two potential modes of action (Figure 3.3a). In its full form, upon activation, it acts as ribosome dissociation factor, leading to reversible ribosome inhibition. Interestingly, the JIP60-mediated ribosome dissociation is only possible in plants that had a prolonged exposure to

MeJA (Reinbothe et al. 1994b). When the C-terminal domain is cleaved off and the inactivation loop on the N-terminal is proteolytically excised, the RIP domain becomes fully activated, leading to degradation via depurination of SRL and permanent ribosome inactivation (Rustgi et al. 2014).

3.1.7 Aims

I hypothesise that JIP60 is a PTI-mediated RIP which plays a crucial role in barley defence against biotrophic fungal pathogens, such as *Blumeria*. Moreover, this study aims to confirm the active site residues and the accuracy of the molecular structure prediction.

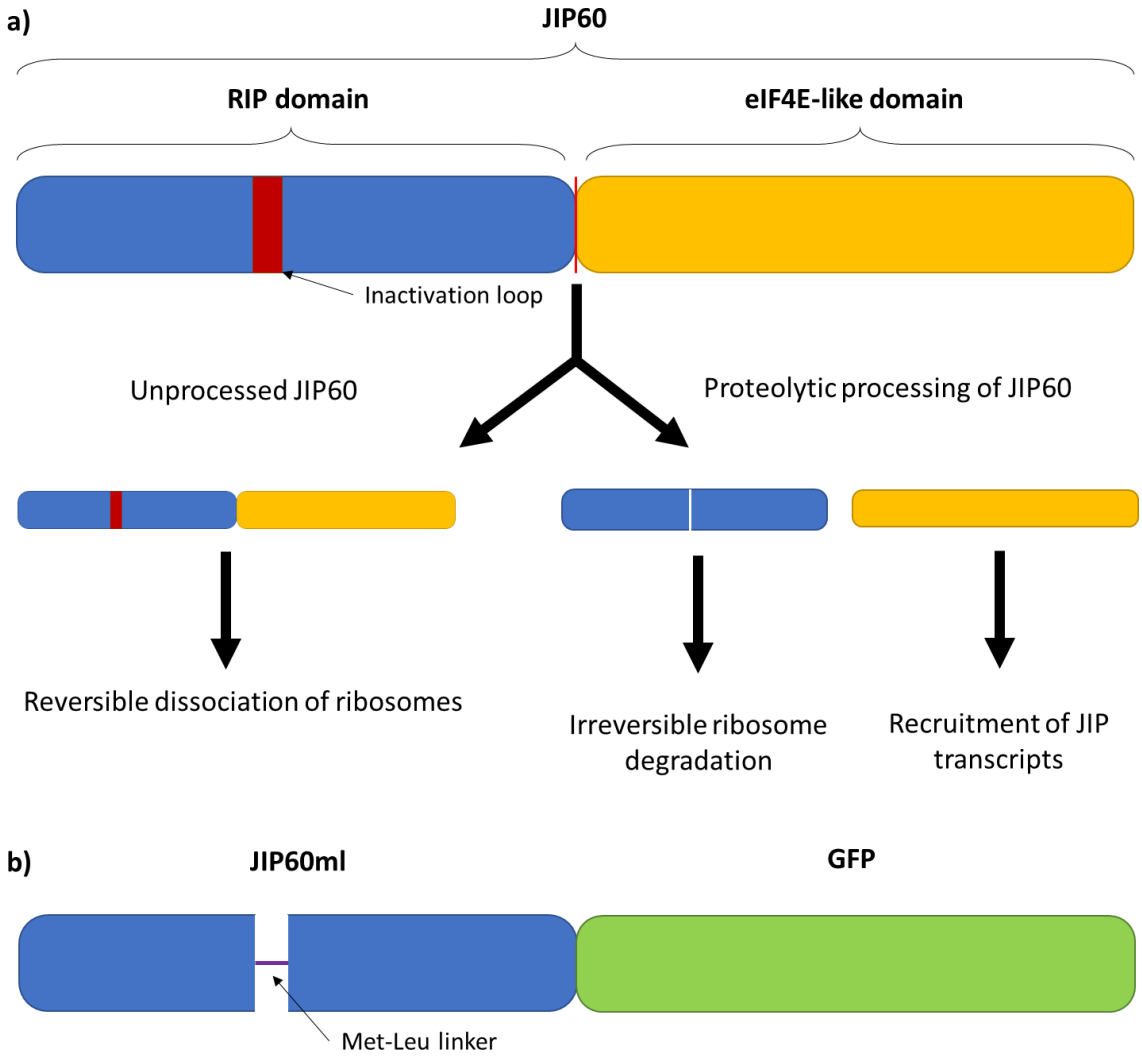


Figure 3.3: Cartoon representation of JIP60 processing and function in barley
a) JIP60 in barely is expressed as a single protein of 30 kDa comprised of two domains: the N-terminal RIP domain (blue) and the C-terminal eIF4E-like domain (yellow). In addition, the RIP domain contains the inactivation loop (red). JIP60 has two distinct mode of actions. First, the unprocessed JIP60 can cause reversible dissociation of ribosomes, thus temporarily inhibits translation. Second, JIP60 undergoes proteolytic processing where the inactivation loop is excised, and the C-terminal domain is cleaved off. At this stage, the activated RIP domain causes irreversible ribosome degradation, thus leading to cell death. The eIF4E domain's function is still uncertain, however, studies suggest it plays a role in recruitment of other JIP transcripts for preferential translation (Reinbothe et al. 1994b; Rustgi et al. 2014). b) This study focuses on the RIP domain of JIP60 only, hence an active version of the domain was created. JIP60ml is the N-terminal domain of JIP60 with its inactivation loop excised and the two fragments are fused with a Met-Leu linker (purple). In case of agroinfiltrations performed in this study, the JIP60ml was in addition fused with GFP (approximately 27 kDa in size) at its C-terminal.

3.2 Results

3.2.1 JIP60 as member of the ribosome inactivating protein family

I carried out a series of bioinformatics-based investigations to test if JIP60 can be classified as a RIP. Firstly, the amino acid sequence of the N-terminal domain of JIP60, predicted to act as a RIP, was used as a query using a HMMER algorithm to find homologous protein sequences in the Pfam database (EMBL-EBI). The HMMER algorithm uses profile Hidden Markov model (HMM) statistical approach to search for protein similarity based on amino acid sequence within given database (Finn et al. 2015). The algorithm recognised the amino acid sequence as an rRNA N-glycosidase (GO: 0030590). Also, based on the JIP60 amino acid sequence as the query, a family of 815 sequences classified as RIPs (PF00161) was found. Interestingly, within that family the RIP domain on average covered only 46.03% of the protein sequences, suggesting the presence of an additional domain. Therefore, most of the sequences in the family seemed to belong to Type II (presence of extra domain), rather than Type I (single domain). Similarly to the nucleic acid sequence similarity, the RIP domain family showed poor amino acids sequence conservation, with average identity of the full family alignment of 18%. However, ClustalO alignment showed that despite poor overall sequence conservation, there were particular residues that showed high level of conservation across the family (Figure 3.4a). Subsequently, an HMM logo graph was plotted to highlight the most conserved residues (Figure 3.4b). I therefore hypothesised, four of these residues (Tyr96, Glu202, Arg205 and Trp235) may be important for the function, hence they were selected for site-directed mutagenesis in this study. Then, I tested the amino acid sequence of the JIP60 N-terminal domain by protein fold prediction using the Phyre^2 tool with "intense" setting (Kelley et al. 2015). The sequence was predicted with 100% confidence to assume RIP-like fold, with sequence identity to known structures ranging from 17% to 29%. The predicted structure was modelled using the PyMOL molecular graphics system software (Schrodinger LLC 2010). The predicted structures of the wild type JIP60 (JIP60 WT) with inactivation loop intact, and of the recombinant with the inactivation loop excised (JIP60ml) were then compared (Figure 3.5a and 3.5b, respectively). The four residues conserved within the RIP

family highlighted by the HMM logo clustered into a single region of the protein, suggesting they might in fact be the active site of JIP60. Interestingly, in the predicted structure of JIP60 WT, the sidechains of the predicted active site pointed away from the centre and each other, whereas in the predicted structure of JIP60ml where the inactivation loop is absent, those sidechains were pointing towards the centre (Figure 3.5c and 3.5d, respectively). This predicted conformational change suggests the potential mechanism of JIP60 switching from inactive to active state, caused by inactivation loop processing seen *in vivo*. It is worth noting that conformational change observed here is only a computational prediction based on physical constraints of individual residues in the protein sequence, derived from similar molecular structures. This change has to be confirm experimentally, e.g. through X-ray crystallography.

3.2.2 Mode of action of JIP60

Considering the fact that the JIP60 N-terminal domain conforms to characteristics of RIPs and taking into account the localisation of the conserved charged residues Glutamate 202 (E202) and Arginine 205 (R205), along with the hydrophobic residues Tyrosine 96 (Y96) and Tryptophan 235 (W235), I propose the chemical mechanism of RNA depurination, based on the mechanism employed by ricin (Endo and Tsurugi 1987). In this model, I suggest that E202 and R205 play the catalytic function of hydrolysis of the glycosidic bond between the purine and the RNA backbone, whereas Y96 and W235 act as stabilisers of the rRNA-protein interaction.

At the usual pH 7.4-7.5 within a plant cell, E202 and R205 should be negatively and positively charged, respectively (Kurkdjian and Guern 1989). This difference in charge would allow splitting of water molecule into a proton (H^+) and hydroxide anion (OH^-), initiating the hydrolysis (Figure 3.6a). If the rRNA molecule is being stabilised by the Y96 and W235, the free electrons from the hydroxide anion are able to 'attack' the glycosidic bond between the purine and the RNA backbone, attaching the OH group onto the ribose (Figure 3.6b). Consequently, the free proton would then be able to stabilise the purine by associating itself with the exposed nitrogen on the purine itself (Figure 3.6c). That concludes the depurina-

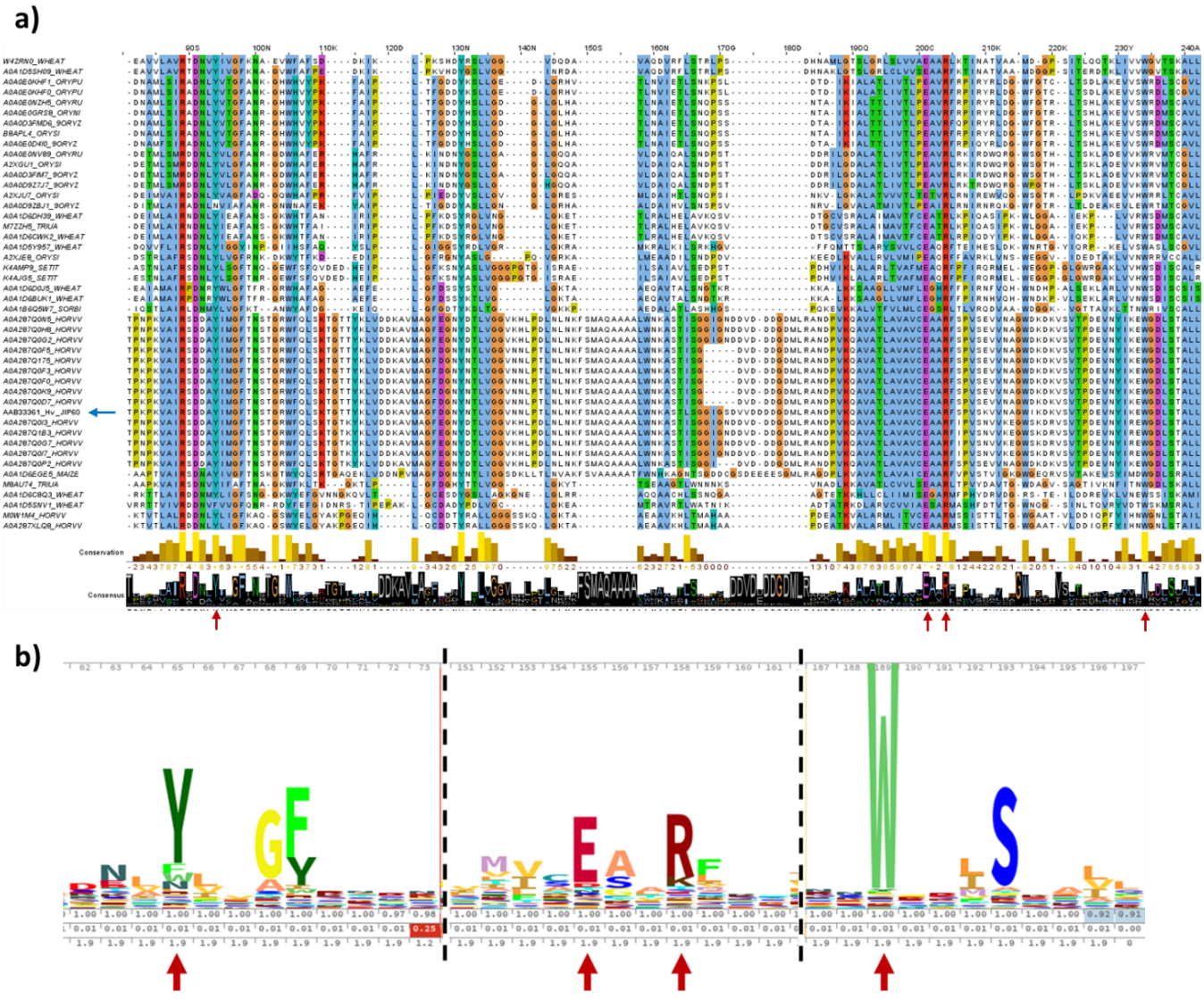


Figure 3.4: Alignment of amino acid sequences and HMM logo representation of RIP domain family
a) Amino acid sequence of JIP60 RIP domain (blue arrow) was used as the query in Plant Ensembl database using HMMER web tool. The sequence was recognised as a part of RIP family (PF00161) consisting of 815 sequences. All of these sequences were then aligned and sorted into neighbour joining tree using BLOSUM62 algorithm. This figure represents a small subset of 45 sequences most closely homogeneous to the JIP60 sequence. The residues are coloured according to the Clustal convention. Red arrows point to residues of interest which represent Tyr96, Glu202, Arg205 and Trp235 on JIP60 RIP domain. b) Figure shows logo representation using hidden Markov model (HMM) of residues conserved in RIP domain family. The amino acid sequence of JIP60 RIP domain was used as the query for this alignment. Red arrows represent residues selected for site-directed mutagenesis.

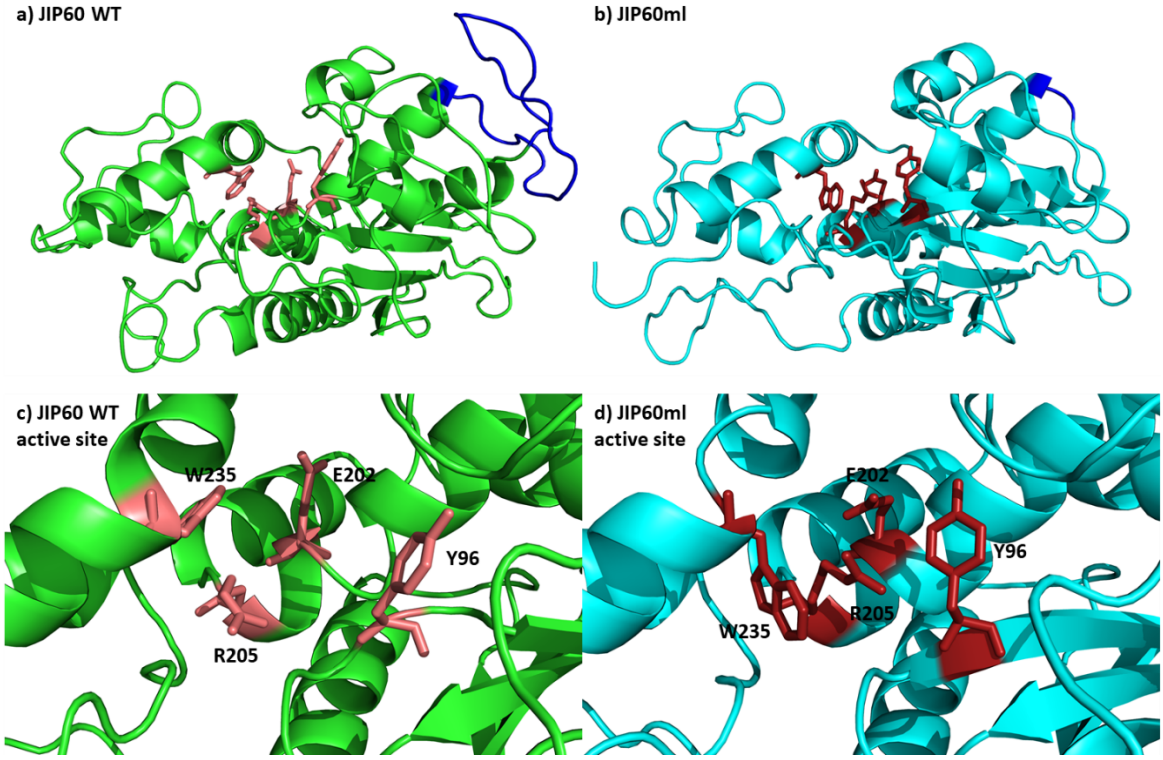


Figure 3.5: Predicted molecular model of the N-terminal RIP domain of JIP60
a) The model represents predicted molecular structure of the wild type N-terminal RIP domain of JIP60 found in barley. The blue region represents the inactivation loop that needs to be excised for JIP60 to be functional. The residues coloured in pink represent the predicted preserved active site. b) This model represents the predicted N-terminal domain of JIP60 based on sequenced deprived of the inactivation loop, replaced with a short Met-Leu linker, JIP60ml. The dark blue region represents the Met-Leu linker. The deep red residues show the predicted JIP60 active site based on the conserved nature of the residues. c) Close-up of the predicted active site of the WT N-terminal domain of JIP60. The pink residues represent the residues which may take active part in JIP60 function. When the inactivation loop is present, the active site residues are predicted to converge in a close proximity, however, their sidechains seem to be point away from one another, suggesting an inactive conformation. d) Close up on the predicted active site of the N-terminal domain of JIP60ml. The deep red residues represent the residues predicted to take active part in JIP60 function. When the inactivation loop is excised, the active site residues are predicted to converge in a close proximity, similarly to the WT, however, their sidechains point inwards, suggesting an active conformation. All models were acquired using intense Phyre^2 predictive algorithm.

tion process and both the purine and the now weakened RNA backbone are released (Figure 3.6d).

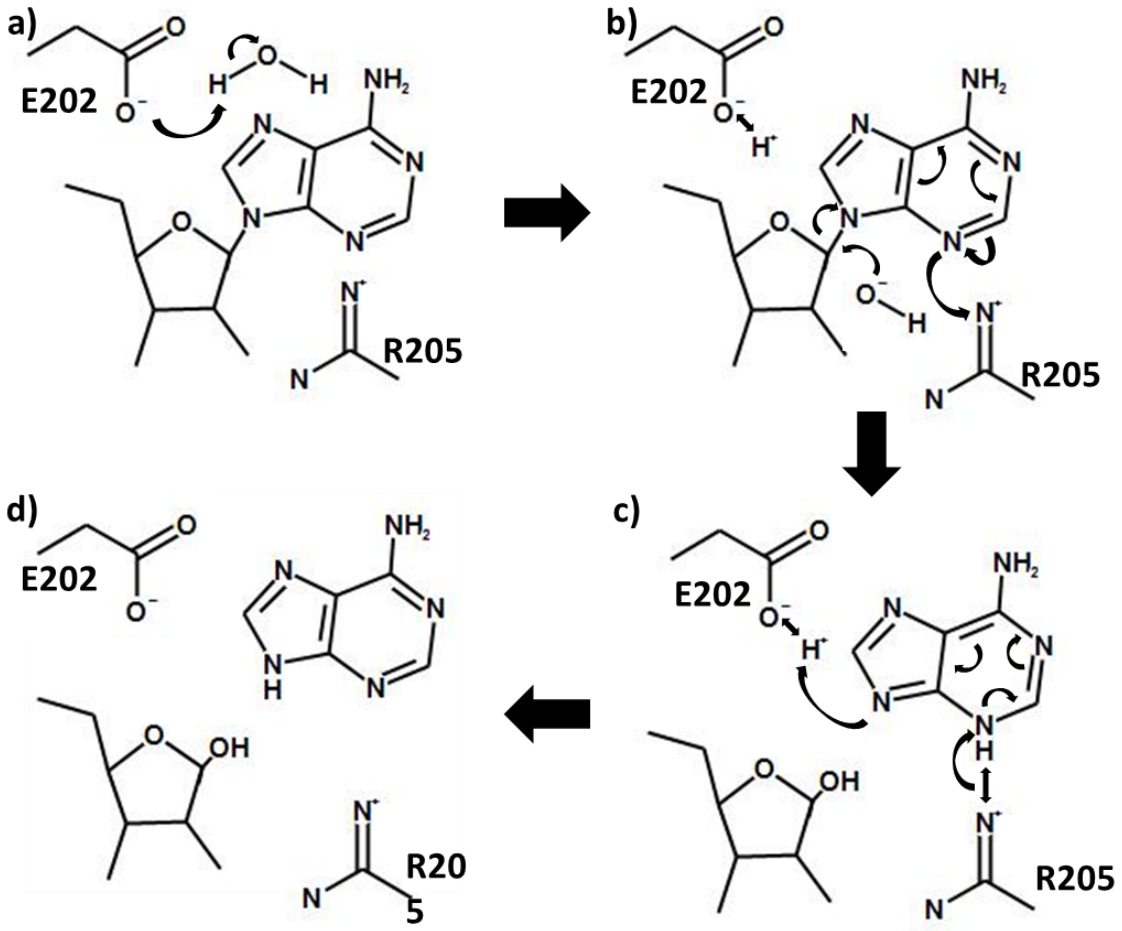


Figure 3.6: Hypothetical mode of action of hydrolytic depurination of adenine by the JIP60 RIP domain
The curly arrows represent movements of electrons while double arrows represent temporary bonds. a) First, a negatively charged glutamic acid (E202) leads to splitting water molecule into H^+ and OH^-. b) Subsequently, OH^- performs an 'attack' on carbon atom located on the ribose and involved in glycosidic bond with the purine. That leads to shift of charges across purine rings, facilitated by the proximity of positively charged arginine (R205), and to a cleavage of the glycosidic bond between the ribose and purine. c) Plant cytoplasmic conditions (pH 7.4-7.5) favours negatively charged glutamic acid and positively charged arginine. Therefore, reverse shift of charges takes place, finalising on a glutamate-associated proton being bound by the nitrogen atom located on purine. d) The glycosidic bond is fully cleaved and the purine is released from the adenine.

3.2.3 The recombinant JIP60 N-terminal domain causes necrosis *in planta*

In order to test whether the recombinant JIP60ml is in fact functional *in vivo*, a set of agroinfiltration experiments was performed. Two strains of *Agrobacterium tumefaciens* GV3101 (Agrobacterium) were created by transforming them with plasmids containing either JIP60ml-GFP construct or GFP-only as a negative control. The Agrobacterium cells were then infiltrated separately into *N. benthamiana* leaf (OD_{600}=1.0). The leaf was observed for any

changes and photographs were taken 2 and 7 days post infiltration (dpi). There were no differences visible to the naked eye between the JIP60ml treatment and the negative control at 2 dpi (Figure 3.7a). However, there was a clear difference at 7 dpi (Figure 3.7b). The leaf zone agroinfiltrated with JIP60ml showed clear signs of necrosis and chlorosis. The leaf lamina in that zone showed substantial thinning and proneness to tearing. The chlorosis-mediated discolouration of the leaf is displayed better when the images are transformed into grey scale (Figure 3.7c and 3.7d for 2 and 7 dpi, respectively). In contrast, the zone agroinfiltrated with the GFP-only negative control showed none of those signs. That indicated recombinant JIP60ml is expressed and is causing a severe effect in the *N. benthamiana in planta* model.

3.2.4 Essential residues of JIP60 active site

Subsequently, in order to investigate experimentally the importance of the four amino acids predicted to be the active site of JIP60, the residues were mutated to an alanine. Alanine was chosen as it is a short, non-interactive amino acid unlikely to cause a structural disruption (Cunningham and Wells 1989; Morrison and Weiss 2001). Moreover, Val62 (V62) was chosen as a structural residue not involved in function, and mutated into an alanine as well, as a mutagenesis control. The mutants were then each agroinfiltrated in a separate leaf zones, alongside the functional JIP60ml as a positive control and the GFP-only as a negative control (Figure 3.8). The leaves were then observed daily, and pictures were taken 3, 7 and 11 dpi. All of the four mutants of the predicted active site, JIP60$_{Y96A}$, JIP60$_{E202A}$, JIP60$_{R205A}$ and JIP60$_{W235A}$, showed loss of function. The zones agroinfiltrated with the JIP60 mutants showed no signs of JIP60-mediated necrosis, whereas the JIP60ml positive control showed progressive degeneration of leaf tissue. That indicates that each residue is necessary for the N-glycosidase function of JIP60. It supports the hypothesis that Y96 and W235 play a structural role in the depurination process, as these residues seem to be essential independently of the catalytic E202 and R205 residues. The JIP60$_{V62A}$ mutant did not show loss of function, showing that not all mutations lead to loss of function in JIP60.

Next, further investigation of the active site residues was performed. Instead of alanine sub-

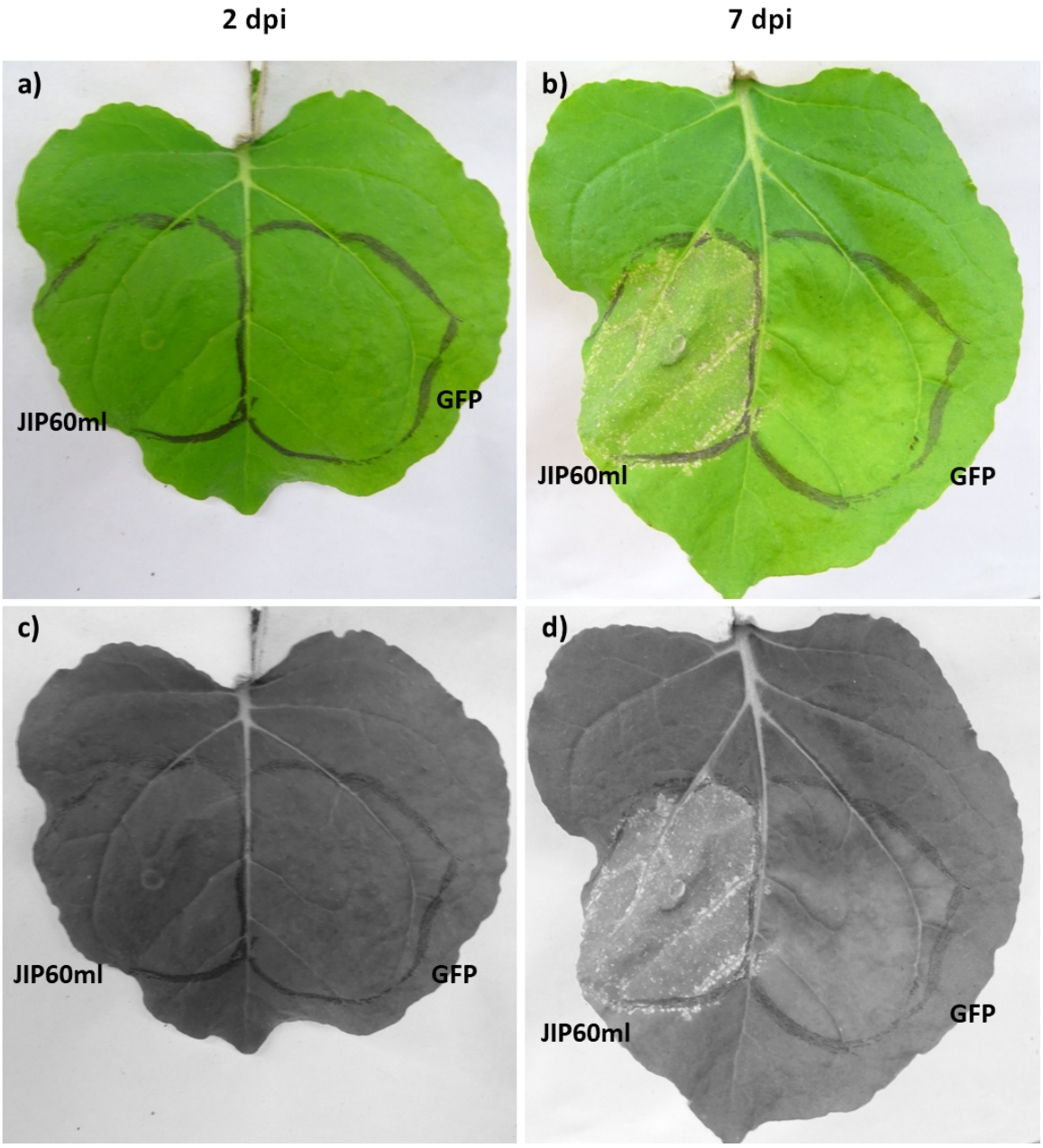


Figure 3.7: Time course of transient expression of active JIP60 via agroinifiltration of *Nicotiana benthamiana* Agrobacterium containing either a plasmid with JIP60ml or with GFP as negative control was infiltrated into *N. benthamiana* leaves (OD_{600}=1.0). Subsequently, pictures of the leaves were taken 2 and 7 days post infiltration (a & b, respectively). At 2 dpi (a), no changes are visible yet on the leaf and there is no visible difference between the JIP60ml treatment and the negative control. At 7 dpi (b), lesions and progressing chlorosis are clearly visible on the zone agroinfiltrated with JIP60ml in comparison with the negative control, showing that transient expression of JIP60ml is sufficient to cause necrosis in non-host plant. c) & d) show the a) & b) in the grey scale, respectively, to highlight the visibility of the lesion on the leaf and chlorosis. (Experiment was repeated three times, one week apart, six leaves (technical repeats) in each repeat; photograph of a representative example shown)

stitutions, a set of amino acids was chosen that were either isofunctional, i.e. possessed an equivalent chemical functional group, or isostructural, i.e. had a similar structure or size. Therefore, the following mutants were created: Y96F (isostructural), Y96S (isofunctional), E202D (isofunctional), R205K (isofunctional), W235F (isostructural) and W235P as a mutagenesis control. The purpose of these mutants was to investigate how fragile the active site is, and whether the JIP60 function can be retained with other, similar residues. These mutants were then agroinfiltrated into *N. benthamiana* leaves, alongside JIP60ml and GFP as a positive and negative controls, respectively. Then, the leaves were monitored for signs of necrosis and pictures were taken 3, 7 and 11 dpi (Figure 3.9). However, throughout the time course, none of the JIP60 mutants showed any sign of activity and the agroinfiltrated leaf zones showed no signs of necrosis, same as the GFP-only negative control. Only the leaf zones infiltrated with JIP60ml showed progressive necrosis and plant tissue degeneration. The results indicated that substitutions of the essential amino acids of the JIP60 active site even with similar residues, either structurally or chemically, disrupted JIP60 function.

3.2.5 Presence of transiently expressed JIP60 *in planta*

Next, we tested whether the lack of necrosis in the leaves agroinfiltrated with the JIP60 mutants was the result of an actual loss of function or simply by lack of expression. Firstly, the agroinfiltrations were repeated and leaf discs of the infiltrated zones were collected 2 dpi. Those leaf discs were investigated with epifluorescence microscopy to look for presence of GFP signal, as all of the JIP60 variants were conjugated to GFP at their C-terminal. The micrographs showed a strong signal from the GFP-only control and a lack of signal from the un-infiltrated leaf disc (Figure 3.10). The strong "jigsaw puzzle" outline of the GFP signal characteristic with the plant epithelial cells suggests a uniform expression throughout the cytosol, without major compartmentalisation into any of the cell organelles. Nonetheless, some of the GFP signal localises into the nucleus, visible as a bright orb within the confines of a cell. Some autofluorescence from plastids, appearing as red signal, is detectable in micrographs with low GFP signal, such as the un-infiltrated sample. The micrographs of leaf discs infiltrated with the functional JIP60 variants, JIP60ml and JIP60$_{V62A}$, also showed lack of

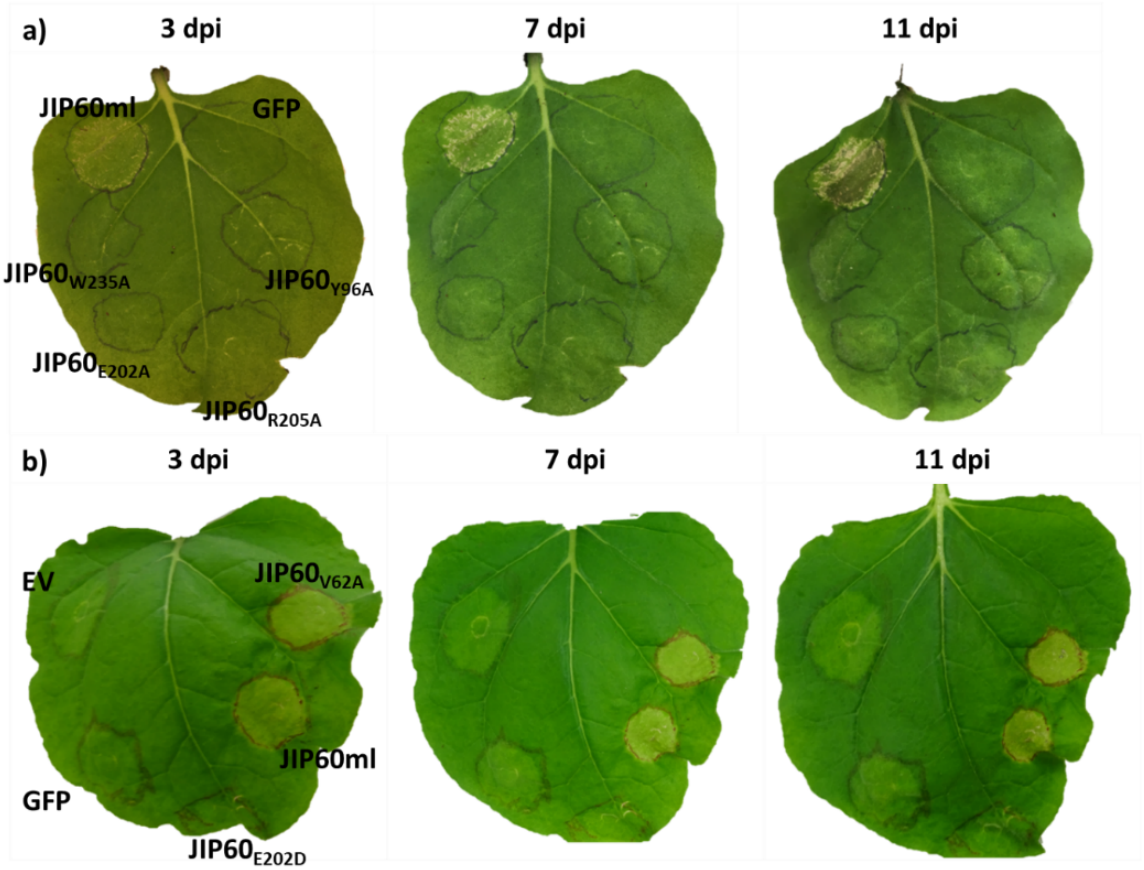


Figure 3.8: Time course of transient expression of JIP60 mutants with alanine substitution
a) Agrobacterium strains containing the four JIP60 mutants, JIP60ml as positive control and GFP as negative control were created. The four JIP60 mutants were following: JIP60$_{Y96A}$, JIP60$_{E202A}$, JIP60$_{R205A}$ or JIP60$_{W235A}$; each with a single alanine substitution of the active side residue. Agrobacterium strains were infiltrated into *N. benthamiana* leaf as indicated (OD_{600}=1.0) and pictures were taken at 3, 7 and 11 dpi. Only JIP60ml showed progressive lesions and chlorosis, whereas all of the mutants showed loss-of-function, indicating that each residue is necessary for the JIP60 function. b) Agrobacterium strains containing JIP60ml, JIP60$_{V62A}$ mutant, JIP60$_{E202D}$ mutant, GFP as a negative control or empty vector (EV) were infiltrated (OD_{600}=1.0) into *N. benthamiana* leaf as indicated, and pictures were taken at 3, 7 and 11 dpi. In this case, both JIP60ml and JIP60$_{V62A}$ mutant showed similar activity, causing lesions and chlorosis, whereas the rest showed no necrotic function. This indicates that JIP60$_{V62A}$ mutant remained active despite the site-directed mutagenesis, hence the loss-of-function of other mutants was caused by lack of necessary residues. (experiments performed and pictures taken by: a) Maya Bruderer and b) Gerard Belmans)(n=3 for each experiment; photograph of a representative example shown)

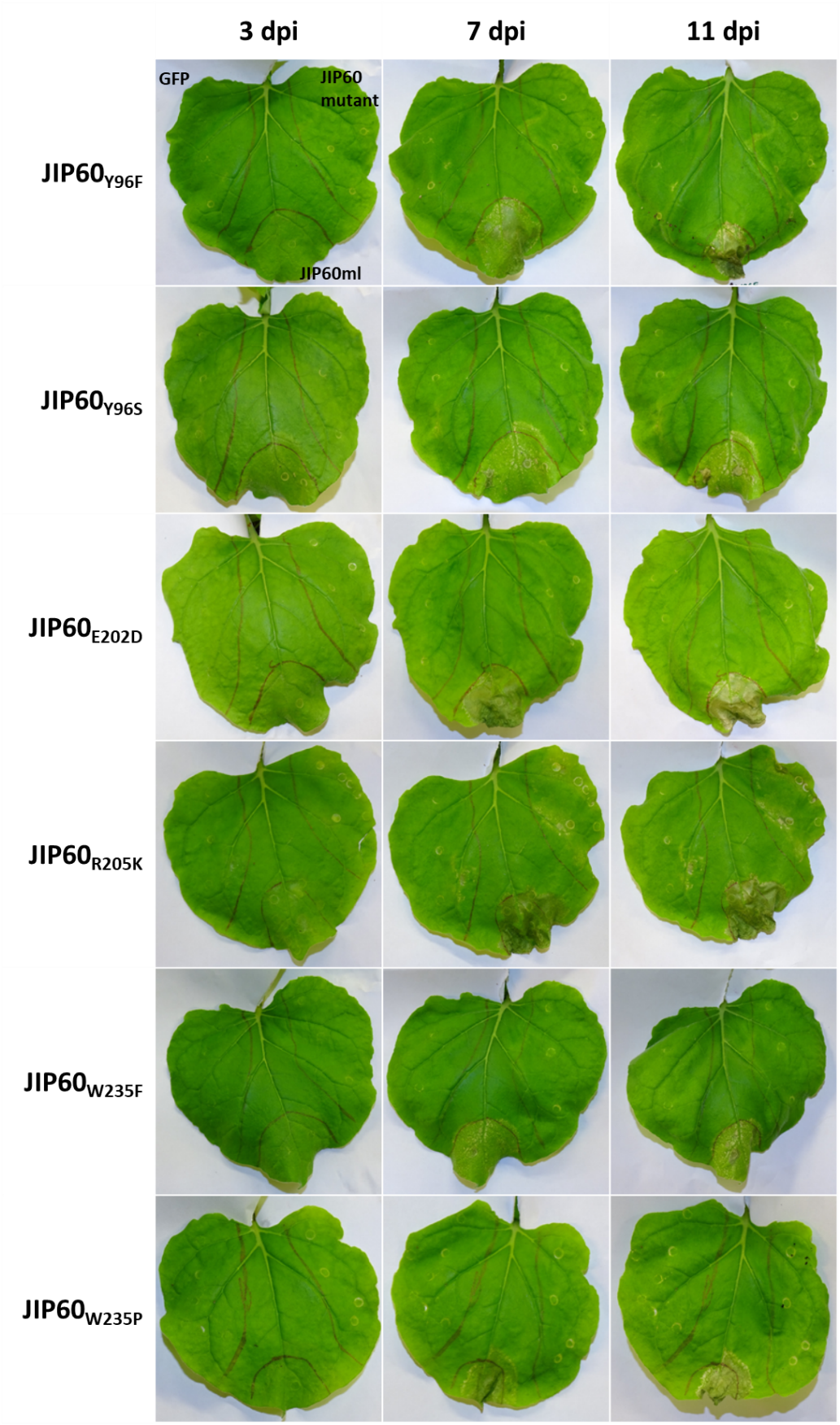


Figure 3.9: Time course of transient expression of isostructural or isofunctional JIP60 mutants in *N. benthamiana*

Agrobacterium strains carrying plasmids with JIP60 mutants or with either JIP60ml or GFP as the positive and negative controls, respectively, were infiltrated into *N. benthamiana* (OD_{600}=1.0) leaf zones as indicated by the marker outlines. Pictures were taken at 3, 7 and 11 dpi. The JIP60 mutants were obtained via site-directed mutagenesis of active site residues substituted with either isostructural or isofunctional amino acid. However, all of the mutants showed loss-of-function and only JIP60ml exhibited progressive necrosis and chlorosis of the infiltrated leaf zone. (Experiment performed and pictures taken by Rachel Greenhill)(n=3, photograph of a representative example shown)

GFP signal; however, the cellular structure within the tissue seemed to have been compromised when compared to the un-infiltrated sample. It manifests through ill-defined "jigsaw puzzle" structure of the cells, as well as by diminished autofluorescence signal. Furthermore, the majority of loss-of-function JIP60 variants exhibited strong GFP signal, indicating successful expression. Moreover, the signal is less uniform than in the case of GFP-only control. These loss-of-function JIP60 mutants seem to congregate throughout the cell cytosol which manifests as small spots. This could be an indication of protein aggregation or sequestration into cell P-bodies. Moreover, the autofluorescence signal tends to be dwarfed here by strong GFP expression and not visible in these micrographs. Out of all the JIP60 loss-of-function variants, only JIP60$_{W235F}$ showed poor GFP signal where only singular cells showed any GFP expression.

Following the epifluorescence microscopy experiments that showed successful agroinfiltration and expression of GFP, a set of western blotting experiments was performed, to establish whether the JIP60-GFP constructs are still intact *in planta*. The agroinfiltrations were repeated and leaf discs of the infiltrated leaf zones with various JIP60 variants were collected at 3 dpi. Then proteins were extracted and analysed by SDS-PAGE on 10% tris-glycine gels. The proteins were then transferred onto PVDF membrane by electroblotting. The membrane was incubated with anti-GFP primary antibody, followed by an incubation with HRP-conjugated secondary antibody. Strong bands were visible on the western blot; this was consistent with the 55 kDA size of the JIP60-GFP chimera and was observed for all of the loss-of-function JIP60 variants except for the JIP60$_{W235F}$ (Figure 3.11). Those lanes also showed bands corresponding to proteins of an apparent molecular weight of 22 kDa: these may be products of protein degradation. The lane with the GFP-only control showed a strong band consistent with recombinant GFP size of 27 kDa. No other lane showed that band, indicating that none of the JIP60 variants expressed solely GFP instead of the full construct. JIP60ml and JIP60$_{W235F}$ showed no bands at all. In case of JIP60ml, it is unlikely due to lack of expression, as the infiltrated leaf zone exhibited necrosis over time, thus the protein had to be present in levels sufficient to cause cell death. Finally, un-infiltrated leaf disc protein extract also showed no bands, indicating lack of unspecific binding in this size range.

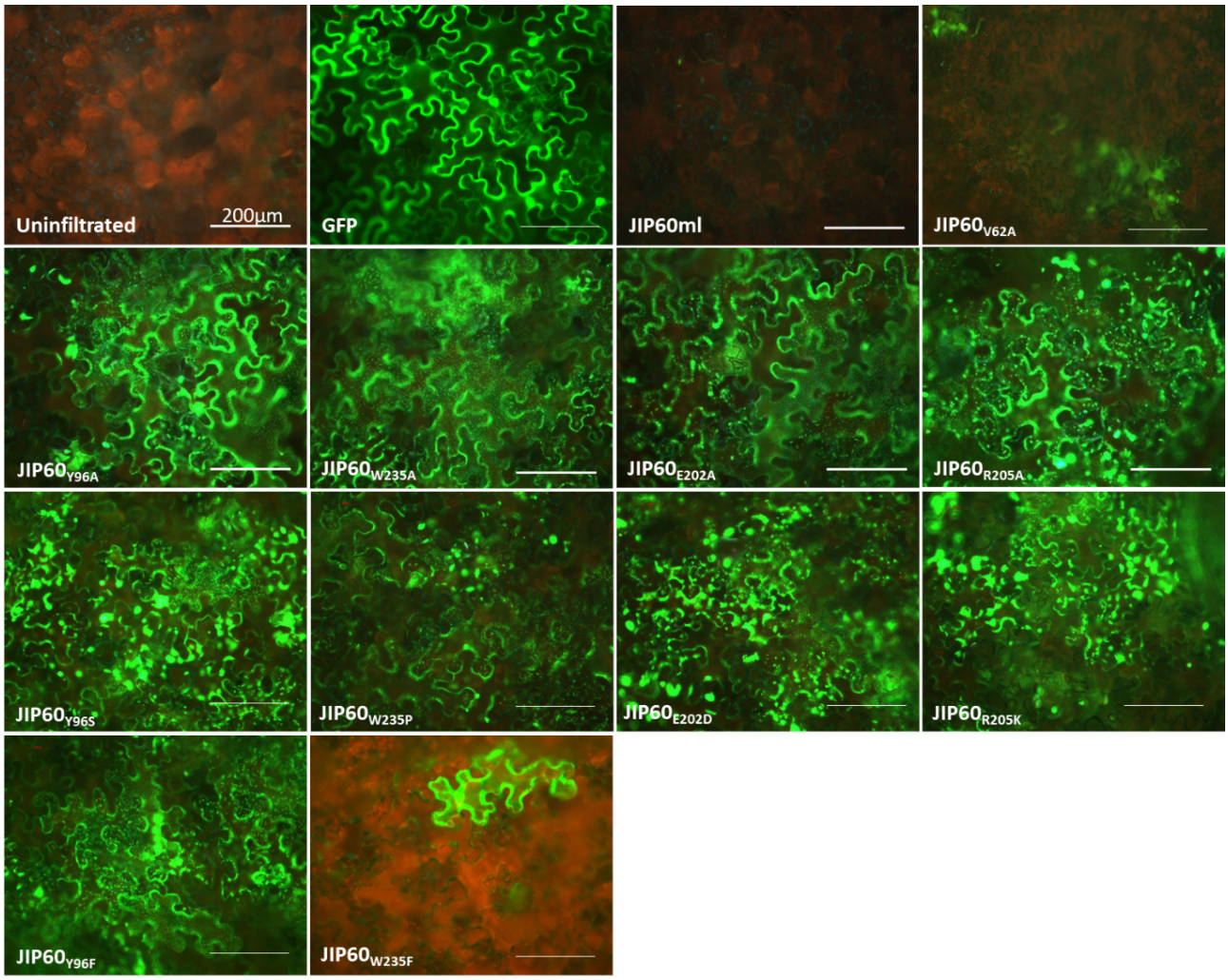


Figure 3.10: Fluorescent micrograph of transiently express JIP60 variants in *N. benthamiana*
Agrobacterium strains carrying plasmids with JIP60 variants conjugated to GFP were infiltrated into *N. bethamiana* (OD_{600}=1.0). At 2 dpi, the samples were observed by epifluorescence microscopy and micrographs were taken. The excitation/emission filters used were those optimised for GFP imaging. All JIP60 variants, apart from JIP60ml, $JIP60_{V62A}$ and $JIP60_{W235F}$ show strong GFP signal, indicating successful expression. JIP60ml and $JIP60_{V62A}$ mutant are both functional variants, hence little to no GFP was detected, possibly because cellular necrosis has already commenced. All the size bars represent 200 μm. (Experiments performed and micrographs taken by Maya Bruderer and Rachel Greenhill)(n=3, photograph of a representative example shown)

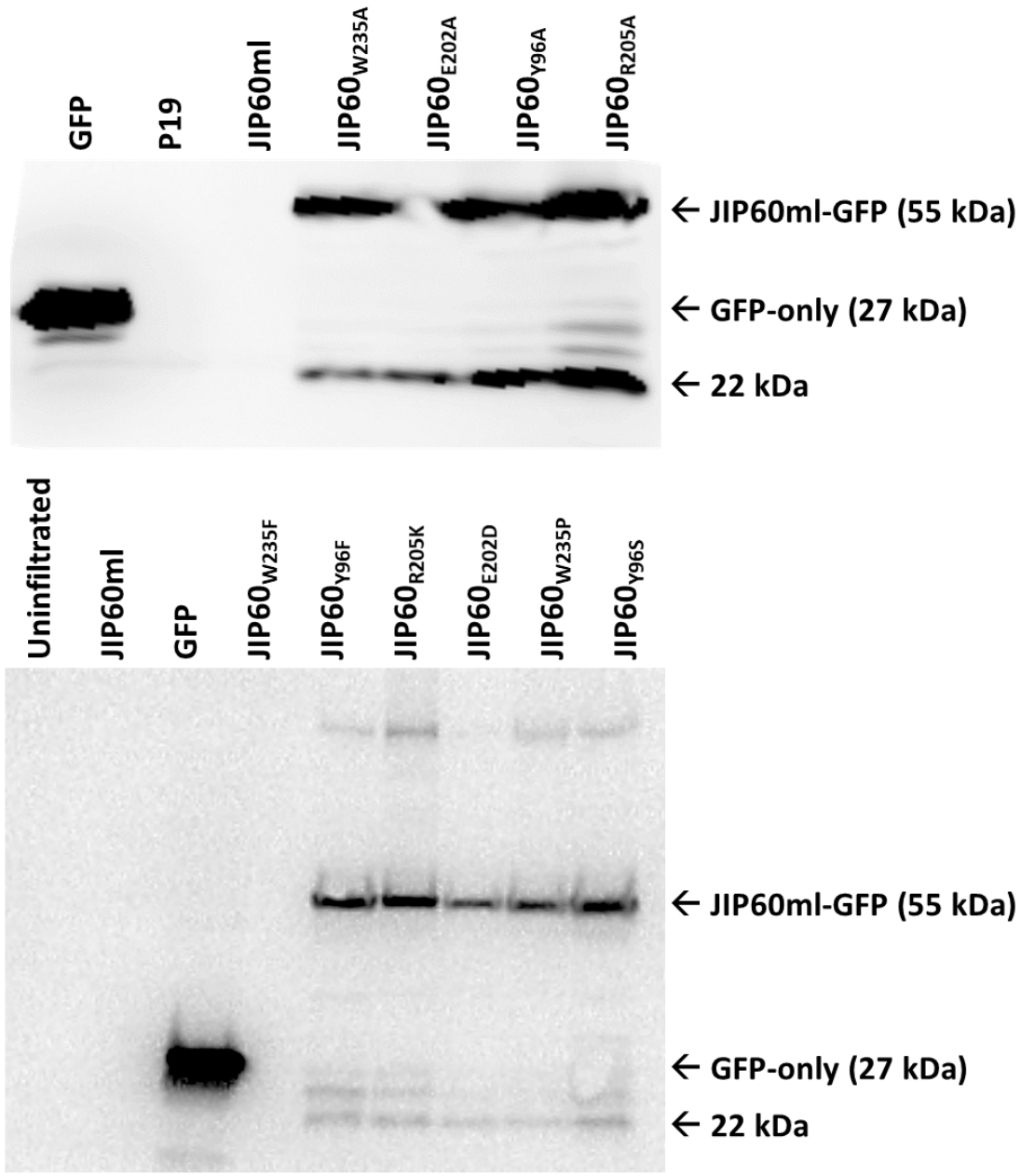


Figure 3.11: Western blot of protein extract from agroinfiltrated *N. bethamiana* leaves
Agrobacterium strains carrying JIP60 variants conjugated to GFP were infiltrated into N. benthamiana leaves (OD_{600}=1.0). At 3 dpi, leaf discs were collected and protein extraction was performed using denaturing buffer. The protein extracts were resolved using SDS-PAGE on 10% tris-glycine gels with 100 V for 90 min. Subsequently, the proteins were electroblotted onto PVDF membrane at 10 V for 45 min. The membrane was incubated with rabbit anti-GFP IgG primary antibody at 1:4000 dilution, followed by incubation with goat anti-rabbit HRP-conjugated secondary antibody at 1:4000 dilution. Strong bands were detected at 55 kDa for all JIP60 mutants apart from $JIP60_{W235F}$, indicating presence of JIP60-GFP conjugates. No bands were detected for un-infiltrated negative control or for either JIP60ml or $JIP60_{W235F}$ mutant. The former was most likely due to cellular necrosis within the leaf discs due to function of JIP60. GFP control showed strong band at 27 kDa, indicating good transient expression. Also, small bands of this size were detected for some of the JIP60 mutants, probably due a degree of protein degradation. For all mutants that a band was detected at 55 kDa, also a smaller, unidentified band was detected at 22 kDa, most likely a product of limited protein degradation. (Experiments performed by Rachel Greenhill and Maya Bruderer)(n=1 for each experiment)

3.2.6 Recombinant JIP60ml leads to translation inhibition *in vitro*

Finally, the effects of JIP60 variants were evaluated *in vitro* using a wheat germ extract translation system. The JIP60 variants genes were first amplified using PCR to add T7 promoter to the products. Then, the T7-JIP60 variants were transcribed into mRNA with MEGAScript T7 transcription kit (Thermo Fisher). Subsequently, 1 μg of each JIP60 variant mRNA was added to wheat germ extract alongside 1 μg of luciferase mRNA and incubated for 2 hr at 25°C to achieve *in vitro* translation. Then luciferin was added to each sample and luminescence was measured to test the efficacy of JIP60 variants in inhibiting translation of the luciferase mRNA. The idea behind the assay was that luciferase mRNA translation would lead to luciferase activity measured as luminescence. In samples where JIP60ml mRNA was present, translation of functional JIP60ml would in turn inactivate the ribosomes, leading to less luciferase being produced, which would be observed as a decrease in luminescence. The experiment was repeated three times and within each experiment five consecutive measurements were taken as technical repeats. To statistically assess the validity of the results, they were tested using linear mixed model where the JIP60 variants were treated as the fixed effect, whereas the difference between experimental repetitions was taken into account as the random effect. Subsequently, the significance between samples was assessed using Tukey test to account for multiple testing. According to the linear mixed model, the difference between the repeats was responsible for almost 49% of the variability between the samples. JIP60ml and JIP60$_{V62A}$ variants produced a consistent, statistically significant, decrease in luciferase activity, with their respective medians at $1.2 * 10^5$ FU and $0.7 * 10^5$ FU, in comparison with luciferase-only positive control (+ve) with its median of $1.9 * 10^5$ FU (*** $p < 0.001$ for both JIP60ml and JIP60$_{V62A}$, according to TukeyHSD test). JIP60 variants JIP60$_{Y96F}$, JIP60$_{Y96S}$, JIP60$_{E202D}$, JIP60$_{R205K}$ and JIP60$_{W235F}$ showed no consistent decrease in luciferase activity, with their medians not varying significantly from the luciferase-only positive control, indicating loss of function. Interestingly, JIP60$_{W235P}$ which was predicted to have structural disruption due to proline substitution, showed statistically significant drop in luciferase activity (*** $p < 0.001$, according to TukeyHSD test) with median of $1.7*10^5$ FU. All conditions were statistically significant from the negative control (-ve), according to the TukeyHSD test. The

above results of JIP60-mediated effect on *in vitro* translation are presented in Figure 3.12.

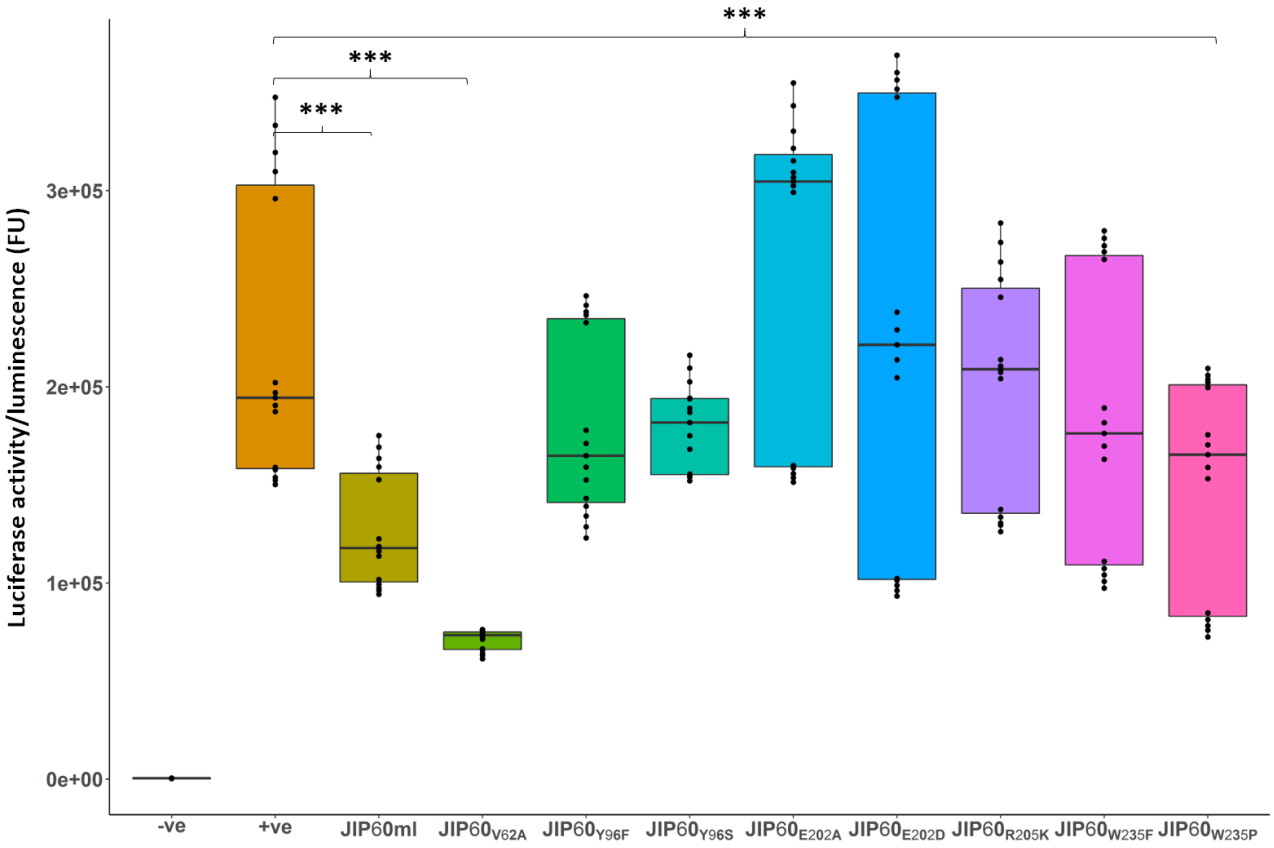


Figure 3.12: ***In vitro*** **translation assay using JIP60 variants in wheat germ extract**
JIP60 variants located on plasmid containing T7 promoter were transcribed into mRNA using MEGAscript T7 transcription kit (Thermo Fisher). Subsequently, 1 μg of mRNA of appropriate JIP60 variant was added to wheat germ extract alongside 1 μg of luciferase mRNA, and incubated at 25°C for 2 hr. Then luciferin was added to each sample and the efficacy of JIP60 variants ribosome inhibition was measured indirectly via drop in luminescence within each sample. JIP60ml and JIP60$_{V62A}$ which both showed to be functional *in planta* led to a consistent and statistically significant drop in luciferase activity (*** $p < 0.001$ for both JIP60ml and JIP60$_{V62A}$, according to TukeyHSD test), with medians $1.2 * 10^5$ FU and $0.7 * 10^5$ FU, respectively. Interestingly, JIP60$_{W235P}$ showed less defined, however also a statistically significant decrease in luciferase activity (*** $p < 0.001$, according to TukeyHSD test), with median $1.7{*}10^5$ FU. Other mutants, JIP60$_{Y96F}$, JIP60$_{Y96S}$, JIP60$_{E202D}$, JIP60$_{R205K}$ and JIP60$_{W235F}$, showed no statistically significant drop in luciferase activity, with their medians falling closely to that of the positive control. According to the linear mixed model which took into account the difference between the experimental repeats as the random effect, these differences explained almost 49% of variability between the samples. The experiment was repeated independently three times. (Experiments performed and raw data obtained by Tia Salter and Gerard Belmans)

3.3 Discussion

Ribosome-inactivating proteins are a widespread group of proteins involved in various physiological processes despite having a single catalytic function. Plants, and cereals in particular, have evolved a whole range of RIPs. Moreover, despite the observations that the RIP domain only exhibit an N-glycosidase function, the proteins are hypothesised to also play a role in plant defence against fungal, bacterial and viral pathogens, in translational regulation, in senescence and even as amino acid storage (Zaeytijd and Damme 2017).

3.3.1 JIP60 as a part of PTI response

JIP60 is associated with barley senescence. It is present in both natural senescence, and in MeJA-induced one (Springer et al. 2015). In both cases, JIP60 is detectable; however, in the case of the MeJA-induced senescence, JIP60 accumulates over time to much greater amounts and the process of plant cell death is much more rapid. Judging from the increased polysome/monosome ratio in *in vitro* studies, the N-terminal JIP60 domain inhibits translation at the elongation step (Dunaeva et al. 1999). JIP60-mediated host cell death seems to be a different process from classic HR seen in ETI. HR is a result of cognate *avr*-R gene product interaction and it is a very rapid process while JIP60-mediated host cell death seems to proceed at a slower rate (Morel and Dangl 1997; Mur et al. 2008). Moreover, JA and their derivatives are produced by the plant upon recognition of generic infection signals by PRRs, rather than a specific effector (Campos et al. 2014). Therefore, it would suggest synthesis of MeJA and subsequent expression of JIP, including JIP60, would be the results of PTI, rather than ETI.

3.3.2 JIP60 as a barley RIP

JIP60 exhibits characteristics consistent with RIPs. Previous bioinformatic searches showed its sequence to be homologous with plant RIPs and it showed N-glycosidase activity and protein translation inhibition properties *in vitro* and *in vivo* (Chaudhry et al. 1994; Dunaeva et

al. 1999). However, its molecular structure has not been solved, to date. The bioinformatic tools are constantly improving and their capabilities are expanding, along with databases of known and solved genomes and protein structures. The tools currently available allow easy comparison and alignment with thousands of genes or proteins, of hundreds of organisms, using various statistical approaches, such as BLAST or HMM (Finn et al. 2015). Phyre^2 is a particularly useful tool that allows prediction of molecular structure of a protein based on its amino acid sequence and their properties, comparing it with structures of proteins that have been solved experimentally, e.g. through X-ray crystallography or Cryo-EM (Kelley et al. 2015). Due to extensive databases populated with experimentally confirmed molecular structures, these structural predictions are often very reliable. Using these modern tools, such as HMMER and Phyre^2, I was able to confirm that amino acid sequence of N-terminal domain of JIP60 contain all the characteristics of a RIP. Moreover, its predicted structure in fact matches that of a RIP with high confidence, meaning when compared to the database the protein sequence composition of JIP60 conformed with those of known RIPs with experimentally confirmed molecular structures.

In this study, we excised the JIP60 inactivation loop *in vitro* and replaced it with a methionine-leucine linker to produce JIP60ml: a recombinant, constantly active N-terminal domain of JIP60. The two-residue Met-Leu linker was based on a similar modification studied in maize RIP1 (Walsh et al. 1991). Moreover, Met-Leu residues are seen roughly within the middle of the inactivation loop of wild-type JIP60, and neither Met nor Leu is likely to cause adverse effects on protein function (Jones, R., pers. comm.). We created the recombinant JIP60ml to study this protein in a model organism such as *N. benthamiana*, because we reasoned that this plant might not possess molecular machinery necessary to process JIP60 into its active form. The resulting gene produces an active form of the N-terminal domain which possesses the N-glycosidase activity inherent to RIPs.

The fact that the N-terminal domain of JIP60 has been used in this study, rather than the full-length protein needs to be borne in mind. In nature, JIP60 exhibits processing into two separate domains, where its N-terminal domain splits from its C-terminal domain, and they appear to act independently (Chaudhry et al. 1994). Focusing only on the N-terminal do-

main is justified as it reflects the natural processes that happen in barley. JIP60ml proved to be active and able to induce necrosis, even in the non-host plant *N. bethamiana*. While JIP60 peptides were shown to cause ribosome inactivation *in vitro* and *in vivo* (Rustgi et al. 2014; Dunaeva et al. 1999; Chaudhry et al. 1994) those experiments had not demonstrated whether JIP60 causes necrosis *in planta*. Gorschen et al. (1997) managed to stably transform full-length JIP60 cDNA into tobacco but only the plants that were expressing JIP60 relatively poorly were able to be regenerated and grown. Those plants exhibited visible gene dose dependant phenotype changes such as severe stunting, premature senescence and poor or no seed production. We showed that transient expression of the JIP60ml gene caused necrosis within the agroinfiltrated zones on a living plant. Moreover, the necrosis was dose-dependent, where the symptoms showed earlier and progressed faster proportionally with increased numbers of Agrobacteria infiltrated. JIP60ml was extremely effective at causing necrosis, even in the non-host plant: infiltration of Agrobacterium at a concentration as low as OD_{600} of 0.02 was sufficient to cause necrosis within the zone. Standard OD_{600} for agroinfiltration is usually around 1.0. In addition, JIP60ml variant was shown to act as a RIP in yeast. Yeast-3 Hybrid experiments, which test RNA-protein interaction, showed that JIP60ml in fact associates and interacts with SRL rRNA sequence but not with other, random rRNA fragment (Pennington 2014; SenGupta et al. 1996).

3.3.3 JIP60 mode of action

Conformational change often is a mechanism of protein activation (Grant et al. 2010). However, in case of maize RIP1 that possesses a similar inactivation loop to JIP60, Yang et al. (2010) proposes it is the physical obstruction by the loop and not any conformational changes in the active site, that prevents the RIP from interacting with ribosomes, thus making the protein inactive. It is unknown whether the same mechanism occurs in JIP60.

Analysis of the predicted structures obtained from the amino acid sequences of JIP60 WT and JIP60ml via Phyre^2 suggested a potential mechanism of function control of the protein. Excision of the inactivation loop led to a conformational change within the active site. The sidechains of the conserved residues shifted their position and started pointing towards each

other, creating a saddle where an rRNA molecule could potentially fit. Even though it is only a computational prediction, it is still worth noting because the Phyre[2] algorithm considers the usual behaviour and arrangement of residue sidechains based on their chemical and physical constraints. Conversely, as it is only a computational prediction, it has to be confirmed experimentally, e.g. with X-ray crystallography, before any solid conclusions can be drawn. Especially, since it regards the orientation of residue sidechains, which can potentially assume different positions without changing the overall structure of the protein.

I was unable to extract intact JIP60ml protein from agroinfiltrated zones. Even though the leaf discs were collected before any symptoms of necrosis were visible, western blotting with anti-GFP antibodies showed no presence of JIP60ml-GFP conjugate. Similarly, micrographs acquired by epifluorescence microscopy revealed no GFP signal in those zones. In contrast, majority of JIP60 loss-of-function mutants, showed both presence of JIP60-GFP conjugates on western blots and a strong GFP signal on micrographs. JIP60ml protein was clearly expressed by the plant as deduced from the observations that necrosis occurred. The possible explanation for the absence of JIP60ml in protein extracts could be that active JIP60 has a quick turn over and is being rapidly degraded. Our efforts to express active JIP60 in bacteria showed it is susceptible to protein degradation (Jones, R., pers. comm.). The necrotic cells with their internal structure compromised are more likely to expose JIP60 to protein degrading conditions and enzymes (Reape et al. 2008). Interestingly, the JIP60 loss-of-function mutants that are showing presence of JIP60-GFP conjugates on western blots, also cause an appearance of GFP signal in distinct, scattered spots in cell cytosol on fluorescent micrographs, that in appearance look similarly to P-bodies (Eulalio et al. 2007; Luo et al. 2018). It would seem the inactive JIP60 variants either aggregated or their association with RNA leads to them being trafficked into cell P-bodies, which in turn could prevent the protein degradation for long enough to be detected via western blotting.

The mutagenesis of the four candidate active site residues (Tyr96, Glu202, Arg205 and Trp235), and the subsequent experiments allowed to conclude that these residues are indeed part of the active site of N-terminal domain of JIP60. They are all necessary for the RIP function of the protein, and any changes of these residues have very strong or detrimental effect on

the function. The transient expression of N-terminal domain of JIP60 *in planta* showed that site-directed mutagenesis of the active site residues, i.e. Tyr96, Glu202, Arg205 and Trp235, in fact led to loss of function. The use of isofunctional and isostructural amino acids showed that the RIP active site is very fragile and even a small variation in a single residue, such as mutation from glutamate to aspartate, is detrimental to its functionality. Substitution of Val62 with alanine did not lead to loss of function, showing that not all mutations would disturb the activity.

Epifluorescence microscopy and western blotting confirmed detectable expression of all of the loss-of-function mutants. The only mutants of JIP60ml that did not show expression of GFP signal or protein levels on a western blot were the $JIP60_{V62A}$ and $JIP60_{W235F}$. These results were not surprising for the $JIP60_{V62A}$, as the mutant was designed to retain its function, as was in fact the case. However, the reason for the lack of satisfactory expression of $JIP60_{W235F}$ is unknown. One of the possibilities is that the regulatory element on the T-DNA of this Agrobacterium strain was mutated so the strain has a low efficiency transformation rate. In that case, recreating the strain could solve the problem of low expression. The *in vitro* assay of the JIP60ml mutants, including the isofunctional mutants such as $JIP60_{Y96S}$, $JIP60_{E202D}$ and $JIP60_{R205K}$, but excluding the $JIP60_{W235P}$ mutant, showed no statistical difference from the positive control in lowering the luciferase activity, suggesting no effect on translation inhibition. Western blot experiments also showed presence of a small fragment of about 22 kDa which most likely emerged due to proteolysis of the JIP60ml-GFP conjugate within the plant cell. When expressing full JIP60 in transgenic tobacco, Dunaeva et al. (1999) detected several small fragments detected by anti-JIP60 antiserum, as small as 20 kDa.

In the case of the $JIP60_{W235P}$ mutant, the *in planta* experiments showed the mutant did not cause any visible necrosis, and the western blotting and fluorescent micrographs confirmed good expression by the plant. However, the *in vitro* translation experiments showed a statistically significant, but not consistent, inhibition of luciferase translation, when variation between repeats is taken into account. This suggests that $JIP60_{W235P}$ mutant retains at least part of its function. It is particularly interesting as this mutant was designed to not retain

its function. Proline residue tends to create a kink within molecular structure, often leading to misfolding of the protein if introduced as a mutation (Yaron et al. 1993). However, taking into consideration that the tryptophan residue does not take part in the catalytic reaction but is rather a scaffold and stabiliser of the interaction with RNA molecule, it is possible that the substitution with proline leads to lowered activity that prevents crossing the threshold that would lead to cell death. The Phyre[2] prediction of $JIP60_{W235P}$ structure shows that presence of the proline leads to a kink in the alpha helix that contacts the rRNA but otherwise does not seem to disturb the rest of the structure or the positioning of other active site residues or their sidechains. Moreover, the orientation of the proline would still allow for potential H-bond creation between the residue and rRNA backbone. More experiments are required to assess whether any vestigial functionality remains in this variant.

The *in vitro* translation assays proved to be problematic and are still requiring optimisation before concrete insights are acquired. The main problem of the assay is there is a big variation between repeats, making it difficult to compare and interpret the results reliably. The linear mixed model statistical approach used attempted to take the big variation between repeats into account. The test itself showed that the differences between repeats are responsible for 49% of variability between samples, which is a substantial amount. Chaudhry et al. (1994) reported that JIP60 inhibited ribosomes from rabbit reticulocyte lysate but not from wheat germ extract, justifying it by saying JIP60 does not work on conspecific ribosomes. However, in my study, I used both wheat germ extract and rabbit reticulocyte lysate ribosomes and achieved similar results in both. From there on, I mainly used wheat germ extract in the assay as I assumed plant ribosomes would be better model. The disparity between my results and that of Chaudhry et al. (1994) highlight the challenges of using an *in vitro* translation assay reproducibly. One of the possible ways to increase specificity of the assay would be to employ an JIP60 N-terminal domain with higher activity. Krawetz & Boston (2000) reported that active maize RIP1 obtained by proteolytic treatment of precursor protein with papain was over 100-fold more active than the recombinant peptide obtained by excision of the inactivation loop region from the gene and replaced by a two amino acid linker. Therefore, it is possible that a more active variant of JIP60 N-terminal domain could be obtained via proteolytic cleavage rather than by expressing recombinant JIP60ml whose inactivation

loop was replaced by a short linker.

Despite expression of JIP60 being described in literature many times, we had no success in expressing and purifying JIP60ml (Reinbothe et al. 1994b; Chaudhry et al. 1994; Dunaeva et al. 1999). The attempts to express an active form of N-terminal domain of JIP60 in *E. coli* led to either death of the bacteria or rapid protein degradation, depending on protein tag (Jones, R., pers. comm.). In contrast, expression of an inactive JIP60 N-terminal domain mutants led to good protein expression; however, the peptide immediately aggregated into inclusion bodies and any attempts to acquire refolded protein were unsuccessful (Cota, E., pers. comm.).

In conclusion, the results strongly suggest that N-terminal domain of JIP60 is a RIP. JIP60, expresses in barley in response to MeJA hormone, thus it is likely to be a result of a PTI-mediated response rather than ETI. Bioinformatics confirmed it contains the conserved residues of other RIPs and it also caused cell death when transiently expressed *in planta*. Moreover, the four conserved residues: Tyr96, Glu202, Arg205 and Trp235, were confirmed to be necessary for the function of the peptide. An interference with any of these residues using alanine scanning mutation resulted in loss of function, thus confirming them to comprise all or part of the active site of JIP60. The fact that JIP60 acts like a RIP and the finding that the conserved residues are important to the function of JIP60 confirms indirectly that the computational prediction of the molecular structure prediction of the peptide was correct.

Chapter 4: *Blumeria* effector BEC1054 interferes with JIP60-mediated host cell death

4.1 Introduction

4.1.1 CSEPs in *Blumeria*

Infection in plants by bacteria, fungi and even some insects is facilitated by the use of effectors (Varden et al. 2017; Lo Presti et al. 2015; Hogenhout and Bos 2011). Effectors are small proteins secreted by an invader that facilitate infection by altering host cell structure or function, or alternatively they cause plant immune response (Hogenhout et al. 2009). *Blumeria graminis* is an example of phytopathogen using effectors to its advantage. Within its genome, an extensive combined genomic, transcriptomic and proteomic search found over 500 CSEPs (Pedersen et al. 2012; Frantzeskakis et al. 2018). CSEPs are classified as proteins with a signal peptide and no transmembrane domain, as well as no known homology outside of powdery mildews. These potential effector genes amount to over 7% of all annotated genes in *Blumeria* genome, which suggests an enormous importance of these proteins (Pedersen et al. 2012).

4.1.2 Host-pathogen interface

The important site of host-pathogen interaction for obligate biotrophs like *Blumeria* is the haustorium, their feeding body. Development of a haustorium marks a successful infection. Apart from drawing nutrients from the host, haustoria are suspected to be the hub for effector secretion (Szabo and Bushnell 2001; Godfrey et al. 2010). Importantly, even though

a haustorium is located inside the host cell, there is no mixing between the cytosols of the plant and the fungus (Glawe 2008). Instead, the haustorium is surrounded by a unique, two-layer lipid extra-haustorial membrane of plant origin, showing a different composition on its inner and outer side, which is the host-pathogen interface (Kemen et al. 2015). The outer layer of the membrane is then enclosed by extra-haustorial matrix which is believed to be the main molecular battleground of infection (Hückelhoven and Panstruga 2011).

The exact delivery mechanism of the fungal effectors is not fully understood. In case of oomycetes, it is suggested they employ host's trafficking system by containing RxLR motif on their effectors, a motif that can also be found in signal peptide on host proteins (Panstruga and Dodds 2009; Birch et al. 2006; Liu et al. 2019). However, this has been contested by biochemical studies that show that, despite being essential for the function of an effector, the RxLR motif is cleaved off before its secretion. This suggests the motif plays a role in the secretion process rather than in the host cell uptake (Wawra et al. 2017). The other route for effector delivery mechanism, seen in bacteria, is injecting them directly into host cell; this happens, for example, in *Pseudomonas syringae* and its syringe-like type III secretion system (Hueck 1998). However, neither of the methods seem apply in case of *Blumeria* effectors.

Proteomic studies showed that most of CSEPs are associated with haustoria. They were either more highly expressed in haustoria in comparison to epiphytic tissues or in some cases they were exclusively found in epidermis containing haustoria (Pedersen et al. 2012).

4.1.3 RNase-like effector proteins expressed in haustoria (RALPHs)

CSEPs are structurally and functionally varied. There is no single way to classify them. For example, CSEPs can roughly be divided into two categories depending on the localisation within the host target: the long, apoplastic effectors, characterised by localising to apoplast and length of 300-400 amino acids, and the short, cytoplasmic effectors, about 100-150 amino acids in length, targeted to host cytoplasm (Pedersen et al. 2012). The bioinformatics study showed that among the CSEPs in *Blumeria graminis*, the most numerous structural group are RALPHs. More than 120 out of more than 500 effectors are predicted to assume the

RNase-like structure, or are similar in sequence to those which are; they are also associated with haustoria (Pedersen et al. 2012). Genomic investigation of RALPHs suggests they might all share a common ancestor, most likely an ancient RNase that underwent multiple events of duplication and diversification (Spanu 2017). RNase fold is a very stable and robust structure, resistant to proteolysis, thus perfect for infiltration and subverting host's immune system (Pace et al. 1988).

4.1.4 Family 21 – crucial effectors in *B. graminis* infection

Among RALPHs in *Blumeria*, effector Family 21 stands out in the impact it has on the success of infection. Family 21 consists of 5 members, including BEC1054 and BEC1011 (syn. CSEP0064 and CSEP0264, respectively) (Pedersen et al. 2012). BEC1054 assumes an RNase-like structure (Pedersen et al. 2012) and the other members of the Family 21 are predicted to do so as well, due to close homology. Expression profiles showed that BEC1054 is most highly expressed at about 24 hr post inoculation, suggesting a role early on in the infection process (Pliego et al. 2013). HIGS studies indicated that both BEC1054 and BEC1011 are very important in facilitating *B. graminis* infection, as their downregulation led to decrease in successful haustoria formation by 60% and 70%, respectively (Pliego et al. 2013; Pennington et al. 2019). BEC1011 is also believed to interfere with host cell death (Pliego et al. 2013).

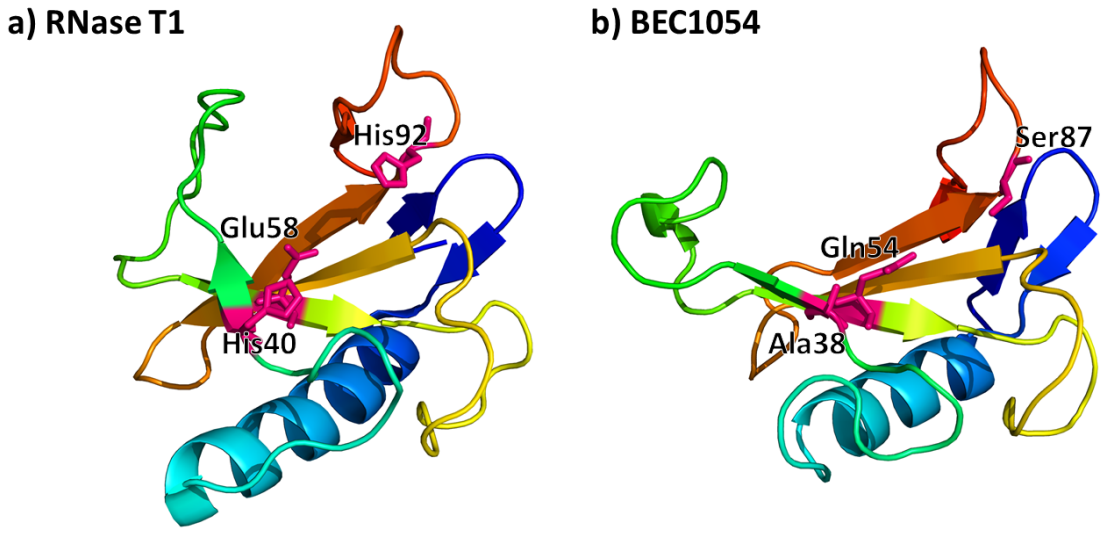


Figure 4.1: Comparison between structures of Ribonuclease T1 and BEC1054
Ribonuclease T1 (*A. oryzae*; PDB ID: 3URP) and BEC1054 (PDB ID: 6FMB) have remarkably similar structures. However, BEC1054 lacks the RNase catalytic residues, i.e. His40, Glu58 and His92 in RNaseT1 are replaced by Ala38, Gln54 and Ser87 in BEC1054, respectively (in purple)

4.1.5 BEC1054 as a potential pseudoenzyme

A structural study confirmed that BEC1054 possesses a RNase-like structure, while lacking the catalytic residues required for RNA cleavage, as predicted computationally (Figure 4.1) (Pedersen et al. 2012; Pennington et al. 2019). This suggests that BEC1054 is *de facto* a pseudoenzyme.

Pseudoenzymes are a type of proteins that lost their catalytical function, however, they are far from useless or simply a mid-step in their molecular evolution. It turns out that their lack of catalytic activity actually can grant them a different function (Adrain and Freeman 2012). Most pseudoenzymes evolved through gene duplication and subsequent loss-of-function mutations of their key catalytic residues (Todd et al. 2002). In addition, majority of described pseudoenzymes are signalling molecules involved in regulatory processes (Pils and Schultz 2004). There are numerous modes of action a pseudoenzyme can have an effect on cellular regulation. Some pseudoenzyme act by interfering with their counterpart active enzymes. For instance, pseudophosphatases EGG-4 and EGG-5 inhibit conventional phosphatase MBK-2 by sequestering it, hence stopping it from accessing its substrate (Cheng et al. 2009). Conversely, iRhoms, inactive rhomboid proteases, inhibit EGFR signalling by binding the ligands of rhomboid proteases, hence occluding them from their active counterparts (Adrain and Freeman 2012). Alternatively, pseudoenzymes can act as allosteric activator or suppressor (Murphy et al. 2017). For examples, pseudoprotease cFLIP binds and inhibits protease caspase-8 involved in apoptosis regulation (Chang et al. 2002).

It is easy to see how properties of pseudoenzymes fit well with the role of effectors in infection and the zig-zag model of plant immunity (see 1.8.1). For example, pseudoenzymes can act as decoys or 'dummys', where they act as ligands of enzymes or receptors, 'keeping them busy' while a different peptide remains undetected and free to act. A 'dummy' pseudoenzyme could be easily used as a distraction for an R gene product, preventing triggering the immune response. That is exactly the case in *Phytophthora sojae*, where the pathogen secretes both enzymatically active effector PsXEG1 as well as PsXEG1-like pseudoenzyme PsXLP1. PsXEG1 is recognised, bound and inactivated by host R gene product GmGIP1.

However, PsXLP1 has higher affinity to GmGIP1 than its active paralog, thus it is bound instead, leaving PsXEG1 free to act and contribute to virulence of *Ph. sojae* (Ma et al. 2017).

4.1.6 Aims

In this chapter I address the role of BEC1054 effector in *Blumeria graminis* infection. I hypothesise that the effector prevents host cell death by acting as a pseudoenzyme and binding to host ribosomes, occluding the SRL site from host RIPs. I investigated the effects of the effector on host ribosomal RNA as well as its relationship with host RIPs, using JIP60 as proof of concept.

4.2 Results

4.2.1 MeJA treatment leads to emergence of novel RNA species in wheat rRNA

In order to investigate the effects of PTI-induced, RIP-mediated host cell death, experiments were performed on MeJA treated wheat leaves. Firstly, I analysed total RNA profiles from the treated leaves. The leaves were floated on 100 ml of H_2O with either 40 μM MeJA or 0.1% DMSO. Then, total RNA was extracted and treated with aniline to induce breakage at depurinated sites, and RNA profiles were obtained using 2100 Bioanalyzer (Agilent) with Agilent RNA 6000 Nano chips (Figure 4.2). The RNA profiles revealed emergence of a novel RNA species (Figure 4.2b). The novel species manifests as a peak that appears on the profile between the peaks representing 16S and 23S rRNAs, and will be referred to as putative peak from now on.

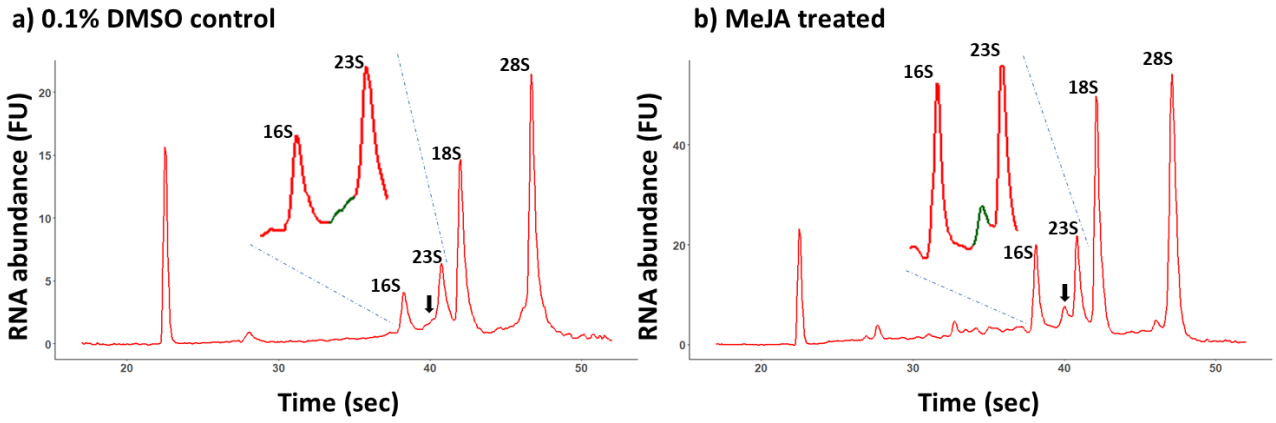


Figure 4.2: Emergence of putative peak in total RNA extracts from MeJA-treated wheat
Wheat was grown for 7 days before the primary leaves were collected and either treated with 40 μM MeJA or kept in 100 ml of 0.1% DMSO for following 4 days. Finally, total RNA was extracted from the samples and treated with aniline before the RNA profiles were obtained using Agilent 2100 Bioanalyzer. a) and b) show total RNA profiles of samples untreated and treated with MeJA, respectively. The identity of the major peaks is indicated (Krupp 2005), whereas the peak of interest is marked by black arrows. The green outline within the magnification illustrates which area was considered in peak abundance measurements. Representative RNA profiles are presented

In order to estimate the size of the putative peak, I used standard RNA markers of known sizes (Agilent RNA 6000 Nano ladder). By extrapolating the relation between the size of an RNA species and the time it appears on RNA profiles, I inferred the size of the putative peak to be around 1180 bases based on its position on the RNA profiles (Figure 4.3). However, it is important to note that due to the fact that the Agilent RNA 6000 Nano chips are a non-

denaturing method and that the RNA is prone to forming secondary structures, the size estimation is not reliable. This is demonstrated by the fact that on the RNA profiles, the bigger 23S rRNA species appears earlier than the smaller 18S rRNA species (Figure 4.3).

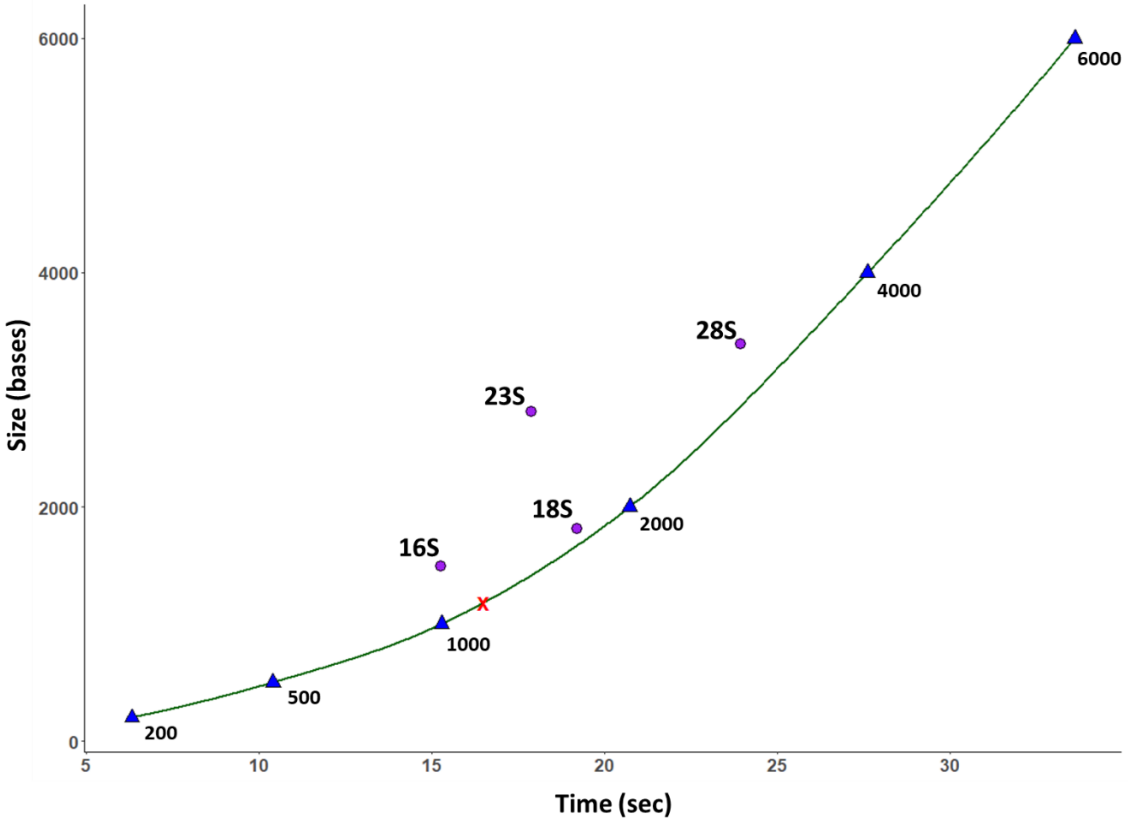


Figure 4.3: Size estimation of the putative peak using standard RNA markers
The size of peak of interest was estimated using standard RNA markers of known sizes resolved on Agilent 2100 Bioanalyzer. The blue triangles indicate the position and sizes of the standard RNA markers (Agilent RNA 6000 nano ladder). The green line illustrates the best fit regression line using loess method. The peak of interests resolves at approximately 16.5 sec; thus the red X shows its position on the regression line, indicating the estimated size of the putative peak to be 1180 bases long. NB: time is counted as a difference between the top point of a peak and a marker 25 bases in size

4.2.2 Effector BEC1054 alone is not sufficient to interfere with MeJA-induced host RNA degradation

I conducted further investigations of the putative peak to see how it is affected by *Blumeria* infection and the presence of BEC1054 effector. To do that, two transgenic wheat lines were used. The first one, was a homozygote possessing BEC1054 gene under constitutive promoter, while the second one was an azygote, a line that underwent the transgenic procedure but resulted in no transgenes; the latter line was used as the negative control. Seven-day-old plants of these two lines were split into two groups, one infected with *B. graminis* for three consecutive days while the other was kept uninfected under identical growth conditions but

in a separate enclosure. Subsequently, primary leaves were harvested and suspended in 100 ml of H_2O with MeJA for four days. Then the total RNA was extracted and the RNA profiles were obtained using 2100 Bioanalyzer (Agilent) with Agilent RNA 6000 Nano chips. The RNA profiles showed that the putative peak was most visible in samples from azygotic plants that were uninfected with *B. graminis* (Figure 4.4a), whereas the peak was visibly diminished in azygotic plants infected with *B. graminis* (Figure 4.4b). Moreover, in RNA profiles from uninfected BEC1054 positive homozygotic plants, the putative peak still appeared smaller than that from the uninfected azygotic plants (Figure 4.4 c&a, respectively). Finally, the putative peak on RNA profiles from the infected homozygotic plants appeared similar to that of the infected azygotic plants (Figure 4.4 d&b, respectively).

Subsequently, I attempted to quantify the putative peak by measuring the area under the peak using Agilent 2100 Expert software and standardising the data by presenting it as a percentage of the area under 28S rRNA peak of each RNA profile (Figure 4.5). The results were tested using first two-way ANOVA assess the effect of the genotype of the plants and their infection status on size of the putative peak. After checking assumptions and homogeneity of the data, the log transformation was applied. Moreover, each group was later tested using Tukey approach to establish statistical differences between each group. The experiment was repeated independently eight times. The ANOVA test showed that the infection status of the leaf is the most influential trait the size of the putative peak, explaining 28% of the variability within the data (*** p=0.0005). The data showed that the putative peak is substantially diminished in infected azygotic plants and infected homozygotes expressing BEC1054 (BEC1054 +ve infected), with respective medians of 2.145 and 1.260, in contrast to uninfected azygotic plants with median 1.010 and those differences are statistically significant (** p=0.002 and * p=0.011, respectively). The putative peak seems smaller on RNA profiles from the uninfected BEC1054 positive homozygotes than that of the uninfected azygotes (medians 1.390 and 2.145, respectively), however, without statistically significant difference (p=0.27), suggesting that BEC1054 effector alone is not sufficient in inhibiting the emergence of the putative peak and other *Blumeria* effectors may play an important, synergistic role in the phenomenon. No other groups showed statistically significant difference to any other group.

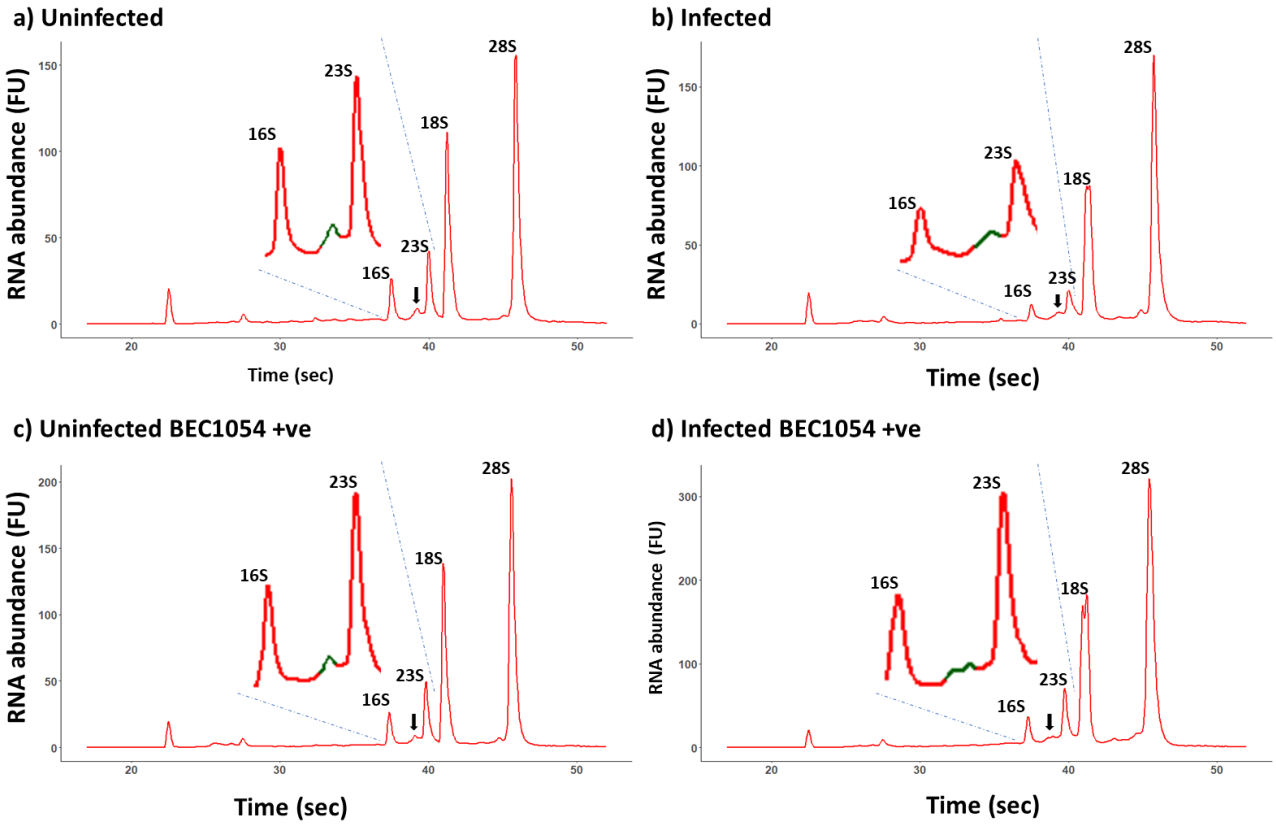


Figure 4.4: Total RNA profiles obtained from MeJA-treated transgenic wheat
Two lines of transgenic *T. aestivum* were used in this study: constitutively expressing BEC1054 effector homozygote and an azogotic control. 7-day-old plants from each line were split into two groups, one of which was inoculated daily with *B. graminis* for 3 days whereas the other was kept uninfected in a separate enclosure. Afterwards, the primary leaves were collected and treated with 40 μM MeJA and 0.1% DMSO in 100 ml of H_2O for following 4 days. Finally, total RNA was extracted from the samples and treated with aniline before the RNA profiles were obtained using Agilent 2100 Bioanalyzer. a) & b) show total RNA profiles obtained from azygotic plants, uninfected and infected with *B. graminis*, respectively. c) & d) show total RNA profiles of BEC1054 positive homozygotic plants, uninfected and infected with *B. graminis*, respectively. The identity of the major peaks is indicated (Krupp 2005), whereas the peak of interest is marked by black arrows, and outlined in green on the enlarged sections of the RNA profiles. The putative peak is visibly smaller in samples obtained from plants infected with *B. graminis*. Moreover, the peak is smaller in plants constitutively expressing BEC1054 in comparison to the control plants suggesting its involvement in the effect. Representative RNA profiles are presented

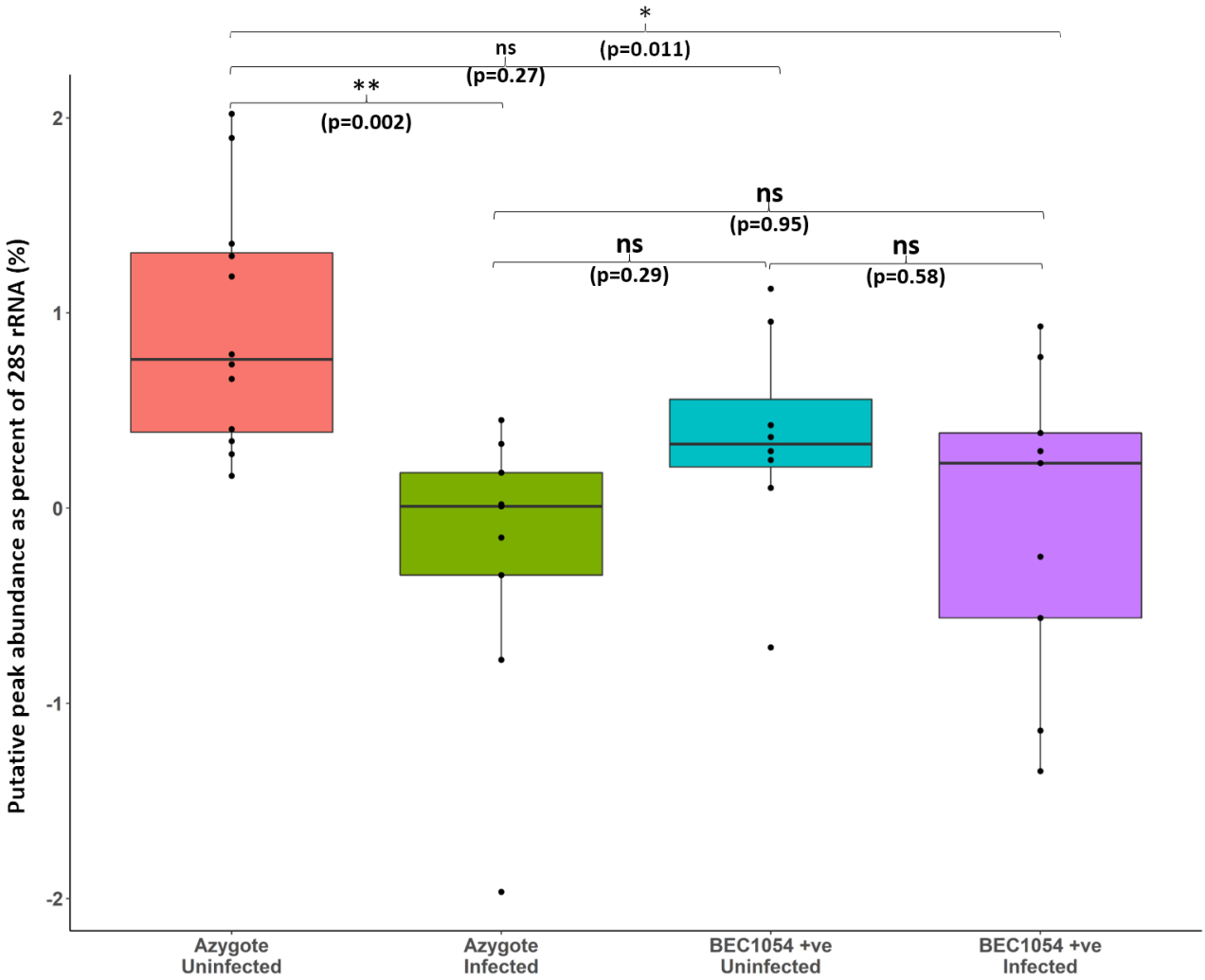


Figure 4.5: Relative abundance of putative RNA peak in total RNA extracts from MeJA-treated transgenic wheat primary leaves in response to presence or absence of *B. graminis*

Two lines of transgenic *T. aestivum* were used in this study: constitutively expressing BEC1054 effector homozygote and an azygotic control. 7-day-old plants from each line were split into two groups, one of which was inoculated daily with *B. graminis* for 3 consecutive days, whereas the other was kept uninfected in a separate enclosure. Afterwards, the primary leaves were collected and treated with 40 μM MeJA and 0.1% DMSO in 100 ml of H_2O for following 4 days. Finally, the total RNA was extracted from the samples and treated with aniline before the profiles were obtained using Agilent 2100 Bioanalyzer and the peak areas were estimated using Agilent 2100 Expert software. The relative abundance of the putative peak was calculated as percentage of the 28S rRNA peak and a log transformation was applied to increase homogeneity of the data. The experiment was repeated independently eight time and statistical analysis was performed using two-way ANOVA with R software, which showed that the infection status of the leaves had the biggest influence on the difference, accounting for 28% of the variability (*** p=0.0005). Subsequently, all group were then tested with TukeyHSD analysis. This indicated the difference in abundance of the putative peak between the uninfected and the infected azygotic plants (medians 2.145 and 1.010, respectively) is statistically significant (** p=0.002). Likewise, the difference in abundance between the uninfected azygote samples and the infected BEC1054 positive transgenic homozygote samples (medians 2.145 and 1.260, respectively) were found statistically significant (* p=0.011). No other groups showed statistically significant difference to each other

4.2.3 Effector BEC1054 inhibits JIP60-mediated necrosis *in planta*

I assumed that the MeJA-induced host rRNA degradation is mediated by RIPs such as JIP60 (Reinbothe et al. 1994a; Reinbothe et al. 1994b). Therefore, a set of experiments were designed to investigate whether BEC1054 could interfere with JIP60-mediated necrosis. Previous work showed that BEC1054 does not directly interact with JIP60 (Pennington et al. 2016b). In order to assess whether the effector could interfere indirectly with the function of JIP60 RIP domain *in planta* both proteins were expressed in plant tissue via agroinfiltrations by injecting leaves of *N. benthamiana* with Agrobacteria carrying constructs containing JIP60ml along with either BEC1054 gene or GFP as a control.

The effects of agroinfiltrations of JIP60ml into the leaves varied from plant to plant in both appearance and timescale. The earliest effects of JIP60ml agroinfiltration visible to the naked eye, were seen at 4 dpi (Spanu, P., pers. comm.); however, they could be delayed up to 8 dpi, by decreasing the amount of Agrobacterium injected to OD_{600}=0.01 (data not shown). JIP60-mediated necrosis also varied in resulting phenotype. Most commonly, it led to loss of pigment within the zone, as well as to visible thinning of the leaf lamina making it prone to tearing (Figure 4.6). Moreover, the texture of the leaf changed noticeably from smooth and flexible to coarse and "leathery". Systematic experimentation and comparison showed that the presence of BEC1054 affected the phenotype caused by JIP60ml (Figure 4.6a). When JIP60ml is co-expressed with GFP, the necrosis proceeds unhindered. The first signs of necrosis were visible on the abaxial surface of the leaves as tiny, glassy spots, even though no discolouration was yet visible (Figure 4.6b). The necrotic lesions likewise varied in appearance rather than affect the entire zone uniformly: from distinct, defined spots of various sizes to marbling and mottling within the infiltration zone (Figure 4.7). Conversely, when JIP60ml is contested with BEC1054, the necrosis is delayed. The infiltration zone still showed chlorosis but the other symptoms of cell death, such as the thinning of leaf lamina and lesions, were not present.

To investigate the effects of BEC1054 effector on JIP60-mediated necrosis, a time course was set up where the active RIP domain JIP60ml was co-agroinfiltrated along with either

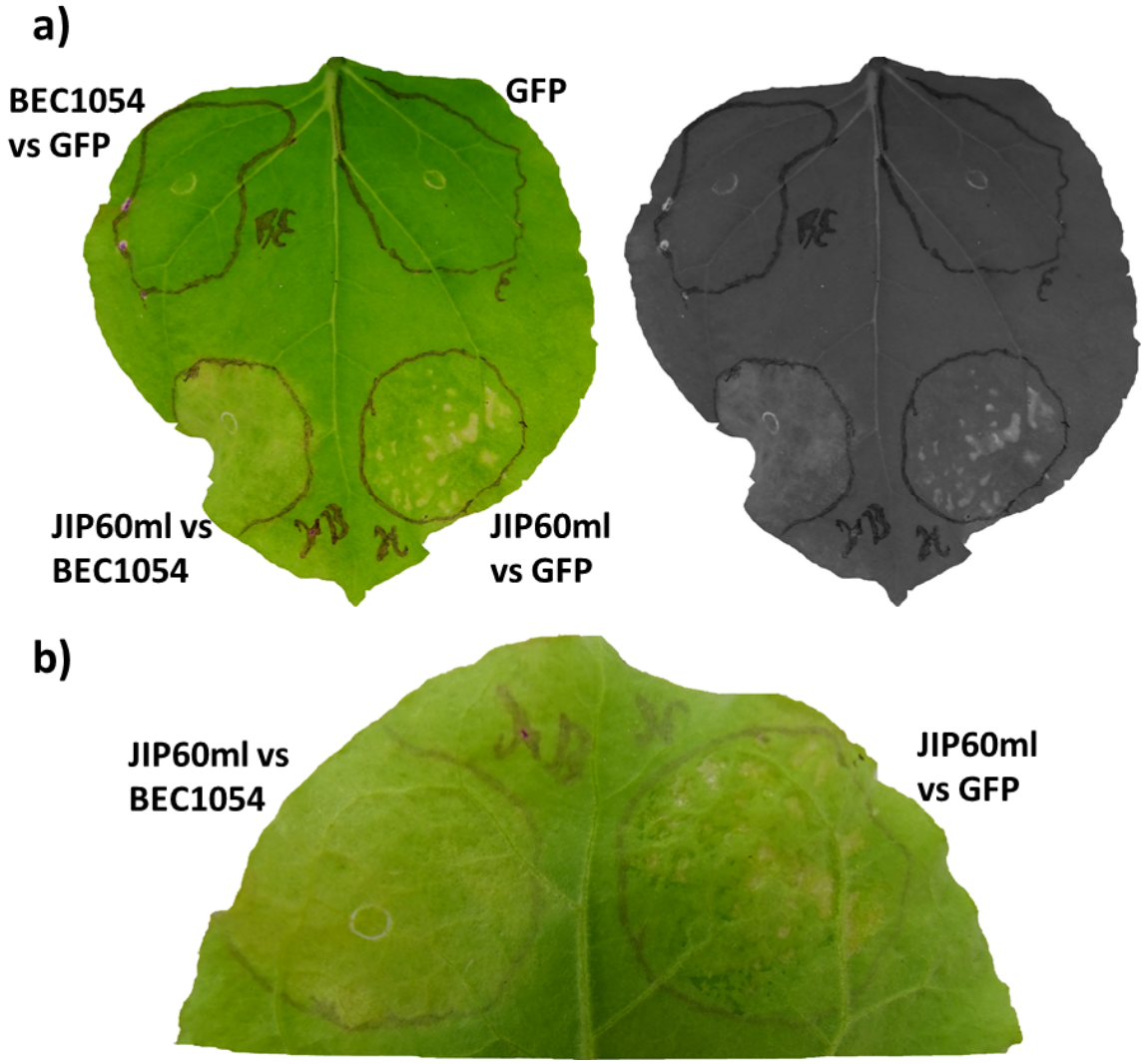


Figure 4.6: Observation of JIP60 RIP domain-mediated necrosis in agroinfiltrated *N. benthamiana*
N. benthamiana leaves agroinfiltrated with JIP60 RIP domain exhibit necrosis. It manifests in loss of pigment due to chlorosis, thinning of the leaf lamina and change in texture from smooth and flexible to coarse and leathery. However, only chlorosis is a quantifiable parameter. Arguably, the loss of pigment is better visible in grey scale, where the picture contrast is increased. The necrosis can be quantified by measuring luminosity, the brightness of pixels. The brighter they are, the greater loss of pigment, hence more progressed necrosis

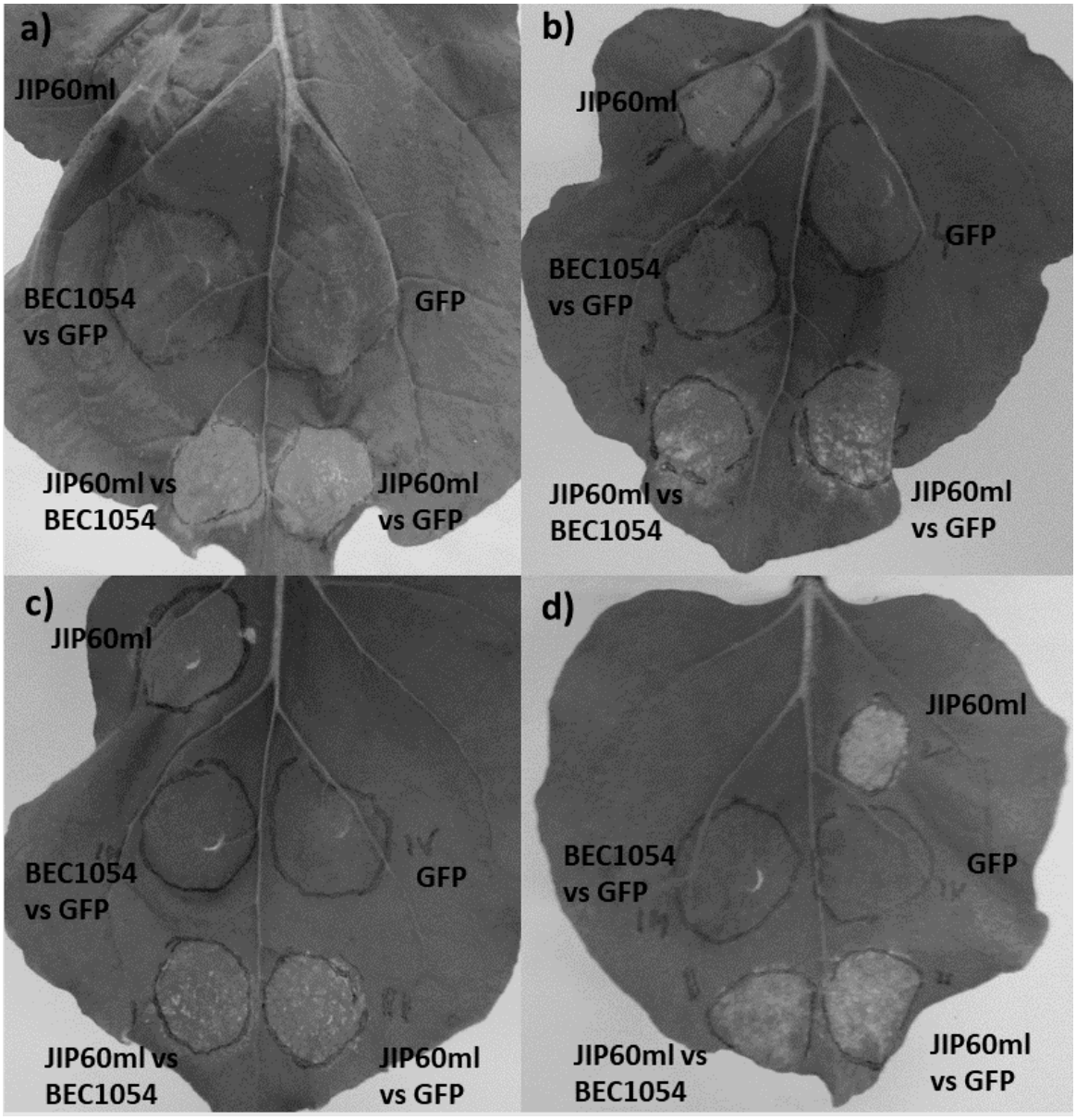


Figure 4.7: Comparison of necrotic phenotypes resulting from agroinfiltration with JIP60 RIP domain
Each *N. benthamiana* leaf was infiltrated with following mixtures of Agrobacteria carrying appropriate plasmids: JIP60ml contested with either BEC1054 or GFP at 1:8 ratio (JIP60ml OD_{600}=0.025, BEC1054 or GFP OD_{600}=0.2), BEC1054 and GFP at 8:1 ratio (OD_{600}=0.2 and OD_{600}=0.025, respectively) and GFP control on its own (OD_{600}=0.225). Additional control includes JIP60ml on its own (OD_{600}=0.025). Infiltration with JIP60/GFP (zones in right bottom corners) produced diverse necrotic phenotypes: a) uniform; b) defined spots; c) mottling; d) marbling

BEC1054 (JIP60ml vs BEC1054, OD_{600}=0.02 and OD_{600}=2.0, respectively) or GFP as a control (JIP60ml vs GFP, OD_{600}=0.02 and OD_{600}=2.0, respectively). Other controls were co-agroinfiltration of BEC1054 with GFP (BEC1054 vs GFP, OD_{600}=2.0 and OD_{600}=0.02, respectively), JIP60ml-only (JIP60ml, OD_{600}=0.02) and Agrobacterium free of plasmids (EV, OD_{600}=2.12). All infiltrates, apart from the EV control, also contained Agrobacterium with P19 plasmid (OD_{600}=0.1); the expression of P19 ensures a better and more uniform expression (Voinnet et al. 2003). Pictures of the agroinfiltrated leaves were taken at 3, 6, 8, 10, 13 and 15 days post infiltration (Figure 4.8).

At 3 dpi, only the zone infiltrated with JIP60ml control showed the early stages of chlorosis, while the other zones showed no visible symptoms of necrosis. At 6 dpi, the chlorosis in zones co-agroinfiltrated with JIP60ml and either BEC1054 or GFP become continuously more apparent as the time-course progresses. From 10 dpi, other control zones start showing signs of stress and exhibit chlorosis but no other signs of necrosis, such as leaf lamina thinning. That stress is most likely due to presence of large amount of bacteria as it is also visible in the zone infiltrated with EV control. As the time course continues, the JIP60ml vs GFP zone exhibits other symptoms of necrosis other than chlorosis, including leaf lamina thinning and lesions. Those symptoms are either not visible or delayed in JIP60ml vs BEC1054 zone. The zone with the fastest progressing necrosis is JIP60ml-only control where it is not encumbered by the presence of bacteria with other plasmids.

Following examination of the phenotype, it became clear that necrosis is a continuous process and needs quantification method to make a comparison between treatments possible. Chlorosis, which is one of the early visible symptoms of necrosis, is due to loss of green pigment and on a grey scale it appears as brighter pixels. Therefore, I quantified necrosis by converting photos of agroinfiltrated leaves into grey scale and analysing luminosity (pixel brightness), the higher the luminosity, the further the progression of necrosis (Figure 4.9). The method was adapted from protocol developed by colleague Dr Linhan Li (Li 2018). The time-course experiment was repeated and the pictures for the necrosis measurement were taken at 4, 7 and 10 dpi.

The experiment was repeated five times using the total of 30 leaves, each counted as an in-

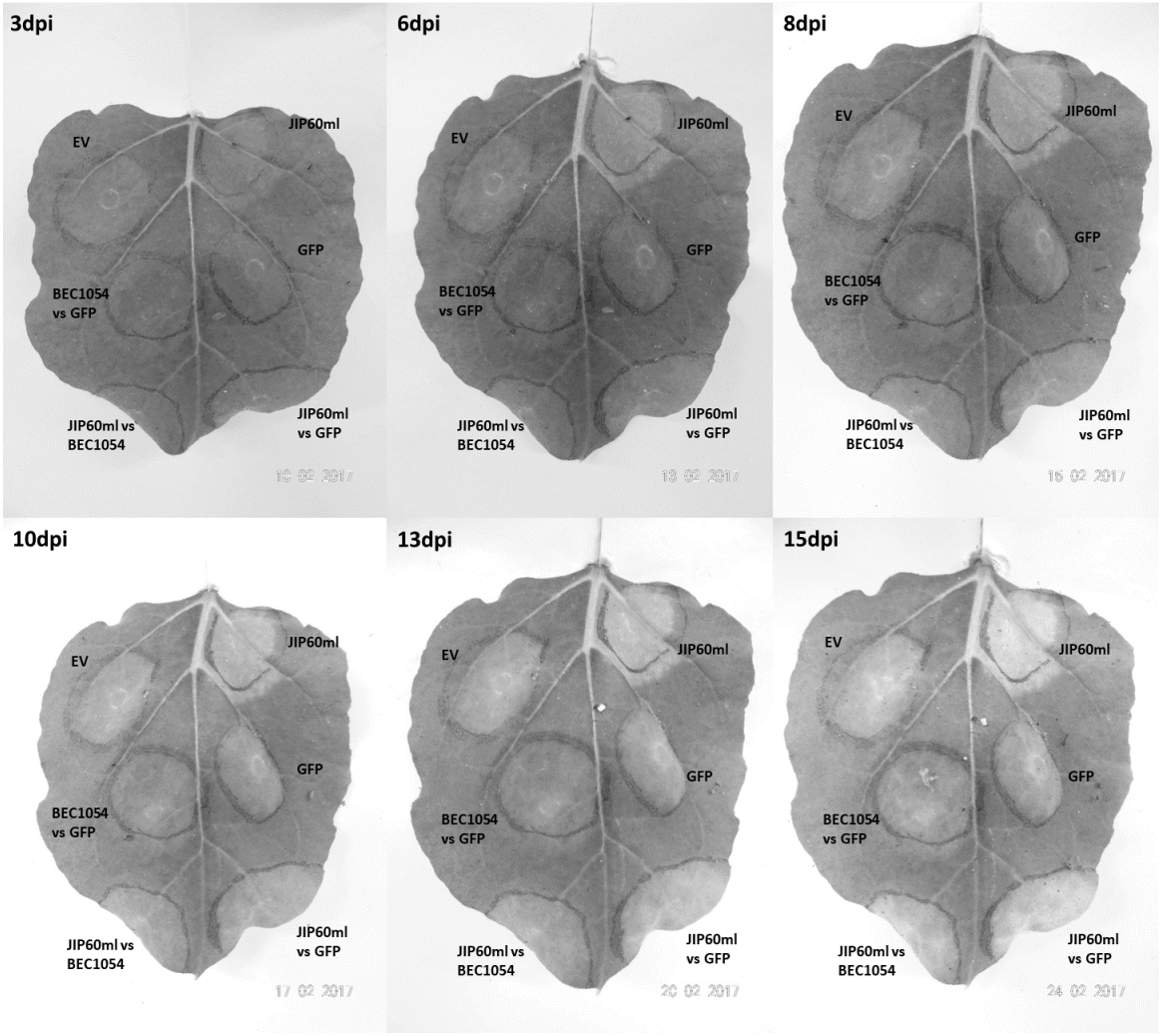


Figure 4.8: Time course of co-agroinfiltration of *N. benthamiana* with JIP60 contested with either BEC1054 or GFP

Each *N. benthamiana* leaf was infiltrated with following mixtures of Agrobacteria carrying appropriate plasmids: JIP60ml contested with either BEC1054 or GFP at 1:100 ratio (JIP60ml OD_{600}=0.02, BEC1054 or GFP OD_{600}=2.0), BEC1054 and GFP at 100:1 ratio (OD_{600}=2.0 and OD_{600}=0.02, respectively) and GFP control on its own (OD_{600}=2.12). Additional controls include Agrobacterium without any plasmid (EV – empty vector; OD_{600}=2.12) and JIP60ml-only (OD_{600}=0.02). All infiltrates included P19 (OD_{600}=0.1), apart from EV control. JIP60/GFP infiltrate led to emergence of lesions within the zone whereas JIP60/BEC1054 infiltrate led to discolouration of the zone but no visible necrosis of the leaf tissue. There were no necrotic effects of either BEC1054/GFP or GFP-only infiltrates on the leaf

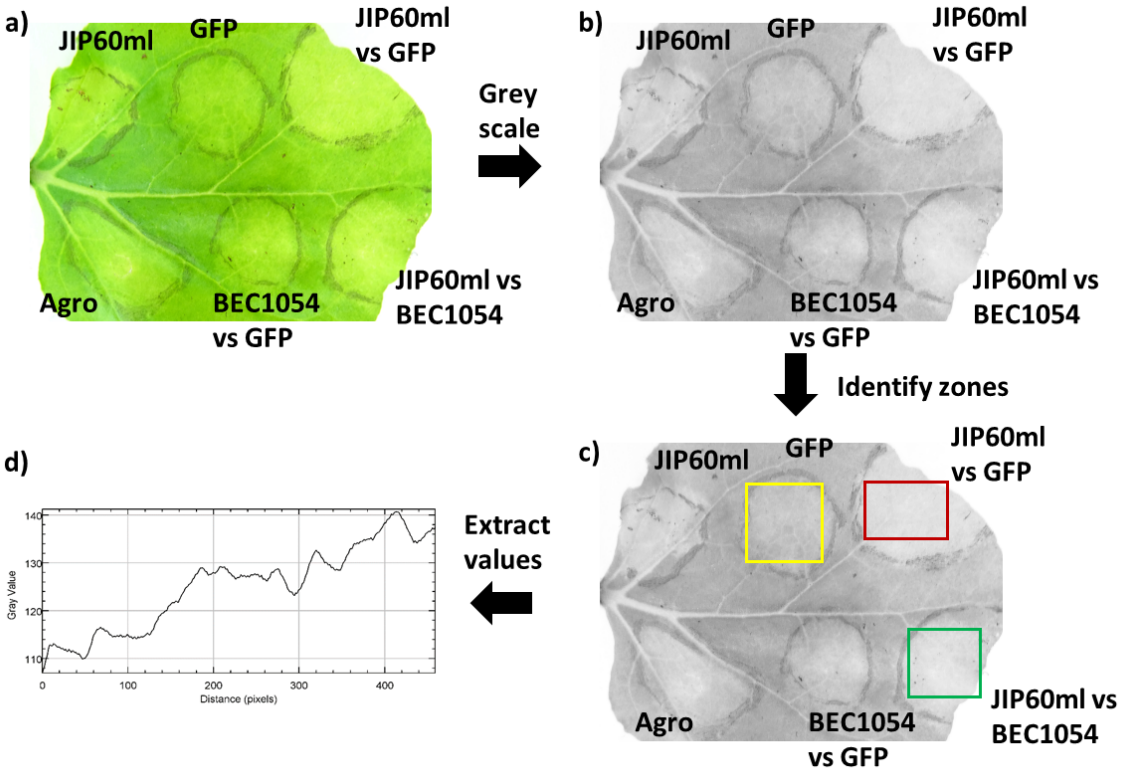


Figure 4.9: Flow chart of measuring grey scale intensity/luminosity of agroinfiltrated zones
Each agroinfiltrated *N. benthamiana* leaf was photographed (a). Subsequently, each photograph was transformed into grey scale to increase contrast (b) and zones were identified and marked for measurement, so all the boxes cover as much of each zone as possible, to avoid introduction of a bias due to picking the most favourable regions within the zone (c): GFP only (yellow), JIP60ml vs GFP (red), JIP60ml vs BEC1054 (green). Luminosity values were measured with ImageJ software (d). JIP60ml vs BEC1054 and JIP60ml vs GFP values were then standardised by subtracting the GFP control value from a corresponding leaf. (Method adapted from protocol developed by Dr Linhan Li)

dividual repeat. Using this method to measure necrosis, the data showed that BEC1054 effector does in fact inhibit JIP60ml-mediated host cell death. The statistical analysis used involved linear mixed model where the presence or absence of BEC1054 was considered the fixed effect, taking into account the variability introduced by the age and the differences between the leaves as random effects. The linear mixed model showed that the presence of BEC1054 has an effect on the luminosity which is statistically significant (* p=0.0136), when the random effects from the age of the leaf and the individual differences between the leaves are considered. The individual differences between the leaves account for 5% of the variability, whereas the age of the leaf explains 12% of the variability between the samples. The overall luminosity time course medians were 36.4 AU and 30.5 AU (Δ=5.9 AU) for JIP60ml vs GFP and JIP60ml vs BEC1054, respectively (Figure 4.10a). When the treatments were considered at specific time points, the medians where BEC1054 was present were consistently lower than where JIP60ml was contested with GFP instead. The respective medians for JIP60ml vs GFP and JIP60ml vs BEC1054 were respectively: 41.1 AU and 36.5 AU (Δ=4.6 AU) at 4 dpi, 31.9 AU and 28.6 AU (Δ=3.3 AU) at 7 dpi, and 34.5 AU and 28.3 AU (Δ=6.2 AU) at 10 dpi. These results were analysed using TukeyHSD test considering differences between individual leaves as a random effect, however, none of the groups within a time point showed statistically significant difference between treatments (Figure 4.10b).

4.2.4 Effect of BEC1054 effector on JIP60 RIP domain and *in vitro* translation

Next, the effect of BEC1054 effector on JIP60 RIP domain-mediated ribosome inhibition was investigated *in vitro*. To that purpose reticulocytes lysate (Thermo Fisher) *in vitro* transcription/translation assay was used. Firstly, cDNA of JIP60ml, BEC1054 effector and 1 kbp fragments of rRNA was amplified with T7 promoter. Subsequently, the 10 μl reaction mixtures were created according to the Table 4.1. The experiment was designed so all tested conditions had the same amount of cDNA. Next, the lysates were incubated at 30°C for 2 hr to allow for the proteins to be transcribed and translated. Then luciferin was added and luminescence from the luciferase activity was measured as an indirect indication of ribosome

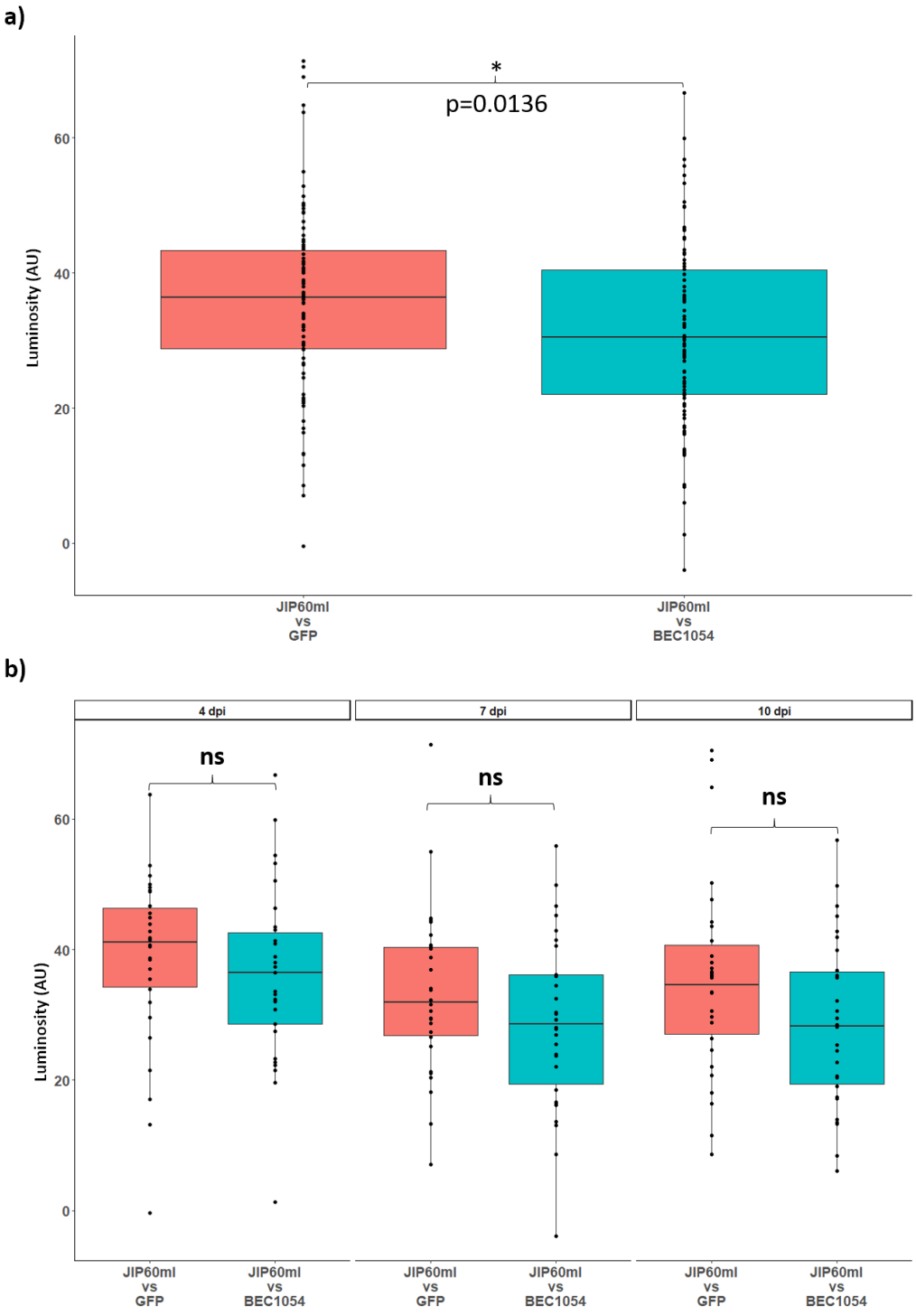


Figure 4.10: Time course of JIP60ml and BEC1054 competition in *N. benthamiana* leaves
N. benthamiana leaves were co-agroinfiltrated with JIP60ml contested with either BEC1054 or GFP at 1:100 ratio (JIP60ml OD_{600}=0.02, BEC1054 or GFP OD_{600}=2.0), BEC1054 and GFP at 100:1 ratio (OD_{600}=2.0 and OD_{600}=0.02, respectively) and GFP control on its own (OD_{600}=2.12). Additional control included JIP60ml on its own (OD_{600}=0.02). All infiltrates included P19 (OD_{600}=0.1). Pictures for measurements of luminosity were taken at 4, 7 and 10 days post infiltration. The experiment was repeated five times using the total of 30 leaves, each considered an independent repeat. a) The leaf zones co-agroinfiltrated with JIP60ml contested with BEC1054 effector showed statistically significant lower necrosis than the control contested with GFP across the whole time course (* p=0.0136). The statistical analysis was performed using linear mixed model where differences introduced by age of the leaf and differences between individual leaves were taken into account as random effects. Those effects explain 5% and 12% of the variability between the samples, respectively. b) When considering individual time points, the data showed consisted trend in which the zones co-agroinfiltrated with JIP60ml and BEC1054 showed lower necrosis than the zones co-agroinfiltrated with JIP60ml and GFP, however, TukeyHSD statistical analysis showed no statistically significant difference between the treatments within the time points.

activity. The experiment was repeated three times and the results were analysed using linear mixed model, taking into account the differences between the repeats as a random effect. The differences between repeats explain 47% of the variability between the samples. Subsequently, TukeyHSD test was used to assess any potential statistically significant differences between the samples. The luciferase-only (positive) control and the rRNA control had medians of $14.8 * 10^5$ FU and $8.8 * 10^5$ FU, respectively. This showed that inclusion of any cDNA alongside luciferase decreases the amount of luciferase produced, indicating competition in ribosome biding between transcripts. Both JIP60ml and BEC1054 translated on their own lead to further drop of luciferase activity, indicating ribosome inhibition by either protein. BEC1054 seems to cause a bigger decrease in luciferase activity than JIP60ml with their respective medians at $5.2 * 10^5$ FU and $6.4 * 10^5$ FU, but there is no statistically significant difference between the two (p=0.38). When both JIP60ml and BEC1054 are present in the reaction, the ribosome inhibition seems to be even more pronounced, with the median of $4.8 * 10^5$ FU. The difference in luciferase activity between BEC1054-only and JIP60ml and BEC1054 together was not statistically significant (p=0.46), while the difference in luciferase activity between JIP60ml-only and JIP60ml together with BEC1054 was statistically significant (** p=0.0026). JIP60-only, BEC1054-only and JIP60 wih BEC1054 together were all statistically significant from the rRNA control (*** $p < 0.001$). Furthermore, all groups were statistically significant from both the negative and the positive controls (*** $p < 0.001$).

	cDNA (ng)				
TnT Reaction	rRNA	JIP60ml	BEC1054	Luciferase	Total
−ve control	0	0	0	0	0
+ve control	0	0	0	160	160
rRNA	120	0	0	160	280
JIP60ml	80	40	0	160	280
BEC1054	40	0	80	160	280
JIP60ml vs BEC1054	0	40	80	160	280

Table 4.1: List of transcription/translation (TnT) reactions for JIP60ml and BEC1054 competition *in vitro* experiment
This table shows a list of reactions used in /textitin vitro transcription/translation experiment using reticulocyte lysate. Each row represents a mixture used and states how much of each cDNA was used in ng. Each cDNA was first amplified with a T7 promoter. The experiment was designed in a way that all tested conditions had the same amount of cDNA

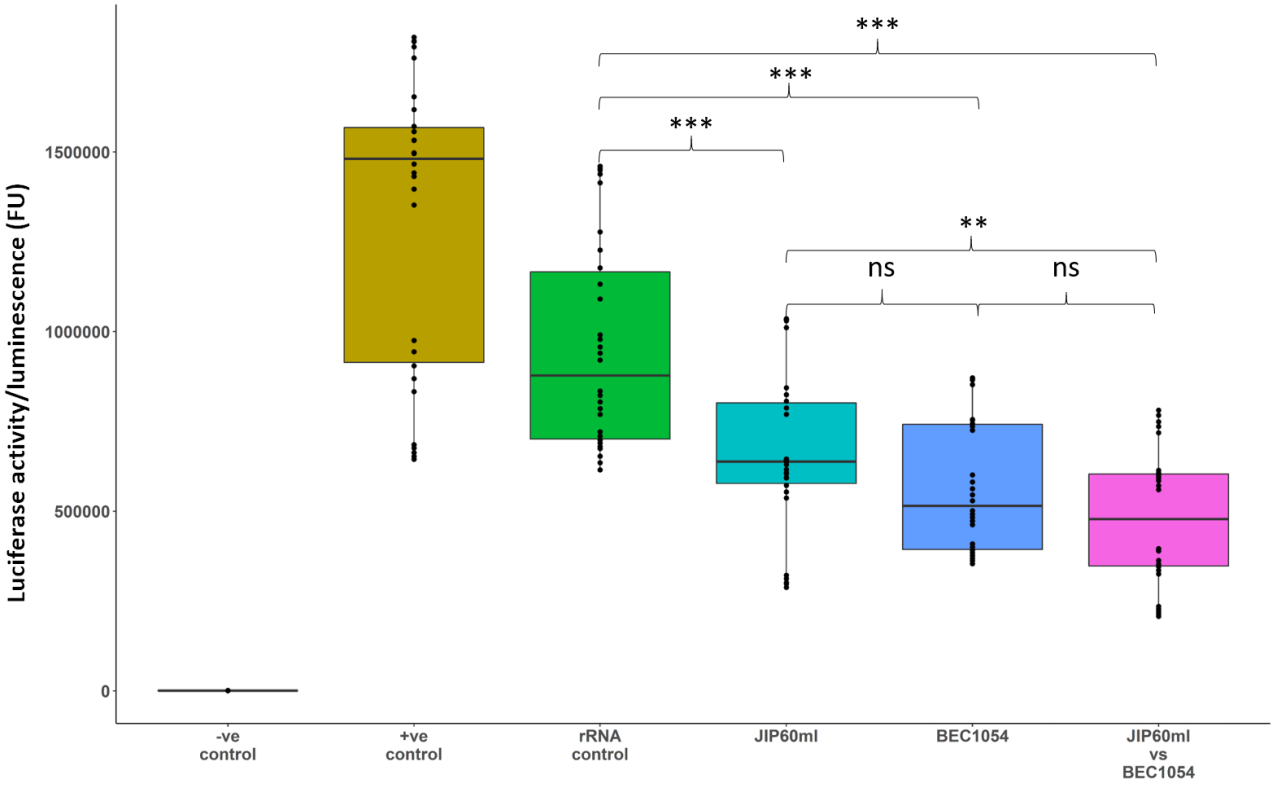


Figure 4.11: Effect of BEC1054 and JIP60ml competition on ribosome inhibition *in vitro*
The effect of BEC1054 effector on JIP60 RIP domain-mediated ribosome inhibition was investigated with reticulocytes lysate (Thermo Fisher) transcription/translation *in vitro* assay. Firstly, cDNA of JIP60ml, BEC1054 effector and 1 kbp fragments of rRNA was amplified with T7 promoter. Subsequently, the following 10 μl reactions were created: rRNA control with 120 ng of T7:rRNA cDNA, JIP60ml with 40 ng of T7:JIP60ml cDNA and 80 ng of T7:rRNA cDNA, BEC1054 with 80ng of T7:BEC1054 cDNA and 40 ng of T7:rRNA cDNA. Each reaction, including the positive control, also contained 160 ng of T7:luciferase cDNA, apart from the negative control which only contained the lysate. The lysates were incubated at 30°C for 2 hr, followed by addition of luciferin and then the luminescence from the luciferase activity was measured as an indirect indication of ribosome activity. The experiment was performed three separate times. The luciferase-only (positive) control and the rRNA control had medians of $14.8 * 10^5$ FU and $8.8 * 10^5$ FU, respectively. JIP60ml and BEC1054 translated on their own lead to further drop of luciferase translation, indicating ribosome inhibition by the produced proteins. BEC1054 seems to cause a bigger decrease in luciferase activity than JIP60ml with their respective medians at $5.2 * 10^5$ FU and $6.4 * 10^5$ FU. When both JIP60ml and BEC1054 are present in the reaction, the ribosome inhibition seems to be even more pronounced, with the median of $4.8 * 10^5$ FU. The difference in luciferase activity between JIP60ml-only and BEC1054-only, as well as between BEC1054-only and JIP60ml and BEC1054 together was not statistically significant (p=0.38 and p=0.46, respectively). However, the difference in luciferase activity between JIP60ml-only and JIP60ml together with BEC1054 was statistically significant (** p=0.0026). JIP60-only, BEC1054-only and JIP60 wih BEC1054 together were all statistically significant from the rRNA control (*** $p < 0.001$). Furthermore, all groups were statistically significant from both the negative and the positive controls (*** $p < 0.001$) The statistical analysis was performed using linear mixed model taking into account the random effect from differences between repeats, and using TukeyHSD test between each group

4.3 Discussion:

4.3.1 BEC1054 inhibits MeJA-mediated host rRNA degradation

Methyl-jasmonate is one of the members of the jasmonates phytohormone family and it plays a crucial role in both plant defence and senescence (Cheong and Choi 2003). Research shows that the outcome of MeJA treatment depends on concentration levels and length of exposure. Relatively short exposure or concentration level below the threshold triggers remodelling of expression patterns, often gearing the plant against biotic and abiotic stresses, and immune defence (Duan et al. 2014). In contrast, prolonged exposure to MeJA or its accumulation to the concentration that above the threshold leads to premature senescence and host cell death (Repka et al. 2001; Reinbothe et al. 1994a). MeJA is sufficient to cause plant cell death in absence of any avirulence trigger in grapevine (Repka et al. 2001).

JIP60 is one of the proteins that are induced by MeJA (Reinbothe et al. 1994b). Bearing in mind that RIPs, such as JIP60, affect translation via ribosome inhibition by SRL depurination, we analysed the total RNA profiles of MeJA treated wheat leaves. The RNA profiles obtained from aniline-treated total RNA extracts from MeJA-treated wheat leaves showed emergence of a novel RNA species, approximately 1180 bases in size. Aniline was used in order to cause breakage of the rRNA backbone at the depurinated site (Peattie 1979). Since this step occurs completely *in vitro* and no transcription apparatus is present, I assume the novel RNA species, the putative peak, is a result of a degradation event, and not *de novo* transcription.

The results of the MeJA treatment experiment on transgenic wheat showed that *B. graminis* infection interferes with host rRNA degradation. The presence of the BEC1054 effector alone was not sufficient to achieve the same level of the interference, but only showed a small, not statistically significant decrease in abundance of the putative peak. However, it is clear that BEC1054 is not the only factor involved. Both the BEC1054 azygotic and homozygotic transgenic wheat lines showed a decreased emergence of the putative peak when infected in comparison to uninfected homozygotic line. In fact, the infection status of the plant seems

to be the most important factor influencing the emergence of the putative peak. This suggests that there are other effectors that play a role in this process. It is hardly surprising. *Blumeria* genome harbours over 500 CSEPs with potentially various functions (Pedersen et al. 2012). Over 120 of them belong to RALPHs. It is not hard to imagine that many of these effectors would work synergistically or there could be a redundancy. For example, BEC1019 also interferes with host cell death, however it is believed to so do via different mechanism, i.e. suppressing HR by outcompeting plant R proteins in binding their ligands, necessary for eliciting immune response (Whigham et al. 2015).

Here, I propose that the BEC1054 effector is involved in the interference with host cell death by physically masking the SRL site on plant ribosome, hence obstructing host RIPs from attachment and depurination of the site, and subsequent host rRNA degradation. That is why, presence of the effectors inhibits the emergence of the putative peak, which is most likely originating from degradation of the 28S rRNA of the host.

Unfortunately, I was not able to determine the precise identity of the putative peak. I attempted mapping of the sequence using northern blot probes, however, this approached proved to be unsuccessful (Data not shown). Furthermore, the size approximation is only a crude estimation which is based on linear extrapolation of resolution of RNA standards. The Agilent 2100 Bioanalyzer used is a non-denaturing method, whereas RNA is prone to creating secondary structures that affect the rate of resolving on a gel, thus rRNA often does not resolve linearly (Krupp 2005). It is possible the actual size of the putative peak is smaller than predicted, but due to the secondary structures it resolves slower through the gel matrix (Goda and Minton 1995). Regardless, the size of the peak seems to be relatively substantial, approximated to be over 1000 bases. As the putative peak is thought to be a result of a degradation event, it had to originate from a larger RNA species. In total RNA, only 23S and 28S are suitably large candidates and since the SRL is located on 28S fragment, suggesting the putative peak originates from it (Shi et al. 2016).

It is necessary to mention that this work was performed in wheat, due to availability of the BEC1054 positive transgenic wheat lines, rather than in barley which JIP60 is native to. This creates a problem of directly interpreting the results. Ideally, similar lines would be

created and tested in barley. However, creating stably expressing transgenic lines in cereals is very costly and time consuming, and it was not within the capacity or time frame of this project. As wheat transgenic lines were available, they were deemed a suitable substitute. Wheat genome possesses a number of RIPs. Even though, due to low sequence conservation in RIPs, they do not share much sequence similarity, they still possess the usually conserved residues and are thought to assume the RIP fold. Moreover, although *B. graminis* f.sp. *tritici* possesses BEC1054 homologs, the effector is native to *B. graminis* f.sp. *hordei* (Oberhaensli et al. 2011; Parlange et al. 2011). Nonetheless, as shown by the rRNA analysis of MeJA treated wheat leaves and co-agroinfiltration experiments, BEC1054 seems to be effective even in non-host species, such as both wheat and *N. benthamiana*, suggesting a generic mode of action (Pliego et al. 2013).

4.3.2 BEC1054 interferes with JIP60

Since we established that BEC1054 inhibits what appears to be RIP-mediated host rRNA degradation, and it does so by employing a generic method, I investigated whether BEC1054 is capable of inhibiting RIP activity *in planta* using direct competition with JIP60ml as a proof of concept.

The co-agroinfiltration experiments showed that BEC1054 seems to interfere with JIP60-mediated host cell death *in planta*. It does not stop it completely, but the effects are delayed in comparison to positive control (JIP60ml vs GFP) and often fewer symptoms of necrosis are present. The interference is shown by a small but consistent drop in luminosity in the samples where JIP60ml is contested with BEC1054 effector. This decrease can be seen as a trend at all the time points the measurements were taken and during the whole time course as an average. Throughout the time course, the difference between the BEC1054 treatment and the control remains small and without statistically significant difference. When the experiment is taken as the whole, there is a clear statistically significant difference between coupling JIP60ml with either BEC1054 or GFP. Moreover, the random effects, i.e. the differences between individual leaves and the age of the leaf, are responsible only for 5% and 12% of the variability, respectively. BEC1054 is a relatively promiscuous protein: a pull-down

it interacts with many proteins, such as GST, MDH or PR5 (Pennington et al. 2016b). However, BiFC and Y2H experiments showed it does not directly interact with JIP60 RIP domain (Pennington 2014; Pennington et al. 2019). Therefore, since BEC1054 seems to have an effect on JIP60-mediated cell death, the interference could be a result of an indirect interaction, in which the effector associates itself with host ribosomes, occluding the SRL site from host RIPs, such as JIP60, hence preventing depurination of the site and subsequent cell death.

The co-agroinfiltration competition assay has a few caveats. Firstly, both JIP60 and BEC1054 are not native to *N. benthamiana*, a dicot plant. Therefore, their efficacy can be altered by the non-native environment. Secondly, measuring progress of necrosis by the intensity of chlorosis is only an indirect measure of the process. A different, more direct methods would be preferable, in order to obtain more solid evidence. For example, other methods, such as use of trypan blue assay to stain dead cells or imaging with UV light, to visualise phenolic compounds released by dying plant cells should be trialled. Finally, the phenotype of necrosis is not always consistent. It is most likely due to the fact that agroinfiltration is not a fully controllable process and the expression can vary between repeats. Throughout this study, many ratios between JIP60ml and BEC1054 Agrobacterium strains were tested, and only a high ratio of 100:1 BEC1054 to JIP60ml gave consistent results. I used such a disproportionate ratio as BEC1054 is expressing relatively poorly in comparison to other constructs (Bruderer, M. and Pennington, H. pers. comm.). To alleviate this, I used Agrobacterium strain carrying P19 within the mixture to ensure a better and more uniform expression of all constructs (Voinnet et al. 2003). Moreover, in order to make sure it is BEC1054 that is having the effect on JIP60-mediated host cell death, GFP was co-agroinfiltrated along JIP60ml as a control at the same ratio. It is worth noting that GFP is more than twice the size of BEC1054, therefore if the effect seen in the infiltration zones with JIP60ml and BEC1054 was due to molecular crowding, that effect would likely be even more pronounced in the zones co-agroinfiltrated with GFP. Unfortunately, no data confirming the presence of the BEC1054 effector was collected for this set of experiments. Therefore, it cannot be unequivocally stated that the effect seen here is due to the presence of the effector. This should be addressed in the future, e.g. by performing western blotting. Moreover, this approach could make it pos-

sible to address the problem of appropriate protein loading and to design the experiment so the ratio between JIP60ml and BEC1054 is not disproportionate.

The *in vitro* competition assay gave no solid conclusions. It would seem that both JIP60ml and BEC1054 cause drop in luciferase translation. Firstly, the *in vitro* translation is a closed system with finite resources and limited number of ribosomes, hence simply a presence of another transcript will lead to fewer copies of the other one to be translated. However, the observed luciferase activity in JIP60ml and BEC1054 reactions is lower than that observed in rRNA loading control. That suggests that both peptides have the capacity to inhibit translation. In fact, previous experiments with BEC1054 showed capability to inhibit translation in yeast most likely due to its association with ribosomes (Pennington et al. 2016a). Interestingly, when JIP60ml and BEC1054 are expressed together, the luciferase activity seems to be even lower than when either of the peptides is expressed individually. That was surprising because as BEC1054 seems to interfere with JIP60ml-mediated cell death *in planta*, I expected the presence of BEC1054 would have rescued the luciferase translation from JIP60ml-mediated inhibition. However, *in vitro* translation assays are notoriously difficult to optimise. Due to varied, and often conflicting results between repeats, more experiments are required to obtain conclusions. The linear mixed model suggested that the differences between repeats are responsible for 47% of variability between the samples, which is a substantial amount. One of the possibilities of optimisation would be to use wheat germ extract instead of reticulocyte lysate, as plant ribosomes would make it more similar to the native environment of the peptides in question.

In conclusion, BEC1054 seems to play a vital role in *Blumeria* infection and it seems to be involved in interference of host cell death which is one of the immune responses to biotrophic invasions. BEC1054 seem to inhibit some of the host rRNA degradation induced by MeJA treatment. Moreover, BEC1054 showed to hinder JIP60-mediated host cell death *in planta*, most likely employing a generic mode of action, such as occlusion of the host ribosome SRL site. BEC1054 was not able to rescue JIP60-mediated translation inhibition *in vitro*. In fact, the effector itself seemed to have an inhibitory effect on translation. Further investigation is necessary to elucidate the precise mode of action of BEC1054 effector.

Chapter 5: Mode of action of RALPH effector BEC1054

5.1 Introduction

5.1.1 *Blumeria* effectors

Analysis of *Blumeria* genome and proteome led to the discovery of a whole arsenal of effectors. First, proteomics study revealed *Blumeria* effector candidates (BECs) which were described as proteins specifically found in host cells colonised by haustoria (Bindschedler et al. 2009). Subsequently, an extensive combined genomics, transcriptomics and proteomics study showed an existence of a wider range of potential effectors, i.e. candidate secreted effector proteins (CSEPs) which were characterised by the presence of a signal peptide and lack of homology outside the *Erysiphales* clade (Spanu et al. 2010; Pedersen et al. 2012). There are now over 500 CSEPs identified in *Blumeria* genome, incorporating many of the BECs as well (Pedersen et al. 2012; Frantzeskakis et al. 2018).

5.1.2 BEC1054 - RALPH effector crucial for powdery mildew infection

Host induced gene silencing (HIGS) experiments highlighted a number of effectors as crucial for powdery mildew infection, including BEC1054 (syn. CSEP0064) and BEC1011 (syn. CSEP0264) (Pliego et al. 2013). BEC1054 is an RNase-like protein predominantly expressed in haustoria at the early stage of powdery mildew infection, perfectly fitting the definition of RALPH (Pliego et al. 2013; Pennington et al. 2019). BEC1054 belongs to CSEP Family 21, a group of five proteins of which all are presumed to be RNase-like proteins based on sequence similarity (Pedersen et al. 2012). Family 21 also includes BEC1011, a close BEC1054

paralogue, whose HIGS-mediated silencing led to 70% and 60% decrease in haustorial index, respectively (Pliego et al. 2013).

The fact that BEC1054 possesses an RNase-like structure while lacking the catalytic residues normally seen in ribonucleases suggests it might be a pseudoenzyme. Pseudoenzyme is a protein that due to gene duplication and mutagenesis, losses the catalytic residues while retaining the overall molecular structure, gaining a new role in regulatory processes (Murphy et al. 2017).

5.1.3 Basis of molecular interaction

Molecular interaction, especially protein-protein interactions, are based on complementarity of surfaces in shape and in corresponding hydrophobic and hydrophilic hot spots on molecular surfaces (Li et al. 2004). That interaction is then often strengthened by conserved residues in strategic positions which also contribute to higher affinity between the molecules (Hubbard and Argos 1994).

The leading force behind molecular interactions is hydrophobicity (Young et al. 2008). The interaction between two hydrophobic surfaces are driven by van der Waals connections and also by gain in free energy from transition from aqueous to non-polar environment caused by the close proximity of two molecules (Moreira et al. 2007). These forces aim to exclude water molecules from immediate vicinity, hence creating an affinity between two hydrophobic surfaces (Fernández and Scheraga 2003).

The other major contributor to molecular interactions are electrostatic forces, such as hydrogen bonds or charge difference in between polar residues (Sheinerman et al. 2000). The complementarity between specific charged residue sidechains in corresponding locations provide specificity between two proteins and also increases the stability of the interaction (Hu et al. 2000).

Not all amino acids have the same potential in contributing to molecular interactions. The most commonly found residues in interaction hot spots are tryptophan, arginine and tyro-

sine (Moreira et al. 2007). Moreover, there is a high frequency of aromatic residues, including phenylalanine, in interaction surfaces, suggesting their high importance in the process. The residues that are the most often excluded from interaction surfaces are leucine, serine, threonine and valine (Moreira et al. 2007). Other residues are considered neutral to interaction potential and mostly contribute to overall shape and structure of the protein.

5.1.4 BEC1054 molecular interaction potential

BEC1054 is a relatively promiscuous protein, i.e. it has an ability to bind to many proteins. Pull-down assay with plant cell lysate showed that BEC1054 has specific affinity to host proteins such as Glutathione-S-Transferase (GST), malate dehydrogenase (MDH) and pathogenesis-related protein 5 (PR5) (Pennington et al. 2016b). All of these are involved in plant immune responses. For example, both GST and MDH play a role in plant oxidative bursts pathway, and PR5 is a thaumatin-like protein with antifungal properties (Pennington et al. 2016b; O'Brien et al. 2012; Dixon et al. 2002; Shatters et al. 2006). Moreover, BEC1054 also binds to some 40S ribosomal proteins and eEF1α, as well as non-specifically to many other proteins (Pennington et al. 2016b). This shows BEC1054 is a relatively "sticky" protein and has a high molecular interaction potential.

Further experimental data from microscale thermophoresis (MST) showed that BEC1054 interacts weakly with nucleic acids while showing a higher affinity towards the SRL consensus sequence (Jones 2015). Moreover, NMR titration with SRL ssDNA showed peak chemical shifts in a specific region of the proteins, highlighting predominantly Phe59 and Tyr100 as the residues likely to be involved in the interaction (Jones 2015; Williamson 2013). In addition, BEC1054 was shown to bind plant ribosomes. When extracted wheat ribosomes were incubated with recombinant BEC1054 and centrifuged through a sucrose cushion, western blotting revealed low amounts of BEC1054 to be still present in the pellet, suggesting a low affinity interaction with plant ribosomes (Przydacz 2015).

5.1.5 Aims

Thus far, this study showed in previous chapters that BEC1054 seems to be involved in inhibition of host rRNA degradation and hindrance of RIP-mediated host cell death. However, the precise nature of its mode of action remains unknown. I hypothesise that BE1054 occludes the SRL site on host ribosomes by associating itself with ribosomes via its hydrophobic surface and attains specificity via its Phe59 and Tyr100 residues.

5.2 Results

5.2.1 Properties of BEC1054 molecular interaction

Further investigation into mode of action of BEC1054 was conducted. Firstly, to test whether the localisation of a GFP tag affects the function of the protein, two BEC1054 constructs were created. One with the GFP tag attached to the N-terminus of the effector, and the other to its C-terminus. *N. benthamiana* leaves were then co-agroinfiltrated with JIP60ml and either of the BEC1054 constructs at 1:100 ratio JIP60ml to BEC1054. Pictures of the infiltrated leaves were taken at 3, 6, 8, 10, 13 and 15 dpi. The exemplar photographs are presented in Figure 5.1. Necrosis was then quantified using pixel luminosity of the infiltrated zones (see Figure 4.9). The experiment was repeated three times, each repeat one week apart, using the total of 30 leaves.

Results showed that the localisation of GFP tag has an effect on the function of BEC1054. The effector in the leaf zones where the GFP tag was localised on its N-terminus exhibited loss-of-function and failed to inhibit JIP60ml-mediated host cell death when compared to the zone where JIP60ml was contested with GFP, with respective medians of 26.65 AU and 24.74 AU (p=0.54). The samples where JIP60ml was co-expressed with BEC1054 with its GFP tag at the C-terminus showed significant decrease in luminosity when compared to its corresponding control, with medians 15.78 AU and 23.82 AU, respectively (** p=0.0013) (Figure 5.2).

Subsequently, I investigated the surface of BEC1054 based on its molecular structure. Each residue of BEC1054 amino acid sequence was coloured according to its hydrophobicity, white representing hydrophilic residues and red representing hydrophobic residues (Figure 5.3a). This showed that BEC1054 possesses many hydrophobic pockets exposed to its surface. The hydrophobic residues cluster on the β-sheet and the surrounding loops of the effector, creating a groove or a "saddle" that potentially could be used to bind to RNA, providing basis for molecular interaction (Figure 5.3b).

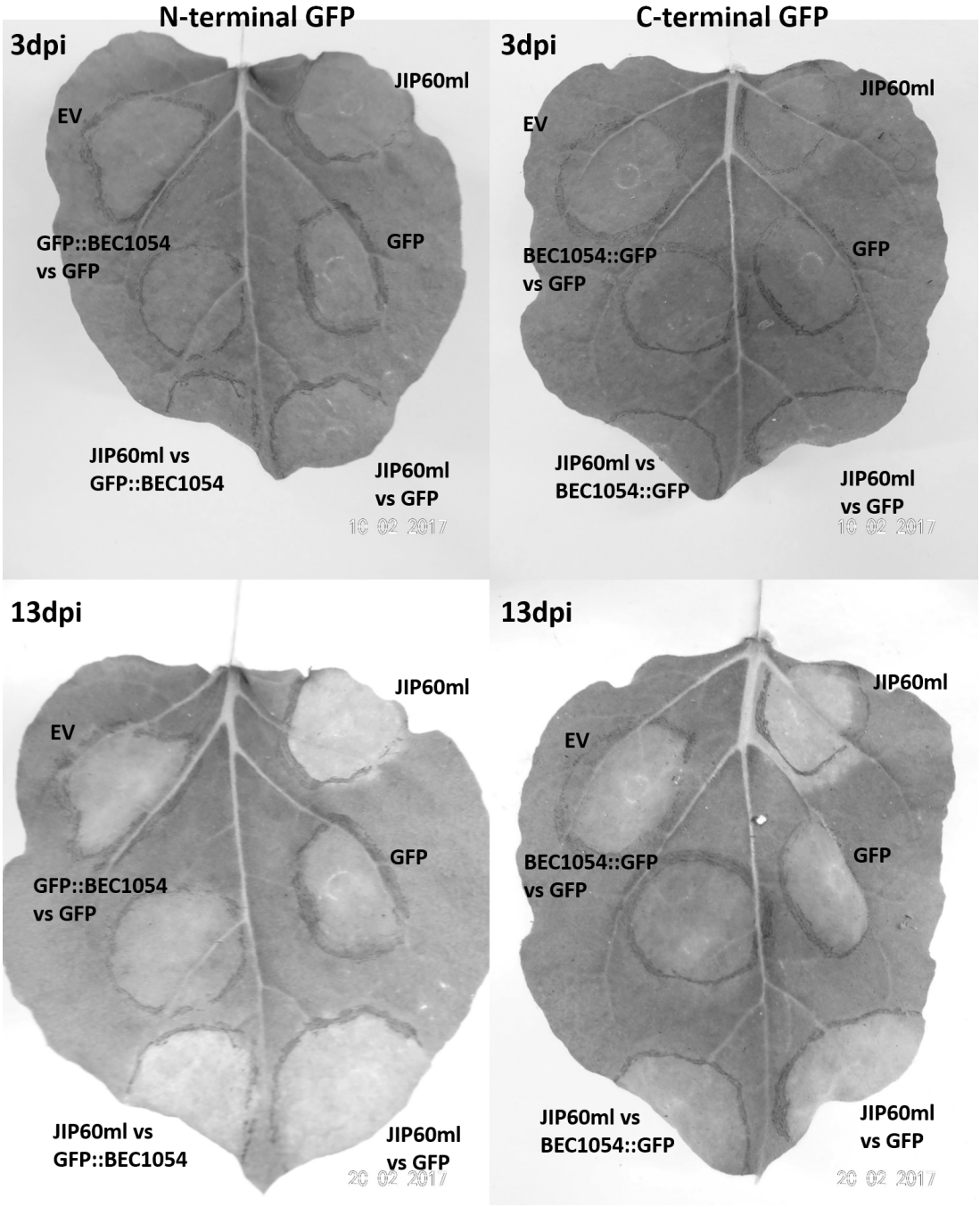


Figure 5.1: Time course of co-agroinfiltration of *N. benthamiana* with JIP60 contested with BEC1054 fused with either N-terminal or C-terminal GFP
Each N. benthamiana leaf was infiltrated with following mixtures of Agrobacteria carrying appropriate plasmids: JIP60ml contested with either BEC1054 or GFP at 1:100 ratio (JIP60ml OD_{600}=0.02, BEC1054 or GFP OD_{600}=2.0), BEC1054 and GFP at 100:1 ratio (OD_{600}=2.0 and OD_{600}=0.02, respectively) and GFP control on its own (OD_{600}=2.12). Additional controls include Agrobacterium without any plasmid (EV – empty vector; OD_{600}=2.12) and JIP60ml-only (OD_{600}=0.02). All infiltrates included P19 (OD_{600}=0.1), apart from EV control. Two variants of BEC1054 were used: one fused with N-terminal GFP(GFP::BEC1054) and the other with C-terminal GFP (BEC1054::GFP). JIP60/GFP infiltrate led to emergence of lesions within the zone. The zones co-agroinfiltrated with JIP60/GFP::BEC1054 infiltrate appeared no different from the JIP60/GFP controls, whereas the JIP60/BEC1054::GFP led to discolouration of the zone but no visible necrosis of the leaf tissue. There were no necrotic effects of either BEC1054/GFP variant or GFP-only infiltrates on the leaf

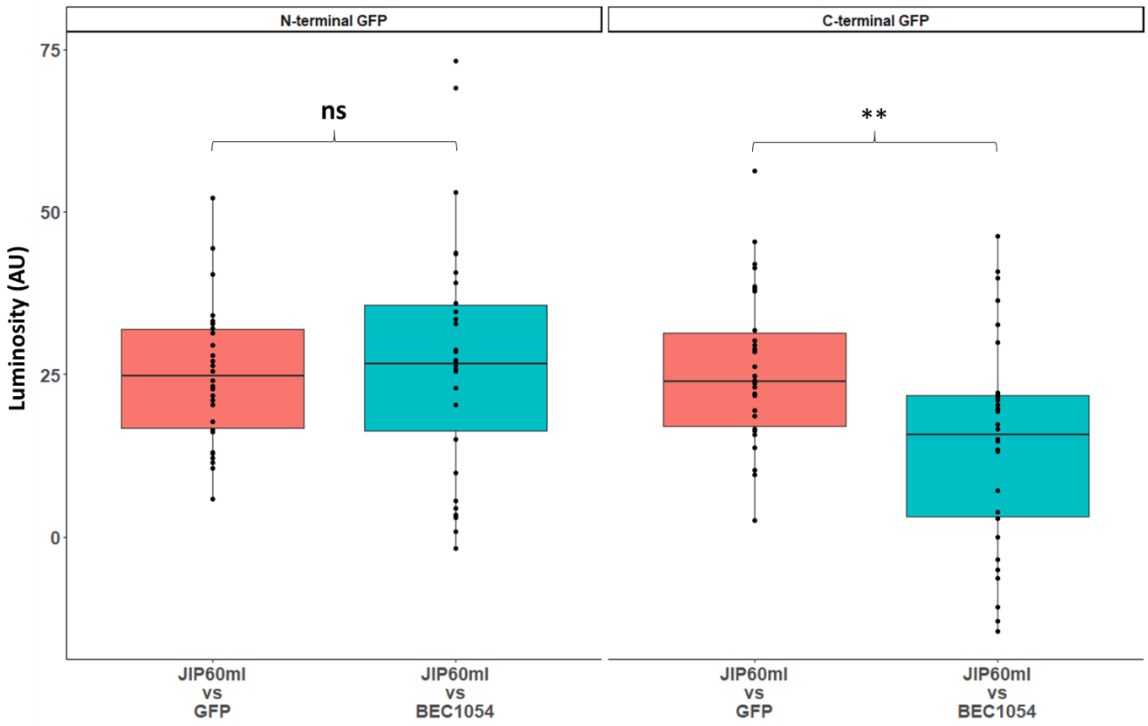


Figure 5.2: The effect of the localisation of the GFP tag on the function of BEC1054
Two versions of BEC1054 effector were created: BEC1054 with N-terminal or C-terminal GFP. Each was co-agroinfiltrated along with JIP60ml at 100:1 ratio of BEC1054 to JIP60ml (OD_{600}=0.02 and OD_{600}=2.0, respectively) into *N. benthamiana*. GFP control at corresponding ratio was co-agroinfiltrated alongside on each leaf (100:1 JIP60ml to GFP; OD_{600}=0.02 and OD_{600}=2.0, respectively). Pictures were taken at 3, 6, 8, 10, 13 and 15 dpi. Necrosis was quantified using pixel luminosity of agroinfiltrated leaf zones (see Figure 4.9), and the samples across the whole time-course were pulled together for each group. The samples where JIP60ml was contested with BEC1054 with the GFP tag localised on the N-terminal of BEC1054 showed no difference from the corresponding control where JIP60ml was contested with GFP only, with respective medians 26.65 AU and 24.74 AU (ns p=0.54). When JIP60ml was contested with BEC1054 with the GFP tag localised on the C-terminal, there was a difference from the corresponding control, with medians 15.78 AU and 23.82 AU, respectively (** p=0.0013). The statistical analysis was performed using paired, one-tailed t test.The experiment was repeated three times, each repeat one week apart, using the total of 30 leaves

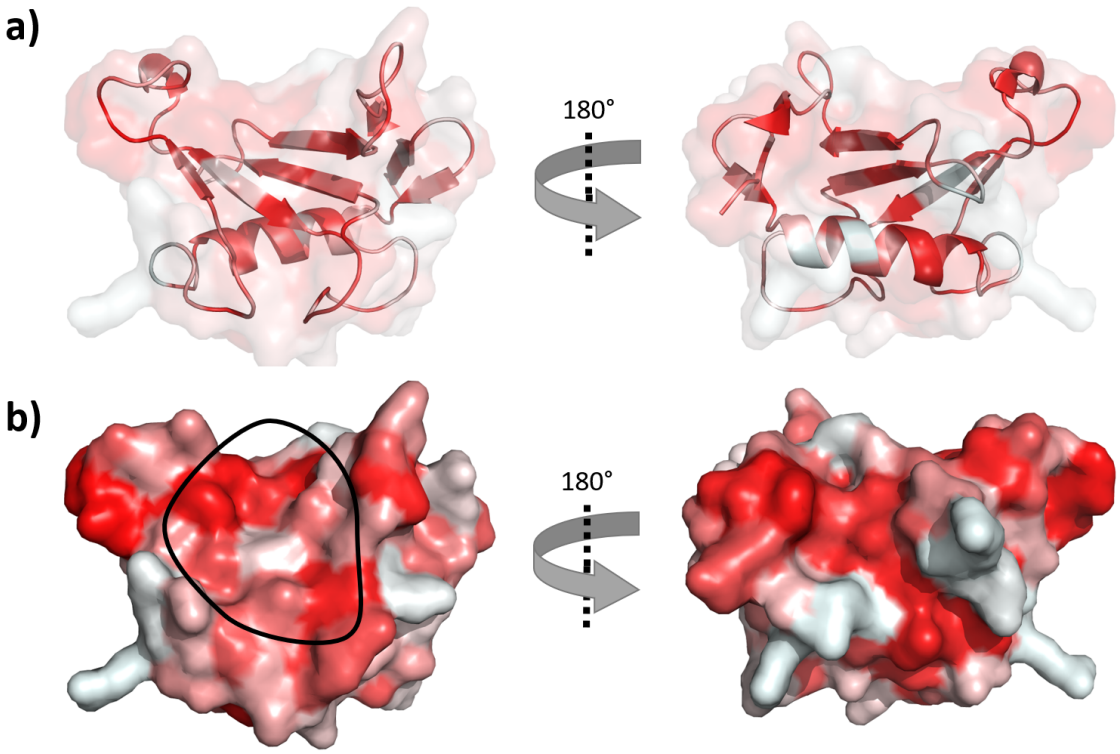


Figure 5.3: Hydrophobic pockets on BEC1054 surface
a) Cartoon of BEC1054 molecular structure with translucent surface, from two opposite angles. Each residue is coloured according to hydrophobic potential of its sidechain, where white represents hydrophilic residues, whereas red represents hydrophobic residues. b) Molecular structure of BEC1054 with its surface superimposed, showed from two opposite angles. The colour of the surface represents hydrophobicity of the residue sidechains exposed to the environment. Red represents hydrophobic pockets likely to contribute to protein-protein interactions. The black outline represents the likely position of the rRNA binding "saddle"

5.2.2 Mutagenesis of suspected active residues of BEC1054

Based on previous experiments involving NMR and MST (Jones 2015), two BEC1054 residues were selected for site-directed mutagenesis as those suspected to play a role in the function of the effector: Phe59 and Tyr100 (Figure 5.4a). Two double mutants of BEC1054 were created in the result: BEC1054$_{F59AY100A}$ (syn. BEC1054$_{FYA}$) and BEC1054$_{F59LY100L}$ (syn. BEC1054$_{FYL}$), where in each, both of the residues Phe59 and Tyr100 were either mutated into alanines or leucines, respectively (Figure 5.4b). Predicted structures of BEC1054$_{FYA}$ and BEC1054$_{FYL}$ are shown in Figure 5.4 c & d, respectively.

Subsequently, the two mutants were transformed into Agrobacterium, using a vector that fused C-terminally attached GFP tag to the constructs. The two Agrobacterium strains were then tested for the ability to elicit transient expression in *N. benthamiana*. Each BEC1054 construct was agroinfiltrated into *N. benthamiana* leaves at OD_{600}=1.0, accompanied by P19 at OD_{600}=0.1 to ensure consistent expression. At 3 dpi leaf discs from infiltrated zones were

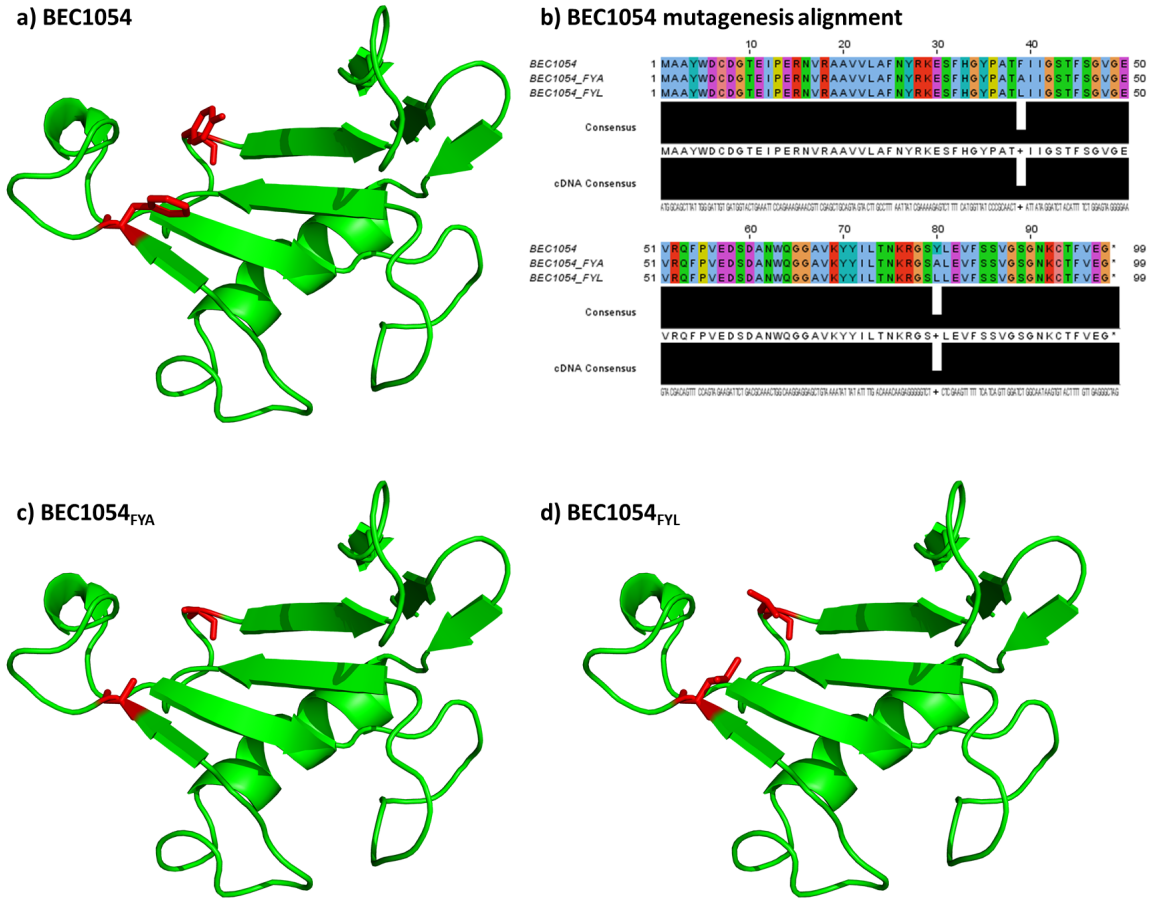


Figure 5.4: Mutagenesis of BEC1054 potential active site residues
a) Cartoon of the molecular structure of BEC1054. The residues in red show the localisation of Phe59 and Tyr100. b) Two double mutants were created: BEC1054$_{F59AY100A}$ (syn. BEC1054$_{FYA}$) and BEC1054$_{F59LY100L}$ (syn. BEC1054$_{FYL}$). The alignment of amino acids sequences of BEC1054 and its two double mutatants. The gaps in consensus show where the mutations occur in the sequence. c) Cartoon representation of BEC1054$_{FYA}$ double mutant. d) Cartoon representation of BEC1054$_{FYL}$ double mutant

collected and observed under fluorescent microscope. Both BEC1054 mutants showed satisfactory expression based on the abundance of the GFP signal, comparable to the wild-type BEC1054 variant (Figure 5.5).

5.2.3 BEC1054 double mutant and JIP60ml competition *in planta*

To investigate whether a double mutation of the residues leads to a loss-of-function of BEC1054, $BEC1054_{FYA}$ was used in a competition with JIP60ml *in planta*. JIP60ml was co-agroinfiltrated with either GFP or $BEC1054_{FYA}$ at 1:100 ratio JIP60ml to GFP or $BEC1054_{FYA}$ (OD_{600}=0.02 and OD_{600}=2.0, respectively). The experiment was repeated five times, using the total of 30 leaves, each being considered a separate repeat. Pictures of the leaves were taken at 4, 7, 10 and 14 dpi, and necrosis was quantified using pixel luminosity. The statistical analysis was performed using linear mixed model taking into account the age of the leaf and the differences between individual leaves as random effects, followed by TukeyHSD test for significance between each group. The results showed that, despite the double mutation, $BEC1054_{FYA}$ still interferes with JIP60ml-mediated host cell death. When the data was pulled across the whole of the time-course, where JIP60ml was contested with GFP the luminosity median was 35.18 AU, whereas when JIP60ml was contested with $BEC1054_{FYA}$ the median was 26.97 AU (Δ=8.21 AU) and the difference was statistically significant (*** p=0.00024) (Figure 5.7a). Each of the random effects explain 6% of the variability between samples. Subsequently, each time point was considered independently. The medians for JIP60ml contested with GFP and with $BEC1054_{FYA}$ were respectively 26.80 AU and 24.13 AU (Δ=2.67) at 4 dpi, 35.23 AU and 20.39 AU (Δ=14.84) at 7 dpi, 43.29 AU and 33.26 AU (Δ=10.03) at 10 dpi, and 47.80 AU and 33.25 AU (Δ=14.55) at 14 dpi. Despite the consistent trend showing lower necrosis in agroinfiltration zones containing $BEC1054_{FYA}$, there were no statistically significant differences between the treatments at any of the time points (Figure 5.7b).

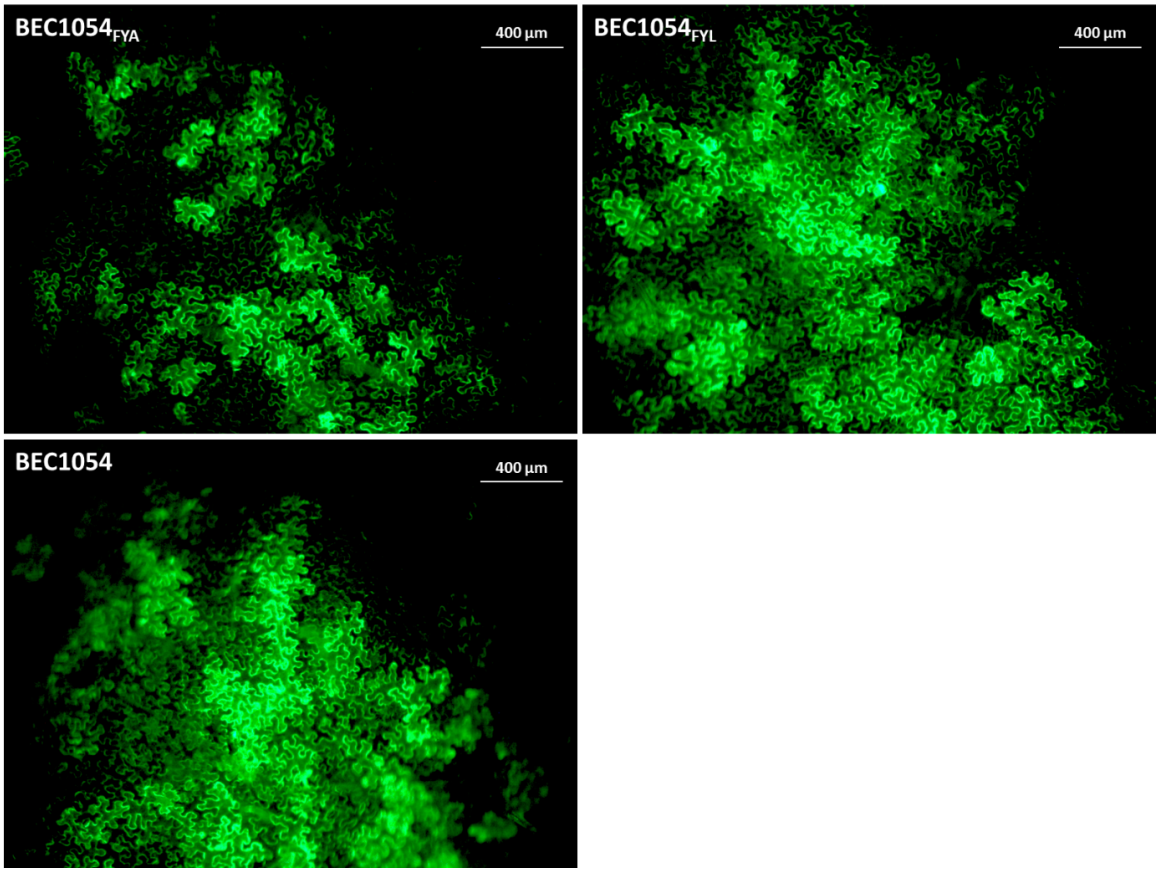


Figure 5.5: Transient expression of BEC1054 variants in *N. benthamiana*
BEC1054 and its two double mutants, BEC1054$_{FYA}$ and BEC1054$_{FYL}$, were transiently expressed in *N. benthamiana* (OD_{600}=1.0). Each variant was co-agroinfiltrated with P19 (OD_{600}=0.1) to ensure consistent expression. As each BEC1054 construct is fused with GFP, epifluorescent micrographs were taken at 3 dpi to test the expression of the constructs. Lack of western blotting data means that the presence of the effector itself is not certain

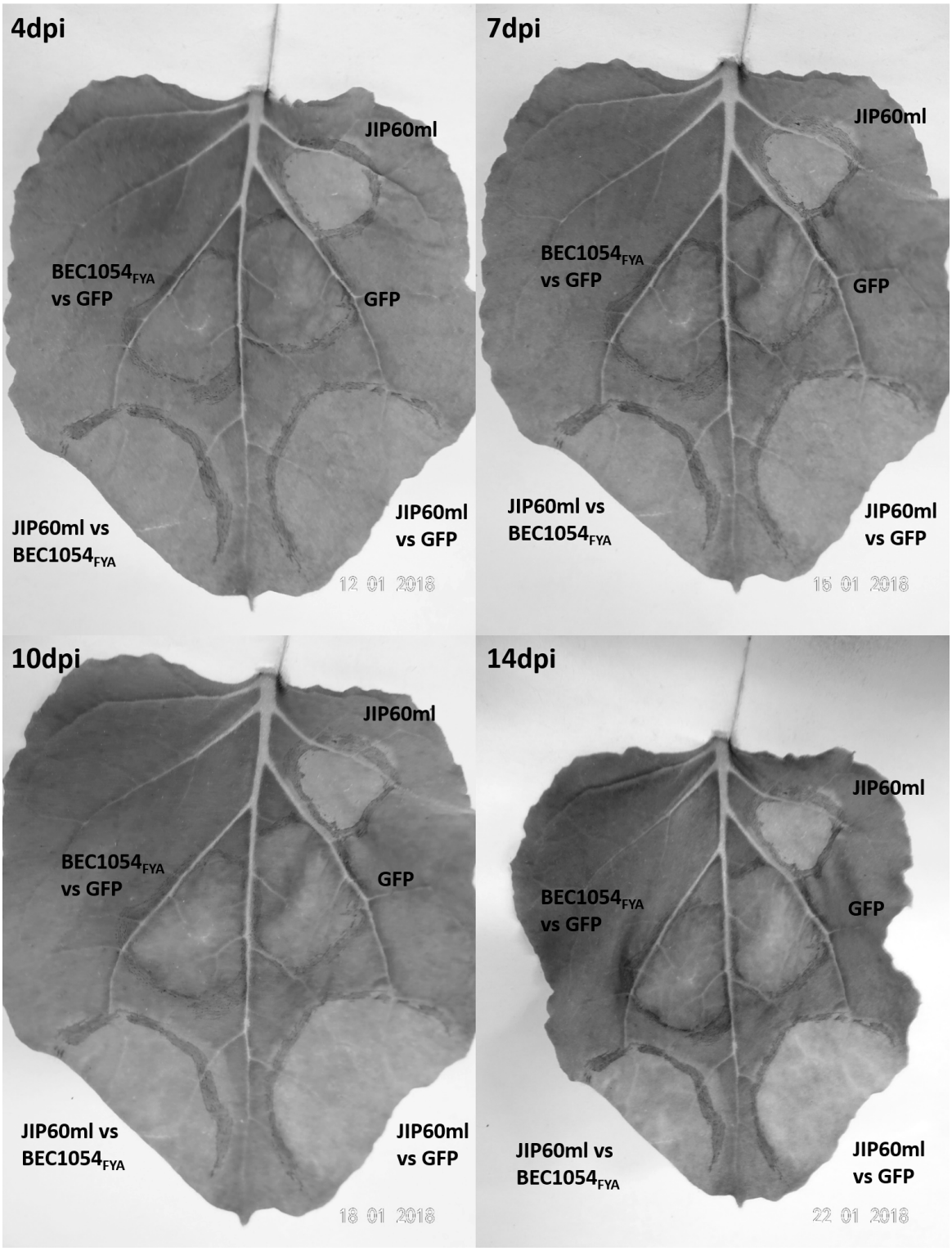


Figure 5.6: Time course of co-agroinfiltration of *N. benthamiana* with JIP60 contested with either BEC1054$_{FYA}$ or GFP

Each N. benthamiana leaf was infiltrated with following mixtures of Agrobacteria carrying appropriate plasmids: JIP60ml contested with either BEC1054 or GFP at 1:100 ratio (JIP60ml OD_{600}=0.02, BEC1054$_{FYA}$ or GFP OD_{600}=2.0), BEC1054$_{FYA}$ and GFP at 100:1 ratio (OD_{600}=2.0 and OD_{600}=0.02, respectively) and GFP control on its own (OD_{600}=2.12). Additional control included Agrobacterium with JIP60ml-only (OD_{600}=0.02). All infiltrates included P19 (OD_{600}=0.1). JIP60/GFP infiltrate led to emergence of lesions within the zone whereas JIP60/BEC1054$_{FYA}$ infiltrate led to discolouration of the zone but no visible necrosis of the leaf tissue. There were no necrotic effects of either BEC1054$_{FYA}$/GFP or GFP-only infiltrates on the leaf

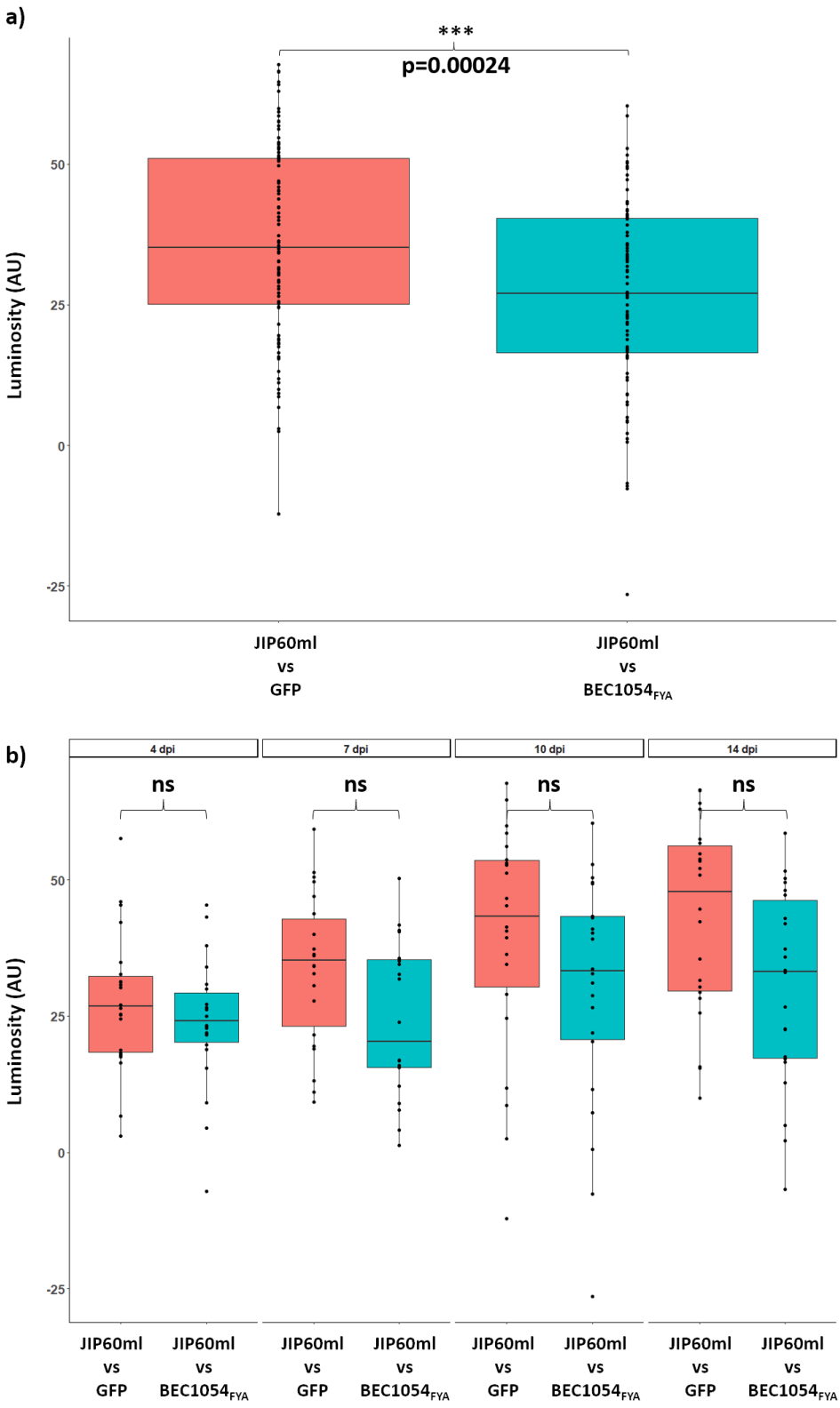


Figure 5.7: The effect of BEC1054$_{FYA}$ double mutant on JIP60ml-mediated host cell death *in planta*
N. benthamiana leaves were co-agroinfiltrated with JIP60ml contested with either BEC1054$_{FYA}$ double mutant or GFP at 1:100 ratio (JIP60ml OD_{600}=0.02, BEC1054 or GFP OD_{600}=2.0), BEC1054 and GFP at 100:1 ratio (OD_{600}=2.0 and OD_{600}=0.02, respectively) and GFP control on its own (OD_{600}=2.12). Additional control included JIP60ml on its own (OD_{600}=0.02). All infiltrates included P19 (OD_{600}=0.1). Pictures for measurements of luminosity were taken at 4, 7, 10 and 14 days post infiltration. The statistical analysis was performed using linear mixed model taking into account the age of the leaf and the differences between individual leaves as random effects, followed by TukeyHSD test for significance between each group. a) The leaf zones co-agroinfiltrated with JIP60ml contested with BEC1054$_{FYA}$ double mutant showed statistically significant lower necrosis than the control contested with GFP across the whole time course, with respective medians at 26.97 AU and 35.18 AU (*** p=0.00024). b) When considering individual time points, the data showed consisted trend in which the zones co-agroinfiltrated with JIP60ml and BEC1054$_{FYA}$ showed lower necrosis than the zones co-agroinfiltrated with JIP60ml and GFP, however, so statistically significant difference between the treatments were found within each time point. Each of the random effects explain 6% of the variability between samples

5.2.4 The effect of BEC1054$_{FYA}$ on *in vitro* translation

The double mutant BEC1054$_{FYA}$ was tested for activity *in vitro*, using reticulocyte lysate. The relevant cDNA, i.e. BEC1054 variants, JIP60ml, 1 kb fragment of rRNA and luciferase, were each amplified with a T7 promoter. Subsequently, the transcription/translation reactions outlined in Table 5.1 were prepared and incubated at 30°C for 2 hours to allow production of the relevant proteins. Next, luciferin was added to each reaction and the luciferase activity was measured. The experiment was designed so each reaction contains the same amount of cDNA. The experiment was repeated three times.The statistical analysis was performed using linear mixed model accounting for random effect caused by differences between repeats, followed by TukeyHSD test for significance between each two groups.

The results showed that BEC1054$_{FYA}$ double mutant behaves similarly to wild-type BEC1054 (Figure 5.8). Both BEC1054 and BEC1054$_{FYA}$, with their respective medians of $5.2 * 10^5$ FU and $5.3 * 10^5$ FU, caused a decrease in luciferase activity when compared to rRNA control with median $8.8 * 10^5$ FU. The difference between the two BEC1054 variants was not statistically significant (p=0.99). Neither BEC1054 nor BEC1054$_{FYA}$ led to a rescue of translation caused by JIP60ml. When JIP60ml was co-expressed with either BEC1054 or BEC1054$_{FYA}$, there was a comparable decrease in luciferase activity, with medians of $4.8 * 10^5$ FU and $5.2 * 10^5$ FU, respectively, which were not statistically different from each other (p=1.0). JIP60-only sample was statistically significantly different from both JIP60 co-expressed with either BEC1054 or BEC1054$_{FYA}$ (** p=0.00156 and ** p=0.00318, respectively). The random effect of the differences between repeats explain 49% of variability between samples. All samples were statistically significantly different from both the negative and the positive controls, as well as from the rRNA control (*** $p < 0.001$). No other groups showed statistically significant differences between each other.

	cDNA (ng)				
TnT Reaction	rRNA	JIP60ml	BEC1054	Luciferase	Total
−ve control	0	0	0	0	0
+ve control	0	0	0	160	160
rRNA	120	0	0	160	280
BEC1054	40	0	80	160	280
$BEC1054_{FYA}$	40	0	80	160	280
JIP60ml	80	40	0	160	280
JIP60ml vs BEC1054	0	40	80	160	280
JIP60ml vs $BEC1054_{FYA}$	0	40	80	160	280

Table 5.1: List of transcription/translation (TnT) reactions for JIP60ml and $BEC1054_{FYA}$ competition *in vitro* experiment
This table shows a list of reactions used in *in vitro* transcription/translation experiment using reticulocyte lysate. Each row represents a mixture used and states how much of each cDNA was used in ng. Each cDNA was first amplified with a T7 promoter. The experiment was designed in a way that all tested conditions had the same amount of cDNA

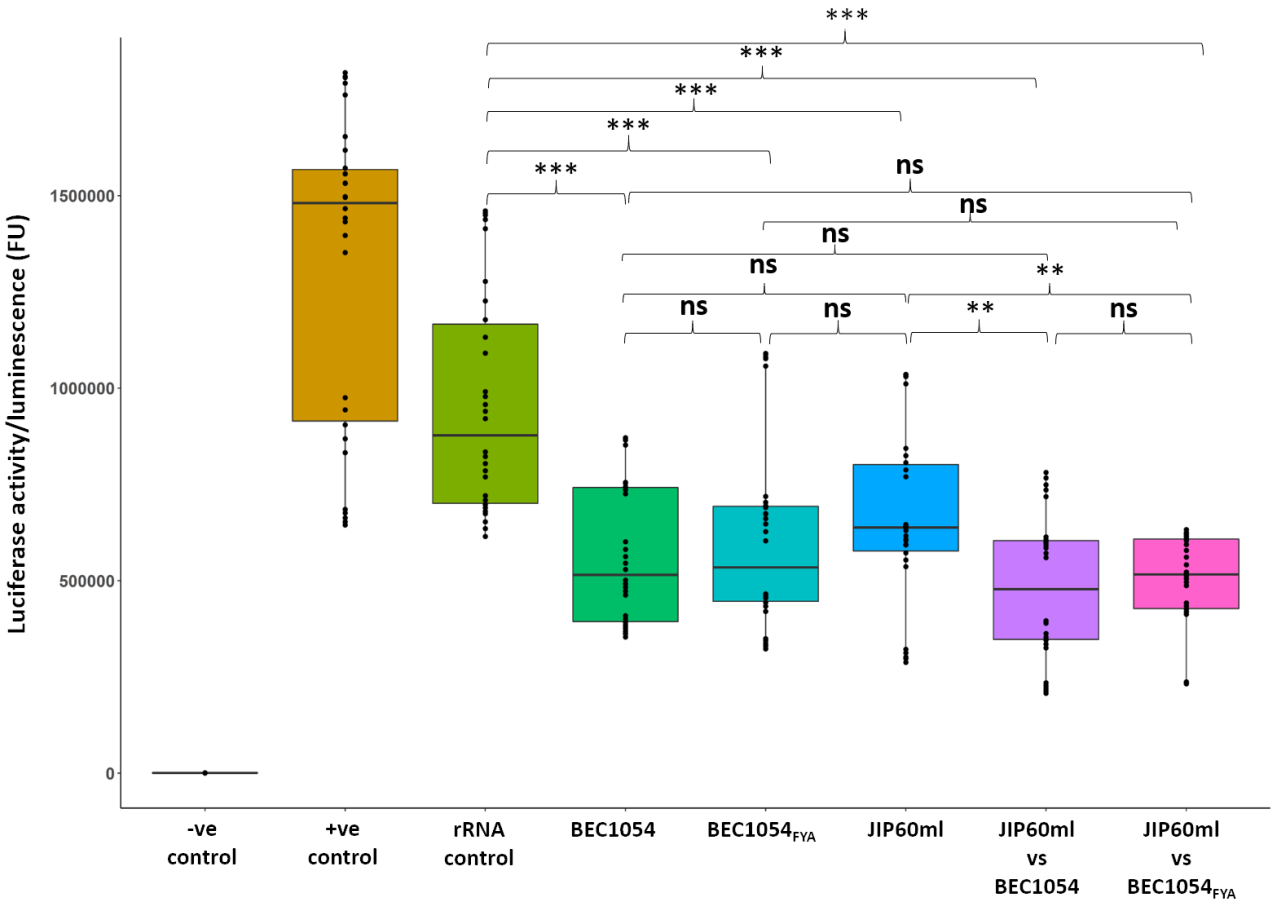


Figure 5.8: Effect of BEC1054 variants on JIP60ml-mediated ribosome inhibition *in vitro*
The effect of BEC1054 effector and its double mutant BEC1054$_{FYA}$ on JIP60 RIP domain-mediated ribosome inhibition was investigated with reticulocytes lysate (Thermo Fisher) transcription/translation *in vitro* assay. cDNA of JIP60ml, BEC1054 variants and 1 kbp fragments of rRNA was amplified with T7 promoter. Subsequently, the following 10 μl reactions were created: rRNA control with 120 ng of T7:rRNA cDNA, JIP60ml with 40 ng of T7:JIP60ml cDNA and 80 ng of T7:rRNA cDNA, BEC1054 with 80ng of T7:BEC1054 cDNA and 40 ng of T7:rRNA cDNA, BEC1054$_{FYA}$ with 80ng of T7:BEC1054$_{FYA}$ cDNA and 40 ng of T7:rRNA cDNA, as well as combination of T7:JIP60ml cDNA at 40 ng with either T7:BEC1054 or T7:BEC1054$_{FYA}$ at 80 ng. Each reaction, including the positive control, also contained 160 ng of T7:luciferase cDNA, apart from the negative control which only contained the lysate. The lysates were incubated at 30°C for 2 hr, then the luciferin was added and the luminescence from the luciferase activity was measured as an indirect indication of ribosome activity. The experiment was repeated three times. Translation of JIP60ml, BEC1054 or BEC1054$_{FYA}$ on their own lead to a drop of luciferase translation, with their respective medians at $6.4 * 10^5$ FU, $5.2 * 10^5$ FU and $5.3 * 10^5$ FU, indicating ribosome inhibition by the produced proteins. When both JIP60ml and either BEC1054 or BEC1054$_{FYA}$ are present in the reaction, the ribosome inhibition is not rescued by the presence of the effectors, with the respective medians of $4.8 * 10^5$ FU and $5.2 * 10^5$ FU. The difference in luciferase activity between JIP60ml only and either BEC1054 only or BEC1054$_{FYA}$ only, as well as between the two BEC1054 variants was not statistically significant (p=0.44, p=0.94 and p=0.99, respectively). The difference in luciferase activity between JIP60ml together with either BEC1054 or BEC1054$_{FYA}$ was also not statistically significant (p=1.0). However, JIP60-only sample was statistically significantly different from both JIP60 co-expressed with either BEC1054 or BEC1054$_{FYA}$ (** p=0.00156 and ** p=0.00318, respectively). All samples were statistically significantly different from both the negative and the positive controls, as well as from the rRNA control (*** $p < 0.001$). No other groups showed statistical significance between each other. The statistical analysis was performed using linear mixed model accounting for random effect from differences between repetitions, followed by TukeyHSD testing for significance between each two groups. The random effect of the differences between repeats explain 49% of variability between samples.

5.3 Discussion

5.3.1 Unoccluded surface is necessary for BEC1054 function

Protein function is often a very fragile phenomenon and sometimes a small change can lead to a loss of the ability to perform that function. For example, presence of a peptide tag can hinder or completely abolish a function of a protein it is attached to. GFP is 238 amino acids long, whereas BEC1054 is barely 99 amino acids long without its signal peptide. Therefore, it is easy to conceptualise that fusion of a tag that is more than double the size of the protein of interest can have a potentially detrimental effect on the function of that protein, depending on positioning and localisation of the tag. At this stage, only GFP tag has been tested, as fluorescence was necessary to establish the expression levels after infiltration. In the future, it would be advisable to also look at other tags, such as myc or FLAG tags, which are much smaller, thus less likely to interfere with BEC1054 function. The presence of the protein could still be examined with methods such as western blotting.

I investigated whether attachment of a GFP tag to either N- or C-terminus of BEC1054 has an effect on its function. The results showed that in fact only one of the two localisations is viable, as the other abolishes the function altogether. When the GFP tag was fused at the N-terminal end of BEC1054, the effector failed to inhibit the JIP60ml-mediated host cell death. One possibility is that the effector is not expressed after the translation of the GFP tag. As in this case the western blotting experiments were not performed, it is not possible to determine if the effector is still attached to the tag. Alternatively, it is possible that the localisation of the GFP tag at the N-terminus of BEC1054 either prevents proper folding of the effector or it physically occludes the surface of the effector responsible for its function. The only way to determine that would be through structural studies, such as X-ray crystallography or NMR. Interestingly, the fact that one localisation of the GFP tag abolishes the function shows that BEC1054 does play an active role in inhibition of JIP60ml-mediated host cell death, and it is not only an artefact caused simply by the presence of any peptide with RNase-like fold.

5.3.2 Role of structure and hydrophobic interactions in BEC1054 function

Majority of RIPs bind to ribosomes based on hydrophobic interactions (Zaeytijd and Damme 2017). Many molecular interactions, such as protein-protein or protein-RNA interactions, rely on hydrophobic sidechains of amino acids being exposed towards the surface (Nooren and Thornton 2003). As the biological cell cytosol is an aqueous environment, hydrophobic residue sidechains are repelled by it, thus they are associating themselves with other hydrophobic surfaces, creating basis for molecular interaction (Jones and Thornton 1996). Analysis of BEC1054 amino acid sequence and its surface created by residue sidechains revealed a few potential hydrophobic pockets. These pockets could explain the promiscuity or "stickiness" of BEC1054 which was found to interact with many various proteins, such as MDH and GST, and it was also binding non-specifically to several other plant proteins (Pennington et al. 2016b; Pennington et al. 2019). This suggests an ability to associate with other molecules based on a generic and unspecific forces, such as hydrophobic interaction. Hydrophobic forces only require another hydrophobic surface to initiate interaction in an aqueous environment. This would explain why BEC1054 seems to be associating itself with many proteins which are unrelated. Conversely, it can also mean that some of the interactors of BEC1054 are completely random and do not add to the functionality of the effector.

Previous experimentation on BEC1054 highlighted potential residues involved in its function. I decided to test two of them: Phe59 and Tyr100. These are both aromatic amino acids known to play a role in protein-nucleotide interactions through ring stacking, with tyrosine also having an ability to form hydrogen bonds (Luscombe et al. 2001; Moreira et al. 2007). A double mutant of the effector, BEC1054$_{F59AY100A}$ (syn. BEC1054$_{FYA}$), was then created and tested. The mutant showed similar levels of transient expression to the wild-type variant following agroinfiltration into *N. benthamiana*. Competition assays, both *in planta* and *in vitro*, showed that despite the double mutation, BEC1054$_{FYA}$ is still functional and behaves similarly to wild-type BEC1054. The co-agroinfiltration experiment showed that both BEC1054 variants seem to be able to hinder the JIP60ml-mediated host cell death with comparable efficacy. Similarly, results from *in vitro* assay showed that both BEC1054 and BEC1054$_{FYA}$

lead to translation inhibition, and when contested with JIP60ml, there was no real difference between the two variants. That suggests that these two residues do not contribute to the efficacy of BEC1054 function. The fact that the mutagenesis of these two residues does not lead to a loss of function also would explain why the NMR HSQC profile did not produce stronger peak shifts which usually indicate direct involvement of residues in molecular interaction. It would also explain why such an abundance of BEC1054 is necessary to counteract JIP60ml-mediated host cell death, as hydrophobic interactions alone often lead to low affinity molecular interactions and they lack the stability and specificity provided by electrostatic forces (Tsai et al. 1997; Moreira et al. 2007). If we consider that BEC1054 is a pseudoenzyme and its main function is prevention of host cell death by occluding the SRL site on host ribosomes from RIPs, it is possible that the effector does not require any catalytic activity in order to fulfil its function. Alanine is a short, hydrophobic amino acids, thus it is unlikely to interfere with protein function which is based on structural compatibility and hydrophobic interaction (Morrison and Weiss 2001; Moreira et al. 2007). In that case, it would be its overall structure that would have to be compatible with its target site, rather than an effect of any active site residues. Further investigation is necessary to discern whether a charged, hydrophilic residue in these positions would lead to disruption of BEC1054 function, which would allow to determine if that surface is involved in the interaction with host ribosomes. It is also possible that there are other, yet undiscovered and untested, residues that are responsible for BEC1054 function.

In conclusion, BEC1054 is a short, secreted protein expressed preferentially in haustorium at the early stages of powdery mildew infection (Pliego et al. 2013). The effector is confirmed to assume a RNase-like structure but lacks the catalytic residues necessary for cleaving RNA (Pennington et al. 2019). Results of this study suggest BEC1054 is a pseudoenzyme whose mode of action is based on hydrophobic interactions. The surface of the effector provides necessary hydrophobic pockets that create interaction potential while presumably the structural shape creates the necessary scaffolding and in itself is responsible for compatibility with ribosomes. The notion that the affinity of the effector is based on hydrophobicity is supported by the fact that even a double mutation that replaced residues that were highlighted as potentially involved in the interaction with ribosomes with hydrophobic residues did not affect

the functionality of the protein. BEC1054$_{FYA}$ performed indistinguishably from the wild-type variant both *in planta* and *in vitro*.

Chapter 6: General Discussion

The continuous growth of human population, the limited agricultural land and the impending climate change all contribute to destabilisation of global food security. Moreover, pests not only become resistant to currently used pesticides, but they also are spreading to new geographical regions due to accidental trafficking and environmental changes (Evans et al. 2008). Despite the control measures in place, crop losses due to pests are on the increase in the last 40 years (Oerke 2006; Fisher et al. 2012). In order to ensure ongoing food availability more effort and innovation is needed to increase food production at a faster rate to sustain the future demand. To that end, an in-depth understanding of host-pathogen interactions is necessary to develop new approaches to combat plant diseases, to achieve higher crop yields.

6.1 Successful plant-microbe interaction depends on effectors

Blumeria graminis is an economically important phytopathogen which causes powdery mildew in commercial crops such as wheat and barley. It is an obligate biotroph, thus it requires a living host cell to grow and reproduce. In response, plant immune system allows them to sacrifice compromised host cells by triggering cell death to limit spread of the infection (Jones and Dangl 2006; Young and Gallie 2000; Lam et al. 2001).

One of the pathways of plant senescence and death can be attributed to activity of MeJA, an important plant hormone belonging to jasmonates (Dong 1998). They are thought to be 'master switches' in both biotic and abiotic stress responses (Rustgi et al. 2014). Presence of MeJA is closely associated with plant senescence especially in monocots, which seem to be more sensitive to it than dicots (Wasternack 2007). MeJA leads to expression of jasmonate-induced proteins, many of them also associated with plant immune defences, including JIP60 which acts as a RIP (Reinbothe et al. 1994b). The N-terminal domain of JIP60 possesses N-glycosidase activity and it causes depurination of a conserved adenine within the SRL motif

located on large subunit of ribosomal RNA (Dunaeva et al. 1999). The apurinic base is then prone to breakage of the nucleic acid chain as the phosphodiester bond is destabilised (Barbieri 1997). This cleavage leads to inactivation of ribosome, thus to inhibition of translation and a subsequent cell death (Park et al. 2006).

Pathogens keep evolving new means to evade or subdue the ever-improving plant defences as described by the zig-zag model (Jones and Dangl 2006). Therefore, in this never-ending arms race, it is easy to understand why pathogens have mechanisms in place to ensure the infected host cells remain alive. This is also consistent with a so called 'green island' phenomenon, where infected parts of a leaf remain green while the surrounding tissue undergoes senescence (Johal et al. 1995).

Studies on the *Blumeria* genome and proteome revealed a vast number of potential effectors which are thought to be secreted into the targeted host cell to subdue and control those plant immune responses (Pedersen et al. 2012; Frantzeskakis et al. 2018). The huge number of effectors within *B. graminis* genome while at the same time exhibiting loss of other genes, shows the clear importance of the effector proteins in the success of the pathogen (Spanu et al. 2010). Effectors are now thought to be crucial in majority of plant-microbe interactions. Even beneficial microbes at first contact are recognised by the host plant as an invader but a combination of specialised effectors leads to downregulation of its immune response and establishment of a symbiotic relationship (Zamioudis and Pieterse 2012). In case of *Blumeria*, the effectors are thought to be secreted into host via specialised pathogen-host interface comprised of haustorium, its feeding body, surrounded by the specialised extra-haustorial membrane (Micali et al. 2011).

6.2 Impact of *Blumeria* RALPH effector BEC1054

The BEC1054 RALPH effector is expressed in haustoria of *Blumeria* (Pedersen et al. 2012). A HIGS study showed that BEC1054 effector as crucial in successful establishment of infection (Pliego et al. 2013). Crystallographic studies confirmed that BEC1054 has an RNase-like structure, suggesting the effector targets RNA of the host. In fact, NMR and MST exper-

iments suggested that BEC1054 has a low affinity interaction with nucleic acids (Pennington et al. 2019; Jones 2015). Moreover, further NMR investigation showed that BEC1054 also displays weak binding to plant ribosomes (Przydacz 2015). Comparison and analysis of amino acid sequence of the effector with ribonucleases indicate that the effector does not possess the key amino acid residues necessary for catalytic function, and is thus predicted to be incapable of cleaving RNA (Pace et al. 1988; Roberts et al. 1969; Rosta et al. 2011; Pedersen et al. 2012). The latter was confirmed experimentally, showing BEC1054 does not exhibit any RNase activity (Zhang R., pers. comm.). Pull-down assays with plant cell lysate reveals that BEC1054 binds to numerous proteins, including eEF1G, a protein associated with ribosomes (Pennington et al. 2016b). Notably, yeast-2-hybid and bimolecular fluorescence complementation experiments showed no direct interaction between BEC1054 and the RIP domain of JIP60 (Pennington 2014).

I propose that BEC1054 associates with host ribosomes and physically obstructs the SRL site from host RIPs, hence prevents ribosome inactivation and subsequent host cell death.

6.3 BEC1054 contributes to inhibition of the host rRNA degradation

Here I found that wheat RNA profiles from aniline treated samples showed an emergence of a novel RNA species that is 1180 bases long, but only in samples from MeJA-treated plants. This putative peak is most likely a result of a degradation event as its emergence occurs *in vitro*, where no translation apparatus is present. The only molecules capable of producing an RNA species of such size are ribosomal RNAs. Interestingly, this degradation RNA species was visibly diminished in samples from plants infected with *B. graminis*. In the experiments performed in transgenic wheat that constitutively expresses BEC1054, the RNA putative peak showed a small, though not statistically significant, decrease in abundance compared to the wild type. It was not as substantial a drop as observed in the infected plants (see Chapter 4). That might suggest BEC1054 is not the only factor responsible for preventing the RNA species from emerging. It is possible that other *Blumeria* effectors perform the same

or similar functions, relying on additive effect of multiple effectors, increasing this way the chance of successful infection. For instance, BEC1011 belongs to the same family as BEC1054 and is predicted to share its RNase-like structure; it is also very likely to assume a similar function. Conversely, there could also be effectors that have the same purpose but a completely different mechanism. For example BEC1019, an effector with a protease-like sequence has been recently also associated with preventing host cell death during infection (Whigham et al. 2015). As it stands, BEC1054 effector was not sufficient to interfere with host rRNA degradation in this environment.

As the sequence of the RNA peak is not known, the range of techniques that can be used to investigate the issue is limited. Even though the genome of wheat has been sequenced, it is currently poorly annotated, especially regarding the sequences of the large ribosomal RNA subunits. Although, the sequence used matches the one used in cryo-EM model of wheat ribosome, a confirmation whether the sequence is in fact of the wheat 28S rRNA is necessary (Armache et al. 2010). Furthermore, there is a possibility that the putative peak does not originates from the largest of rRNA species but from the smaller one instead, such as 23S or 18S rRNA. Furthermore, SRL is not the only target of RIPs, as some RIPs depurinate more than one adenine within rRNA (Barbieri et al. 1992). Other regions of ribosomal RNA will have to be investigated to confirm the nature of the BEC1054 function. Establishing the precise identity and RNA sequence of the putative peak would be invaluable for deducing the exact mode of action of BEC1054; regrettably I was not able to achieve this, here.

6.4 BEC1054 affects RIP-mediated host cell death

One of the major challenges in studying *Blumeria*, a strict obligate biotroph, is it is currently impossible to be cultivated on any synthetic medium. Therefore, performing transgenics on this pathogen is not feasible as no selection can be applied. That inability to directly manipulate the pathogen's genes deprives us of one of the most powerful tools in molecular biology. Instead, it is necessary to use indirect methods, such as *in vitro* and *in planta* models and substitutes.

The effects of BEC1054 on RIP-induced cell death was tested *in vivo* via co-agroinfiltrations of the effector with the JIP60 RIP domain (JIP60ml) into *N. benthamiana* as a proof of concept. Even though JIP60 is not native to dicots, it has N-glycosidase activity in transgenic tobacco (Dunaeva et al. 1999) and I showed that transient expression of its N-terminal domain triggers cell death in *N. benthamiana* (see Chapter 3).

Initial results were showing an emerging trend suggesting that BEC1054 effector can hinder the cell death, however, the effect was not always consistent and reproducible, regardless of the ratio between the effector and RIP. Fluorescent microscopy of agroinfiltrated leaves showed that expression of BEC1054 was very limited and short-lived, suggesting that the expression of the gene can be silenced by the host. It is not surprising, as *Nicotiana* plants are very different from grasses such as wheat and barley, and *Blumeria* shows extreme host specificity which could potentially be attributed to its effectors. Therefore, BEC1054 effector might not be ideally expressed in the non-host. Alternatively, the effector might require an assisting protein from the arsenal of *Blumeria* effectors to be fully functional. Another explanation is that due to its association with ribosomes, BEC1054 can itself interfere with translation; such an effect was observed in yeast (Pennington et al. 2016a). This effect of translational inhibition by BEC1054 was also seen in the *in vitro* experiments using reticulocyte lysates. Also, as no western blotting experiments were conducted for the benefit this thesis regarding BEC1054 expression and presence *in planta*, it is possible that the effector is not expressing correctly at all. This oversight should be addressed in the future, to ensure that BEC1054 is in fact present in the plant tissue.

To ensure a sustained expression of BEC1054 in *Nicotiana* plants, I used P19 protein, a repressor of gene silencing from TBSV. P19 enhances the abundance and extends the time of transient expression achieved by agroinfiltration (Voinnet et al. 2003). Following application of P19, BEC1054 showed a more consistent interference and delay effect on JIP60ml-mediated host cell death. Although examination of the infiltrated zones showed that the part of leaves agroinfiltrated with BEC1054 and JIP60ml still showed signs of chlorosis, it was not immediately associated with necrosis, as it was in the case of zones co-agroinfiltrated with JIP60ml and GFP-only control. There was a statistically significant difference in necro-

sis score between leaf zones treated with JIP60ml RIP domain contested with C-terminally tagged BEC1054 in comparison with the zones co-expressed only with GFP (see Chapter 4).

The translation inhibition and decrease in luciferase activity in the *in vitro* assays caused by the presence of BEC1054 is rather surprising. The expected phenotype was a rescue of translational inhibition caused by JIP60ml. It is even more surprising as constitutively expressed BEC1054 showed no effect on growth and seed production of wheat in comparison with wild-type plant (Pennington et al. 2019). One explanation of this could be that the effector affects different ribosomes differently. In this study, BEC1054 was not tested with ribosomes sourced from wheat germ extract but only with ones from reticulocyte lysate. It is possible that the subtle differences between the ribosomes are enough to elicit a different result. For example, some RIPs were shown to be able to distinguish between conspecific and non-conspecific ribosomes, so it is possible that a similar specificity can be present in BEC1054 (Massiah and Hartley 1995). In fact this notion is supported by the fact that transgenic wheat expressing BEC1054 constitutively showed no difference in growth in comparison with the control plants, whereas similar transgenic *N. benthamiana* were prone to show stunted growth compared to wild-type plants (Pennington et al. 2019; Kanja 2018). Therefore, ribosomes not derived from barley might be unintentionally inhibited by the presence of BEC1054 instead of the hypothesised occlusion of the SRL site from host RIPs by the effector happening in barley-derived ribosomes, which BEC1054 evolved to interact with.

6.5 BEC1054 – a molecular Swiss penknife of *Blumeria*

Although not completely conclusive, taken as a whole, the results of this study create an initial picture of BEC1054 mechanism. Based on them, I propose that BEC1054 is employing a generic mode of action, founded on non-specific molecular interactions rather than on complementary target-specific residues, and associates itself with host ribosomes to physically occlude any interaction with the SRL site. This is supported by the fact that BEC1054 remains functional in distinct non-native environments in which it specifically did not evolve in, such as both monocotyledonous wheat and dicotyledonous *N. benthamiana*. In each case,

BEC1054 either interfered with the degradation of host rRNA or the JIP60ml-mediated host cell death. Moreover, BEC1054 facilitates infection of other pathogens than the native *B. graminis* f. sp *hordei*. Presence of BEC1054 significantly increased successful infection of wheat by the related *B. graminis* f. sp *tritici*, as well as by the unrelated downy mildew pathogen, *Peronospora tabacina*, in infecting *N. benthamiana* (Pennington et al. 2019; Yang 2018).

BEC1054 mode of action is likely to be based on hydrophobic interactions, as the effector possesses extensive hydrophobic surface, clustered on its β-sheet and the surrounding loops, creating a hydrophobic groove (Figure 5.3). It would be consistent with a generic mode of action, as it would be driven by the molecular structure compatible with possible interactors and by the hydrophobic potential created by residue sidechains exposed to the surface, rather than by specific electrostatic residues complementary with its target. The fact that BEC1054 seems to interact with a range of host proteins also supports this notion, as interactions based on electrostatic interactions tend to show far more specificity, hence the amount of protein interactors is usually limited only to a specific molecule or a single family, which does not seem to be the case in BEC1054 (Jones and Thornton 1996; Sheinerman et al. 2000).

BEC1054 NMR titration experiments with nucleic acids indicated through chemical shifts that Phe59 and Tyr100 residues are likely to be involved in the interaction. However, both *in vitro* and *in planta* experiments on BEC1054 double mutant BEC1054$_{FYA}$ showed they are not essential for the JIP60ml-mediated host cell death inhibition, and the mutant behaved indistinguishable from the wild-type effector in both assays. This is in further support of the notion that BEC1054 interaction is based on hydrophobic surface potential, as alanine substitution, which is hydrophobic and was used in place of both Phe59 and Tyr100, did not disrupt the function of the effector (see Chapter 5). Conversely, it is possible that these two residues were simply incorrectly identified as important and their contribution to the function is in fact negligible. As such, it is likely there are other, yet untested, residues that are responsible for functionality of BEC1054. For example, Tyr55 and Tyr91 were also indicated as potential residues by minor chemical shifts appearing in NMR titration experiments (Jones 2015). In order to test whether any residues are important for the effector's function, a full

alanine scanning mutagenesis should be performed.

It is possible that the capability of BEC1054 to bind a wide range of proteins gives the effector a *de facto* multifunctionality, well suited for an effector active in the early stages of the infection. As such, BEC1054 can prevent host cell death by blocking the SRL site on host ribosomes for the RIPs while at the same time impeding formation of oxidative bursts cascade by association with GST and MDH. This multifunctionality is made possible because the effector employs a generic mode of action, making it compatible with many unrelated targets. It is worth noting that the "mutlifunctionality" is likely to be a coincidence due to the high hydrophobicity and "stickiness" of the effector, making it compatible with many host targets. The evolutionary pressure seems to have led to an emergence of an effector that can interfere with plant immune system at multiple points, making it an useful tool in establishing successful infection.

With regards to the potential inhibition of the host ribosome inhibition by the BEC1054 effector, I hypothesise, that the effector associates itself with either ribosomal proteins or rRNA of the host, by employing its hydrophobic structure. Upon binding to the ribosome, BEC1054 occludes the SRL located on the 28S rRNA, thus preventing the host RIPs, such as JIP60 from binding. That in turn unables the host-mediated ribosome inactivation. It is possible that the presence of BEC1054 hinders the performance of the host ribosomes but not enough to stop translation altogether, as no cell death due to expression of BEC1054 was ever observed.

To better discern the precise mode of action of BEC1054 in regard to host ribosomes, a series of additional experiments is necessary. For example, an optimised *in vitro* translation assay with ribosomes extracted from barley would be able to show if BEC1054 is able to rescue JIP60ml-mediated translational inhibition. Moreover, a series of yeast-three hybrid experiments between BEC1054 and fragments of host rRNA, including the SRL sequence, would be able to show if the effector in fact associates itself with the SRL site of host ribosomes. Also, to determine whether the effector inhibits specifically JIP60 action or it prevents other RIPs from functioning, co-expression with other RIPs should be performed. Additionally, more experiments should be performed to enhance the reliability of the results already obtained. For

example, other peptide tags than GFP should be trialled. GFP, due to its size, is quite likely to distort the actual function or its efficacy when fused to such as small protein as BEC1054. Thus smaller tags should be considered. Also, the ambiguity of the presence of the effector in plant tissue should be addressed, e.g. with use of western blotting. This would allow drawing more convincing conclusions on the function of BEC1054. Finally, a better method for quantifying necrosis should be devised. Assays such as trypan blue or UV light imaging should be tested to see if more conclusive results can be obtained in the JIP60 and BEC1054 competition assays.

It is worth mentioning that all of the work contained in this study was conducted using a modified JIP60 protein consisting only of the recombinant N-terminal RIP domain, JIP60ml. Therefore, it would be interesting to see if an inclusion of the C-terminal eIFIV-like domain would change some of the outcomes. For example, BEC1054 could potentially directly target the C-terminal domain of JIP60 and prevent its full activation, as the effector is capable of binding other translation factors, such as eEF1G (Pennington et al. 2016b).

6.6 Conclusions

The results obtained during this project brought us a little bit closer to understanding the mode of action of *Blumeria* effector BEC1054. BEC1054 binds a wide range of unrelated host proteins and it shows affinity to nucleic acids and ribosomes. Moreover, BEC1054 slightly inhibits plant rRNA degradation and it seems to hinder RIP-mediated host cell death, as shown by the experiments with JIP60ml *in planta*. Furthermore, the two residues thought to be involved in this process, Phe59 and Tyr100, were shown not to be important in the function. In addition, BEC1054 remains functional in non-host environments, like dicotyledonous *N. benthamiana*. All of these together suggest that BEC1054 employs a generic mode of action, which is most likely based on its overall structure and hydrophobic surface. This would explain the ability of the effector to bind unrelated proteins as well as nucleic acids and ribosomes. The latter also suggests the mechanism of inhibition of RIP-mediated host cell death by the effector. I propose that the RALPH effector BEC1054 associates itself with host ribo-

somes and occludes the SRL site from host RIPs, thus preventing the ribosome inactivation and the subsequent cell death, allowing the pathogen to establish itself in the cell (Figure 6.1).

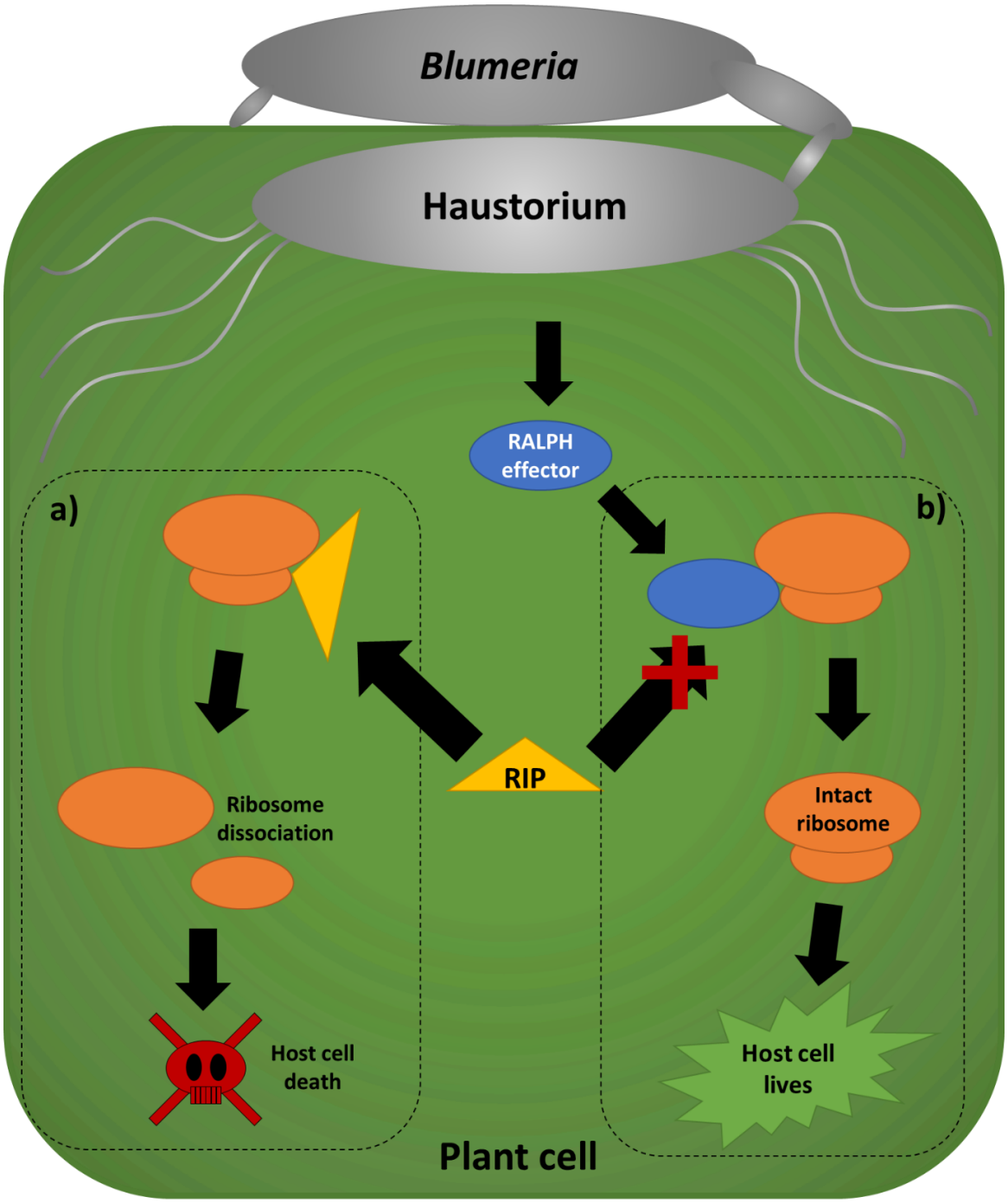


Figure 6.1: Mechanism of inhibition of RIP-mediated host cell death by *Blumeria* RALPH effectors
a) RIP-mediated host cell death. Upon recognition of the pathogen, host expresses and activates RIPs, such as JIP60, which in turn cleave the SRL loop located on the 28S rRNA subunit. The host ribosomes becomes inactivated and either dissociates or degrades, and protein translation is halted. This leads to the host cell death and the biotrophic pathogen is unable to estbalish itself on the host. b) The pathogen secreted RALPH effector, such as BEC1054, into host. The effector associates itself with host ribosomes and occludes the SRL site from host RIPs, preventing the cleavage of rRNA. Therefore, ribosomes remains intact and active and the host cell death is inhibited. The biotrophic pathogen can establish itself in host cell and the infection is successful.

References

Abbott, A. (2018). "Italy's olive crisis intensifies as deadly tree disease spreads". In: *Nature* 563.7731, pp. 306–307.

Adrain, C. and M. Freeman (2012). "New lives for old: evolution of pseudoenzyme function illustrated by iRhoms". In: *Nature Reviews Molecular Cell Biology* 13.8, pp. 489–498.

Andersson, A. A. et al. (2004). "Molecular weight and structure units of (1->3, 1->4)-β-glucans in dough and bread made from hull-less barley milling fractions". In: *Journal of Cereal Science* 40.3, pp. 195–204.

Andresen, I. et al. (1992). "The identification of leaf thionin as one of the main jasmonate-induced proteins of barley (*Hordeum vulgare*)". In: *Plant Molecular Biology* 19.2, pp. 193–204.

Armache, J.-P. et al. (2010). "Cryo-EM structure and rRNA model of a translating eukaryotic 80S ribosome at 5.5-A resolution". In: *Proceedings of the National Academy of Sciences* 107.46, pp. 19748–19753.

Baik, B. K. (2016). "Current and Potential Barley Grain Food Products". In: *Cereal Foods World* 61.5, pp. 188–196.

Baik, B. K. and S. E. Ullrich (2008). "Barley for food: Characteristics, improvement, and renewed interest". In: *Journal of Cereal Science* 48.2, pp. 233–242.

Barbieri, L. (1997). "Polynucleotide:adenosine glycosidase activity of ribosome-inactivating proteins: effect on DNA, RNA and poly(A)". In: *Nucleic Acids Research* 25.3, pp. 518–522.

Barbieri, L. et al. (1992). "Some ribosome-inactivating proteins depurinate ribosomal RNA at multiple sites". In: *Biochemical Journal* 286.1, pp. 1–4.

Barrett, L. G. et al. (2009). "Diversity and Evolution of Effector Loci in Natural Populations of the Plant Pathogen Melampsora lini". In: *Molecular Biology and Evolution* 26.11, pp. 2499–2513.

Bieri, S., I. Potrykus, and J. Fütterer (2003). "Effects of combined expression of antifungal barley seed proteins in transgenic wheat on powdery mildew infection". In: *Molecular Breeding* 11.1, pp. 37–48.

Bindschedler, L. V., R. Panstruga, and P. D. Spanu (2016). "Mildew-Omics: How Global Analyses Aid the Understanding of Life and Evolution of Powdery Mildews". In: *Frontiers in Plant Science* 7, p. 123.

Bindschedler, L. V. et al. (2009). "In planta proteomics and proteogenomics of the biotrophic barley fungal pathogen *Blumeria graminis* f. sp. hordei." In: *Molecular & cellular proteomics* 8.10, pp. 2368–2381.

Bindschedler, L. V. et al. (2011). "Proteogenomics and in silico structural and functional annotation of the barley powdery mildew *Blumeria graminis* f. sp. hordei". In: *Methods* 54.4, pp. 432–441.

Birch, P. R. et al. (2006). "Trafficking arms: oomycete effectors enter host plant cells". In: *Trends in Microbiology* 14.1, pp. 8–11.

Bohlmann, H. et al. (1988). "Leaf-specific thionins of barley-a novel class of cell wall proteins toxic to plant-pathogenic fungi and possibly involved in the defence mechanism of plants." In: *The EMBO journal* 7.6, pp. 1559–65.

Boller, T. and G. Felix (2009). "A Renaissance of Elicitors: Perception of Microbe-Associated Molecular Patterns and Danger Signals by Pattern-Recognition Receptors". In: *Annual Review of Plant Biology* 60.1, pp. 379–406.

Boller, T. and S. Y. He (2009). "Innate immunity in plants: An arms race between pattern recognition receptors in plants and effectors in microbial pathogens". In: *Science* 324.5928, pp. 742–4.

Bolognesi, A. et al. (2016). "Ribosome-Inactivating Proteins from Plants: A Historical Overview". In: *Molecules* 21.12, p. 1627.

Both, M. (2005). "Gene Expression Profiles of *Blumeria graminis* Indicate Dynamic Changes to Primary Metabolism during Development of an Obligate Biotrophic Pathogen". In: *the Plant Cell Online* 17.7, pp. 2107–2122.

Both, M. and P. D. Spanu (2004). "*Blumeria graminis* f.sp. hordei, an obligate pathogen of barley". In: *Plant-pathogen Interactions*. CRC Press. Chap. 8, pp. 202–218.

Boudsocq, M. et al. (2010). “Differential innate immune signalling via Ca2+ sensor protein kinases”. In: *Nature* 464.7287, pp. 418–422.

Bourras, S. et al. (2016). “Avirulence genes in cereal powdery mildews: the gene-for-gene hypothesis 2.0”. In: *Frontiers in Plant Science* 7.241, pp. 1–7.

Bourras, S. et al. (2015). “Multiple avirulence loci and allele-specific effector recognition control the Pm3 race-specific resistance of wheat to powdery mildew”. In: *the Plant Cell* 27.10, pp. 2991–3012.

Bozkurt, T. O. et al. (2012). “Oomycetes, effectors, and all that jazz”. In: *Current Opinion in Plant Biology* 15.4, pp. 483–492.

Brooks, D. M., C. L. Bender, and B. N. Kunkel (2005). “The Pseudomonas syringae phytotoxin coronatine promotes virulence by overcoming salicylic acid-dependent defences in Arabidopsis thaliana”. In: *Molecular Plant Pathology* 6.6, pp. 629–639.

Brown, L. R. (2012). *Outgrowing the Earth: The Food Security Challenge in an Age of Falling Water Tables and Rising Temperatures*. Taylor & Francis.

Caarls, L., C. M. J. Pieterse, and S. C. M. Van Wees (2015). “How salicylic acid takes transcriptional control over jasmonic acid signaling”. In: *Frontiers in Plant Science* 6, p. 170.

Campos, M. L., J.-H. Kang, and G. A. Howe (2014). “Jasmonate-Triggered Plant Immunity”. In: *Journal of Chemical Ecology* 40.7, pp. 657–675.

Challinor, A. J. et al. (2016). “Current warming will reduce yields unless maize breeding and seed systems adapt immediately”. In: *Nature Climate Change* June, pp. 1–31.

Chan, D. S. et al. (2007). “Interaction between trichosanthin, a ribosome-inactivating protein, and the ribosomal stalk protein P2 by chemical shift perturbation and mutagenesis analyses”. In: *Nucleic Acids Research* 35.5, pp. 1660–1672.

Chang, D. W. et al. (2002). “c-FLIPL is a dual function regulator for caspase-8 activation and CD95-mediated apoptosis”. In: *The EMBO Journal* 21.14, pp. 3704–3714.

Chang, X. et al. (2016). “Jasmonates are induced by the PAMP flg22 but not the cell death-inducing elicitor Harpin in Vitis rupestris”. In: *Protoplasma*, pp. 1–13.

Chaudhry, B. et al. (1994). “The barley 60 kDa jasmonate-induced protein (JIP60) is a novel ribosome-inactivating protein”. In: *The Plant Journal* 6.6, pp. 815–824.

Che, F. S. et al. (2000). “Flagellin from an incompatible strain of Pseudomonas avenae induces a resistance response in cultured rice cells.” In: *The Journal of biological chemistry* 275.41, pp. 32347–56.

Chen, X.-Y., P. J. Berti, and V. L. Schramm (2000). “Ricin A-Chain: Kinetic Isotope Effects and Transition State Structure with Stem-Loop RNA”. In: *Journal of the American Chemical Society* 122.8, pp. 1609–1617.

Cheng, K. C.-C. et al. (2009). “Regulation of MBK-2/DYRK by CDK-1 and the Pseudophosphatases EGG-4 and EGG-5 during the Oocyte-to-Embryo Transition”. In: *Cell* 139.3, pp. 560–572.

Cheong, J.-J. and Y. D. Choi (2003). “Methyl jasmonate as a vital substance in plants”. In: *Trends in Genetics* 19.7, pp. 409–413.

Chisholm, S. T. et al. (2006). “Host-microbe interactions: Shaping the evolution of the plant immune response”. In: *Cell* 124.4, pp. 803–814.

Chuang, W.-P. et al. (2014). “Caterpillar attack triggers accumulation of the toxic maize protein RIP2”. In: *New Phytologist* 201.3, pp. 928–939.

Clarke, S. M. et al. (2009). “Jasmonates act with salicylic acid to confer basal thermotolerance in Arabidopsis thaliana”. In: *New Phytologist* 182.1, pp. 175–187.

Coll, N. S., P. Epple, and J. L. Dangl (2011). “Programmed cell death in the plant immune system.” In: *Cell Death & Differentiation* 18.8, pp. 1247–56.

Conway, J. M. and K. M. Behall (2006). *Health Effects of Barley Consumption*. Tech. rep. 22. Beltsville: Beltsville Human Nutrition Research Center, pp. 1–8.

Cook, D. E., C. H. Mesarich, and B. P. Thomma (2015). “Understanding Plant Immunity as a Surveillance System to Detect Invasion”. In: *Annual Review of Phytopathology* 53.1, pp. 541–563.

Cunningham, B. C. and J. A. Wells (1989). “High-resolution epitope mapping of hGH-receptor interactions by alanine-scanning mutagenesis.” In: *Science (New York, N.Y.)* 244.4908, pp. 1081–5.

Dean, R. et al. (2012). “The Top 10 fungal pathogens in molecular plant pathology”. In: *Molecular Plant Pathology* 13.4, pp. 414–430.

Deutsch, C. A. et al. (2018). "Increase in crop losses to insect pests in a warming climate". In: *Science* 361.6405, pp. 916–919.

Di, R. and N. E. Tumer (2015). "Pokeweed antiviral protein: its cytotoxicity mechanism and applications in plant disease resistance." In: *Toxins* 7.3, pp. 755–72.

Dixon, D. P., A. Lapthorn, and R. Edwards (2002). "Plant glutathione transferases". In: *Genome Biology* 3.3, reviews3004.1.

Dodds, P. N. and J. P. Rathjen (2010). "Plant immunity: towards an integrated view of plant-pathogen interactions". In: *Nature Reviews Genetics* 11.8, pp. 539–548.

Dong, X. (1998). "SA, JA, ethylene, and disease resistance in plants." In: *Current opinion in plant biology* 1.4, pp. 316–323.

Du, L. et al. (2009). "Ca2+/calmodulin regulates salicylic-acid-mediated plant immunity". In: *Nature* 457.7233, pp. 1154–1158.

Duan, Z. et al. (2014). "The role of jasmonic acid signalling in wheat (*Triticum aestivum* L.) powdery mildew resistance reaction". In: *European Journal of Plant Pathology* 140.1, pp. 169–183.

Dubcovsky, J. and J. Dvorak (2007). "Genome Plasticity a Key Factor in the Success of Polyploid Wheat Under Domestication". In: *Science* 316.5833, pp. 1862–1866.

Dunaeva, M. et al. (1999). "The jasmonate-induced 60 kDa protein of barley exhibits N-glycosidase activity in vivo". In: *FEBS Letters* 452.3, pp. 263–266.

Eckardt, N. A. (2017). "The Plant Cell Reviews Plant Immunity: Receptor-Like Kinases, ROS-RLK Crosstalk, Quantitative Resistance, and the Growth/Defense Trade-Off." In: *The Plant cell* 29.4, pp. 601–602.

Ehrlich, P. (1891a). "Experimentelle Untersuchungen über Immunitat. I Ueber Ricin". In: *Deutsche Medizinische Wochenschrift* 97.32, pp. 1–4.

— (1891b). "Experimentelle Untersuchungen über Immunität. II Ueber Abrin". In: *Deutsche Medizinische Wochenschrift* 32.44, p. 976.

Eiklid, K., S. Olsnes, and A. Pihl (1980). "Entry of lethal doses of abrin, ricin and modeccin into the cytosol of HeLa cells". In: *Experimental Cell Research* 126.2, pp. 321–326.

Ellis, C., I. Karafyllidis, and J. G. Turner (2002). "Constitutive Activation of Jasmonate Signaling in an Arabidopsis Mutant Correlates with Enhanced Resistance to Erysiphe ci-

choracearum , Pseudomonas syringae , and Myzus persicae". In: *Molecular Plant-Microbe Interactions* 15.10, pp. 1025–1030.

Ellis, M. A., D. C. Ferree, and D. E. Spring (1981). "Photosynthesis, Transpiration, and Carbohydrate Content of Apple Leaves Infected by Podosphaera leucotricha". In: *Physiology and Biochemistry* 71.4, pp. 392–395.

Endo, Y. and K. Tsurugi (1987). "RNA N-glycosidase activity of ricin A-chain. Mechanism of action of the toxic lectin ricin on eukaryotic ribosomes". In: *Journal of Biological Chemistry* 262.17, pp. 8128–8130.

Eulalio, A., I. Behm-Ansmant, and E. Izaurralde (2007). "P bodies: at the crossroads of post-transcriptional pathways". In: *Nature Reviews Molecular Cell Biology* 8.1, pp. 9–22.

European Commission Directorate-General for Agriculture and Rural Development (2011). *Prospects of agricultural markets and income.* Tech. rep.

Evans, A. (2009). *The Feeding of the Nine Billion, Global Food Security for the 21st Century.* Tech. rep. Chatham House, pp. 1–59.

Evans, N. et al. (2008). "Range and severity of a plant disease increased by global warming". In: *Journal of The Royal Society Interface* 5.22, pp. 525–531.

Faltermaier, A. et al. (2014). "Common wheat (*Triticum aestivum* L.) and its use as a brewing cereal - a review". In: *Journal of the Institute of Brewing* 120.1, pp. 1–15.

FAO (2017). *World cereal projections 2017.* Tech. rep., pp. 4–5.

FAO, IFAD, and WFP. (2015). *The State of Food Insecurity in the World: Meeting the 2015 international hunger targets: taking stock of uneven progress.* Pp. 1–54.

Feldman, M. and A. A. Levy (2005). "Allopolyploidy–a shaping force in the evolution of wheat genomes." In: *Cytogenetic and genome research* 109.1-3, pp. 250–8.

Fernández, A. and H. A. Scheraga (2003). "Insufficiently dehydrated hydrogen bonds as determinants of protein interactions." In: *Proceedings of the National Academy of Sciences of the United States of America* 100.1, pp. 113–8.

Finn, R. D. et al. (2015). "HMMER web server: 2015 update". In: *Nucleic Acids Research* 43.W1, W30–W38.

Fisher, M. C. et al. (2012). "Emerging fungal threats to animal, plant and ecosystem health." In: *Nature* 484.7393, pp. 186–94.

Fitch, C. A. et al. (2015). “Arginine: Its pKa value revisited.” In: *Protein science : a publication of the Protein Society* 24.5, pp. 752–61.

Frantzeskakis, L. et al. (2018). “Signatures of host specialization and a recent transposable element burst in the dynamic one-speed genome of the fungal barley powdery mildew pathogen”. In: *BMC Genomics* 19.1, p. 381.

Friedt, W. et al. (2011). “Barley Breeding History, Progress, Objectives, and Technology”. In: *Barley*. Juillet. Oxford, UK: Wiley-Blackwell, pp. 160–220.

Gao, X. et al. (2013). “Bifurcation of Arabidopsis NLR Immune Signaling via Ca2+-Dependent Protein Kinases”. In: *PLoS Pathogens* 9.1. Ed. by S. He, e1003127.

Glawe, D. A. (2008). “The Powdery Mildews: A Review of the World’s Most Familiar (Yet Poorly Known) Plant Pathogens”. In: *Annual Review of Phytopathology* 46.1, pp. 27–51.

Glazebrook, J. (2005). “Contrasting Mechanisms of Defense Against Biotrophic and Necrotrophic Pathogens”. In: *Annual Review of Phytopathology* 43.1, pp. 205–227.

Goda, S. K. and N. P. Minton (1995). “A simple procedure for gel electrophoresis and northern blotting of RNA.” In: *Nucleic acids research* 23.16, pp. 3357–8.

Godfray, H. C. J. et al. (2010). “Food Security: The Challenge of Feeding 9 Billion People”. In: *Science* 327.5967, pp. 812–818.

Godfrey, D. et al. (2010). “Powdery mildew fungal effector candidates share N-terminal Y/F/WxC-motif.” In: *BMC genomics* 11.1, p. 317.

Görschen, E. et al. (1997). “Expression of the ribosome-inactivating protein JIP60 from barley in transgenic tobacco leads to an abnormal phenotype and alterations on the level of translation”. In: *Planta* 202.4, pp. 470–478.

Gout, E., R. Bligny, and R. Douce (1992). “Regulation of intracellular pH values in higher plant cells.” In: *The Journal of Biological Chemistry* 267.20, pp. 13903–13909.

Grando, S. and H. G. Macpherson (2005). “Food Barley: Importance, Uses and Local Knowledge”. In: *International Workshop on Food Barley Improvement*. International Center for Agricultural Research in the Dry Areas ICARDA. Aleppo, Syria.

Grant, B. J., A. A. Gorfe, and J. A. McCammon (2010). “Large conformational changes in proteins: signaling and other functions”. In: *Current Opinion in Structural Biology* 20.2, pp. 142–147.

Gregory, P. J. et al. (2009). "Integrating pests and pathogens into the climate change/food security debate". In: *Journal of Experimental Botany* 60.10, pp. 2827–2838.

Habben, J. E., A. W. Kirleis, and B. A. Larkins (1993). "The origin of lysine-containing proteins in opaque-2 maize endosperm". In: *Plant Molecular Biology* 23.4, pp. 825–838.

Hannukkala, A. O. et al. (2007). "Late-blight epidemics on potato in Finland, 1933-2002; increased and earlier occurrence of epidemics associated with climate change and lack of rotation". In: *Plant Pathology* 56.1, pp. 167–176.

Hause, B. et al. (1994). "Intracellular Localization of Jasmonate-Induced Proteins in Barley Leaves". In: *Botanica Acta* 107.5, pp. 333–341.

Hause, B. et al. (1999). "Cultivar-Specific Expression of the Jasmonate-Induced Protein of 23 kDa (JIP-23) Occurs in *Hordeum vulgare* L. by Jasmonates but not During Seed Germination". In: *Plant Biology* 1.1, pp. 83–89.

He, S. Y. et al. (1994). "Hypersensitive Response Elicitedby Erwinia amylovora Harpin RequiresActive Plant Metabolism". In: *Molecular Plant-Microbe Interactions* 7.2, p. 289.

Henchoz, Y. et al. (2007). "Rapid determination of pKa values of 20 amino acids by CZE with UV and capacitively coupled contactless conductivity detections". In: *Analytical and Bioanalytical Chemistry* 389.6, pp. 1869–1878.

Ho, M.-C. et al. (2009). "Transition state analogues in structures of ricin and saporin ribosome-inactivating proteins." In: *Proceedings of the National Academy of Sciences of the United States of America* 106.48, pp. 20276–81.

Hogenhout, S. A. and J. I. Bos (2011). "Effector proteins that modulate plant-insect interactions". In: *Current Opinion in Plant Biology* 14.4, pp. 422–428.

Hogenhout, S. A. et al. (2009). "Emerging concepts in effector biology of plant-associated organisms." en. In: *Molecular plant-microbe interactions : MPMI* 22.2, pp. 115–22.

Hu, Z. et al. (2000). "Conservation of polar residues as hot spots at protein interfaces". In: *Proteins: Structure, Function, and Genetics* 39.4, pp. 331–342.

Hubbard, S. J. and P. Argos (1994). "Cavities and packing at protein interfaces". In: *Protein Science* 3.12, pp. 2194–2206.

Hückelhoven, R. and R. Panstruga (2011). "Cell biology of the plant-powdery mildew interaction". In: *Current Opinion in Plant Biology* 14.6, pp. 738–746.

Hudak, K. A., J. D. Dinman, and N. E. Tumer (1999). "Pokeweed antiviral protein accesses ribosomes by binding to L3." In: *The Journal of biological chemistry* 274.6, pp. 3859–64.

Hueck, C. J. (1998). "Type III protein secretion systems in bacterial pathogens of animals and plants." In: *Microbiology and molecular biology reviews : MMBR* 62.2, pp. 379–433.

International Wheat Genome Sequencing Consortium (2018). "Shifting the limits in wheat research and breeding using a fully annotated reference genome." In: *Science (New York, N.Y.)* 361.6403, eaar7191.

Jaillais, Y. and J. Chory (2010). "Unraveling the paradoxes of plant hormone signaling integration". In: *Nature Structural & Molecular Biology* 17.6, pp. 642–645.

Jiang, S.-Y. et al. (2008). "Genome-wide survey of the RIP domain family in Oryza sativa and their expression profiles under various abiotic and biotic stresses". In: *Plant Molecular Biology* 67.6, pp. 603–614.

Jiang, S.-Y. et al. (2012). "Over-expression of OSRIP18 increases drought and salt tolerance in transgenic rice plants". In: *Transgenic Research* 21.4, pp. 785–795.

Johal, G. S., S. H. Hulbert, and S. P. Briggs (1995). "Disease lesion mimics of maize: A model for cell death in plants". In: *BioEssays* 17.8, pp. 685–692.

Jones, J. T. et al. (2013). "Top 10 plant-parasitic nematodes in molecular plant pathology". In: *Molecular Plant Pathology* 14.9, pp. 946–961.

Jones, J. D. G. and J. L. Dangl (2006). "The plant immune system". In: *Nature* 444.7117, pp. 323–329.

Jones, R. (2015). "Structural and functional characterisation of adhesin and effector proteins from pathogenic fungi". PhD thesis. Imperial College London.

Jones, S. and J. M. Thornton (1996). "Principles of protein-protein interactions." In: *Proceedings of the National Academy of Sciences of the United States of America* 93.1, pp. 13–20.

Kamoun, S. et al. (2015). "The Top 10 oomycete pathogens in molecular plant pathology". In: *Molecular Plant Pathology* 16.4.

Kanja, C. (2018). *FYP: Studying structure-function relations of the barley powdery mildew effector, BEC1054*. Tech. rep. Imperial College London, pp. 1–51.

Kanyuka, K. and J. J. Rudd (2019). "Cell surface immune receptors: the guardians of the plant's extracellular spaces". In: *Current Opinion in Plant Biology* 50, pp. 1–8.

Kelley, L. A. et al. (2015). "The Phyre2 web portal for protein modeling, prediction and analysis". In: *Nature Protocols* 10.6, pp. 845–858.

Kemen, A. C., M. T. Agler, and E. Kemen (2015). "Host-microbe and microbe-microbe interactions in the evolution of obligate plant parasitism". In: *New Phytologist* 206.4, pp. 1207–1228.

Kim, Y. and J. D. Robertus (1992). "Analysis of several key active site residues of ricin a chain by mutagenesis and x-ray crystallography". In: *Protein Engineering, Design and Selection* 5.8, pp. 775–779.

Krawetz, J. E. and R. S. Boston (2000). "Substrate specificity of a maize ribosome-inactivating protein differs across diverse taxa". In: *European Journal of Biochemistry* 267.7, pp. 1966–1974.

Krivdova, G. et al. (2014). "Antiviral and Antifungal Properties of RIPs". In: *Ribosome-inactivating Proteins*. Oxford: John Wiley & Sons, Ltd., pp. 198–211.

Krupp, G. (2005). *Stringent RNA quality control using the Agilent 2100 bioanalyzer*. Tech. rep.

Kurkdjian, A. and J. Guern (1989). "Intracellular pH: Measurement and Importance in Cell Activity". In: *Annual Review of Plant Physiology and Plant Molecular Biology* 40.1, pp. 271–303.

Lam, E., N. Kato, and M. Lawton (2001). "Programmed cell death, mitochondria and the plant hypersensitive response". In: *Nature* 411.6839, pp. 848–853.

Lancaster, L. et al. (2008). "The sarcin-ricin loop of 23S rRNA is essential for assembly of the functional core of the 50S ribosomal subunit." In: *RNA (New York, N.Y.)* 14.10, pp. 1999–2012.

Langner, T., S. Kamoun, and K. Belhaj (2018). "CRISPR Crops: Plant Genome Editing Toward Disease Resistance". In: *Annual Review of Phytopathology* 56.1, pp. 479–512.

Lapadula, W. J., M. V. Sánchez Puerta, and M. Juri Ayub (2013). "Revising the Taxonomic Distribution, Origin and Evolution of Ribosome Inactivating Protein Genes". In: *PLoS ONE* 8.9. Ed. by A. Moustafa, e72825.

Leah, R. et al. (1991). "Biochemical and molecular characterization of three barley seed proteins with antifungal properties". In: *Journal of Biological Chemistry* 266.3, pp. 1564–1573.

Lee, B.-G. et al. (2012). "Structures of the ribosome-inactivating protein from barley seeds reveal a unique activation mechanism". In: *Acta Crystallographica Section D Biological Crystallography* 68.11, pp. 1488–1500.

Leopold, J. et al. (1996). "Isolation, characterization and expression of a cDNA coding for a jasmonate-inducible protein of 37 kDa in barley leaves". In: *Plant, Cell and Environment* 19.6, pp. 675–684.

Li, L. (2018). "Investigations of Barley Powdery Mildew Effectors (CSEPs) in the Non-host Plant Wheat and Host Plant Barley". PhD thesis. Imperial College London.

Li, X. et al. (2004). "Protein-Protein Interactions: Hot Spots and Structurally Conserved Residues often Locate in Complemented Pockets that Pre-organized in the Unbound States: Implications for Docking". In: *Journal of Molecular Biology* 344.3, pp. 781–795.

Liebrand, T. W., H. A. van den Burg, and M. H. Joosten (2014). "Two for all: receptor-associated kinases SOBIR1 and BAK1". In: *Trends in Plant Science* 19.2, pp. 123–132.

Lin, J. Y. et al. (1970). "Abrin and ricin: new anti-tumour substances." In: *Nature* 227.5255, pp. 292–3.

Lin, W. et al. (2013). "Big roles of small kinases: the complex functions of receptor-like cytoplasmic kinases in plant immunity and development." In: *Journal of integrative plant biology* 55.12, pp. 1188–97.

Liu, L. et al. (2019). "Arms race: diverse effector proteins with conserved motifs". In: *Plant Signaling & Behavior* 14.2, p. 1557008.

Lo Presti, L. et al. (2015). "Fungal Effectors and Plant Susceptibility." In: *Annual review of plant biology* 66.1, pp. 513–545.

Logemann, J. et al. (1992). "Expression of a Barley Ribosome-Inactivating Protein Leads to Increased Fungal Protection in Transgenic Tobacco Plants". In: *Nature Biotechnology* 10.3, pp. 305–308.

Luna, E. et al. (2012). "Next-generation systemic acquired resistance." In: *Plant physiology* 158.2, pp. 844–53.

Luo, Y., Z. Na, and S. A. Slavoff (2018). "P-Bodies: Composition, Properties, and Functions." In: *Biochemistry* 57.17, pp. 2424–2431.

Luscombe, N. M., R. A. Laskowski, and J. M. Thornton (2001). "Amino acid-base interactions: a three-dimensional analysis of protein-DNA interactions at an atomic level". In: *Nucleic Acids Research* 29.13, pp. 2860–2874.

Lyngkjaer, M. F. et al. (2000). "The Barley mlo gene: an important powdery mildew resistance source". en. In: *Agronomie* 20.7, pp. 745–756.

Ma, Z. et al. (2017). "A paralogous decoy protects Phytophthora sojae apoplastic effector PsXEG1 from a host inhibitor." In: *Science (New York, N.Y.)* 355.6326, pp. 710–714.

Mansfield, J. et al. (2012). "Top 10 plant pathogenic bacteria in molecular plant pathology". In: *Molecular Plant Pathology* 13.6, pp. 614–629.

Mascher, M. et al. (2017). "A chromosome conformation capture ordered sequence of the barley genome". In: *Nature* 544.7651, pp. 427–433.

Massiah, A. J. and M. R. Hartley (1995). "Wheat ribosome-inactivating proteins: Seed and leaf forms with different specificities and cofactor requirements". In: *Planta* 197.4.

Maucher, H. et al. (2000). "Allene oxide synthases of barley (*Hordeum vulgare* cv. Salome): tissue specific regulation in seedling development". In: *The Plant Journal* 21.2, pp. 199–213.

Maucher, H. et al. (2004). "The allene oxide cyclase of barley (*Hordeum vulgare* L.):cloning and organ-specific expression". In: *Phytochemistry* 65.7, pp. 801–811.

McCluskey, A. J. et al. (2008). "The Catalytic Subunit of Shiga-like Toxin 1 Interacts with Ribosomal Stalk Proteins and is Inhibited by Their Conserved C-Terminal Domain". In: *Journal of Molecular Biology* 378.2, pp. 375–386.

Memelink, J. (2009). "Regulation of gene expression by jasmonate hormones". In: *Phytochemistry* 70.13-14, pp. 1560–1570.

Micali, C. O. et al. (2011). "Biogenesis of a specialized plant-fungal interface during host cell internalization of Golovinomyces orontii haustoria". In: *Cellular Microbiology* 13.2, pp. 210–226.

Miller, R. N. G., G. S. Costa Alves, and M.-A. Van Sluys (2017). "Plant immunity: unravelling the complexity of plant responses to biotic stresses". In: *Annals of Botany* 119.5, pp. 681–687.

Monzingo, A. F. and J. D. Robertus (1992). "X-ray Analysis of Substrate Analogs in the Ricin A-chain Active Site". In: *jr. Mol. Biol* 227.

Moore, D., G. D. Robson, and A. P. J. Trinci (2011a). *21st century guidebook to fungi*. Cambridge University Press, p. 627.

Moore, J. W., G. J. Loake, and S. H. Spoel (2011b). "Transcription dynamics in plant immunity." In: *The Plant cell* 23.8, pp. 2809–20.

Moreira, I. S., P. A. Fernandes, and M. J. Ramos (2007). "Hot spots-A review of the protein-protein interface determinant amino-acid residues". In: *Proteins: Structure, Function, and Bioinformatics* 68.4, pp. 803–812.

Morel, J.-B. and J. L. Dangl (1997). "The hypersensitive response and the induction of cell death in plants". In: *Cell Death and Differentiation* 4.8, pp. 671–683.

Morrison, K. L. and G. A. Weiss (2001). "Combinatorial alanine-scanning". In: *Current Opinion in Chemical Biology* 5.3, pp. 302–307.

Mur, L. A. J. et al. (2006). "The outcomes of concentration-specific interactions between salicylate and jasmonate signaling include synergy, antagonism, and oxidative stress leading to cell death." In: *Plant physiology* 140.1, pp. 249–62.

Mur, L. A. J. et al. (2008). "The hypersensitive response; The centenary is upon us but how much do we know?" In: *Journal of Experimental Botany*. Vol. 59. 3, pp. 501–520.

Murphy, J. M., H. Farhan, and P. A. Eyers (2017). "Bio-Zombie: the rise of pseudoenzymes in biology." In: *Biochemical Society transactions* 45.2, pp. 537–544.

Murray, G. M. and J. P. Brennan (2010). "Estimating disease losses to the Australian barley industry". In: *Australasian Plant Pathology* 39.1, p. 85.

Narayanan, S. et al. (2005). "Ribosome inactivating proteins and apoptosis". In: *FEBS Letters* 579.6, pp. 1324–1331.

Nellemann, C., United Nations Environment Programme., and GRID–Arendal. (2009). *The environmental food crisis : the environment's role in averting future food crises : a UNEP rapid response assessment*. UNEP, p. 101.

Nielsen, K. and R. S. Boston (2001). "Ribosome-inactivating proteins: A Plant Perspective." In: *Annual review of plant physiology and plant molecular biology* 52, pp. 785–816.

Nomura, K., M. Melotto, and S.-Y. He (2005). "Suppression of host defense in compatible plant-Pseudomonas syringae interactions". In: *Current Opinion in Plant Biology* 8.4, pp. 361–368.

Nooren, I. M. and J. M. Thornton (2003). "Diversity of protein-protein interactions". In: *The EMBO Journal* 22.14, pp. 3486–3492.

Nürnberger, T. et al. (2004). "Innate immunity in plants and animals: Striking similarities and obvious differences". In: *Immunological Reviews* 198.1, pp. 249–266.

Oberhaensli, S. et al. (2011). "Comparative sequence analysis of wheat and barley powdery mildew fungi reveals gene colinearity, dates divergence and indicates host-pathogen co-evolution". In: *Fungal Genetics and Biology* 48.3, pp. 327–334.

O'Brien, J. A. et al. (2012). "Reactive oxygen species and their role in plant defence and cell wall metabolism". In: *Planta* 236.3, pp. 765–779.

Oerke, E. (2006). "Crop losses to pests". In: *The Journal of Agricultural Science* 144.01, p. 31.

Olsnes, S. (2004). "The history of ricin, abrin and related toxins". In: *Toxicon* 44.4, pp. 361–370.

Oome, S. et al. (2014). "Nep1-like proteins from three kingdoms of life act as a microbe-associated molecular pattern in Arabidopsis." In: *Proceedings of the National Academy of Sciences of the United States of America* 111.47, pp. 16955–60.

Pace, C. N. et al. (1988). "Conformational stability and activity of ribonuclease T1 with zero, one, and two intact disulfide bonds". In: *Journal of Biological Chemistry* 263.24, pp. 11820–11825.

Panstruga, R. and P. N. Dodds (2009). "Terrific protein traffic: the mystery of effector protein delivery by filamentous plant pathogens." In: *Science (New York, N.Y.)* 324.5928, pp. 748–50.

Pap, P., B. Ranković, and S. Maširević (2012). "Significance and need of powdery mildew control (Microsphaera alphitoides Griff. et Maubl.) in the process of regeneration of the

pedunculate oak (Quercus robur L.) stands in the Ravni Srem area". In: *Periodicum Biologorum* 114.1, pp. 91–102.

Park, S.-W. et al. (2006). "Isolation and purification of ribosome-inactivating proteins." In: *Methods in molecular biology (Clifton, N.J.)* 318, pp. 335–47.

Parlange, F. et al. (2011). "A major invasion of transposable elements accounts for the large size of the *Blumeria graminis* f.sp. tritici genome". In: *Functional & Integrative Genomics* 11.4, pp. 671–677.

Pastan, I., V. Chaudhary, and D. J. FitzGerald (1992). "Recombinant Toxins as Novel Therapeutic Agents". In: *Annual Review of Biochemistry* 61.1, pp. 331–354.

Peattie, D. A. (1979). "Direct chemical method for sequencing RNA." In: *Proceedings of the National Academy of Sciences of the United States of America* 76.4, pp. 1760–4.

Pedersen, C. et al. (2012). "Structure and evolution of barley powdery mildew effector candidates." In: *BMC genomics* 13.1, p. 694.

Peng, Y., R. van Wersch, and Y. Zhang (2018). "Convergent and Divergent Signaling in PAMP-Triggered Immunity and Effector-Triggered Immunity". In: *Molecular Plant-Microbe Interactions* 31.4, pp. 403–409.

Pennington, H. G. (2014). "Investigating the interactors of the *Blumeria* Effector BEC1054". PhD thesis. Imperial College London.

Pennington, H. G., L. Li, and P. D. Spanu (2016a). "Identification and selection of normalization controls for quantitative transcript analysis in *Blumeria graminis*". In: *Molecular Plant Pathology* 17.4, pp. 625–633.

Pennington, H. G. et al. (2016b). "Interactions between the Powdery Mildew Effector BEC1054 and Barley Proteins Identify Candidate Host Targets". In: *Journal of Proteome Research* 15.3, pp. 826–839.

Pennington, H. G. et al. (2019). "The fungal ribonuclease-like effector protein CSEP0064/BEC1054 represses plant immunity and interferes with degradation of host ribosomal RNA". In: *PLOS Pathogens* 15.3. Ed. by P. N. Dodds, e1007620.

Peumans, W. J., C. Shang, and E. J. M. Van Damme (2014). "Updated Model of the Molecular Evolution of RIP Genes". In: *Ribosome-inactivating Proteins*. Oxford: John Wiley & Sons, Ltd., pp. 134–150.

Pieterse, C. M. et al. (2012). "Hormonal Modulation of Plant Immunity". In: *Annual Review of Cell and Developmental Biology* 28.1, pp. 489–521.

Pils, B. and J. Schultz (2004). "Inactive Enzyme-homologues Find New Function in Regulatory Processes". In: *Journal of Molecular Biology* 340.3, pp. 399–404.

Pinstrup-Andersen, P. (2009). "Food security: definition and measurement". In: *Food Security* 1.1, pp. 5–7.

Pliego, C. et al. (2013). "Host-induced gene silencing in barley powdery mildew reveals a class of ribonuclease-like effectors." In: *Molecular plant-microbe interactions : MPMI* 26.6, pp. 633–42.

Pretty, J. (2008). "Agricultural sustainability: concepts, principles and evidence." In: *Philosophical transactions of the Royal Society of London. Series B, Biological sciences* 363.1491, pp. 447–65.

Przydacz, M. (2015). *MRes Thesis: The mode of action of the cereal mildew RNase-like effectors*. Tech. rep. Imperial College London, pp. 1–35.

R Core Team (2013). *R: A language and environment for statistical computing*. Vienna.

Rao, M. V. et al. (2000). "Jasmonic Acid Signaling Modulates Ozone-Induced Hypersensitive Cell Death". In: *The Plant Cell* 12.9, pp. 1633–1646.

Reape, T. J., E. M. Molony, and P. F. McCabe (2008). "Programmed cell death in plants: distinguishing between different modes". In: *Journal of Experimental Botany* 59.3, pp. 435–444.

Reinbothe, C., B. Parthier, and S. Reinbothe (1997). "Temporal pattern of jasmonate-induced alterations in gene expression of barley leaves". In: *Planta* 201.3, pp. 281–287.

Reinbothe, S., B. Mollenhauer, and C. Reinbothe (1994a). "JIPs and RIPs: the regulation of plant gene expression by jasmonates in response to environmental cues and pathogens." In: *The Plant cell* 6.9, pp. 1197–209.

Reinbothe, S., C. Reinbothe, and B. Parthier (1993). "Methyl jasmonate-regulated translation of nuclear-encoded chloroplast proteins in barley (*Hordeum vulgare* L. cv. salome)". In: *Journal of Biological Chemistry* 268.14, pp. 10606–10611.

Reinbothe, S. et al. (1994b). "JIP60, a methyl jasmonate-induced ribosome-inactivating protein involved in plant stress reactions." In: *Proceedings of the National Academy of Sciences of the United States of America* 91.15, pp. 7012–6.

Repka, V., I. Fischerová, and K. Silhárová (2001). "Methyl jasmonate induces a hypersensitive-like response of grapevine in the absence of avirulent pathogens". In: *Vitis* 40.1, pp. 5–10.

Reymond, P. and E. E. Farmer (1998). "Jasmonate and salicylate as global signals for defense gene expression". In: *Current Opinion in Plant Biology* 1.5, pp. 404–411.

Richardson, J., J. Outlaw, and J. M. Raulston (2006). *Impact of the Wheat Industry on the U.S. Economy*. Tech. rep.

Riehl, S., M. Zeidi, and N. J. Conard (2013). "Emergence of Agriculture in the Foothills of the Zagros Mountains of Iran". In: *Science* 341.6141, pp. 65–67.

Roberts, G. C. et al. (1969). "The mechanism of action of ribonuclease." In: *Proceedings of the National Academy of Sciences of the United States of America* 62.4, pp. 1151–8.

Rosta, E. et al. (2011). "Catalytic mechanism of RNA backbone cleavage by ribonuclease H from quantum mechanics/molecular mechanics simulations". In: *Journal of the American Chemical Society* 133.23, pp. 8934–8941.

Rustgi, S. et al. (2014). "JIP60-mediated, jasmonate- and senescence-induced molecular switch in translation toward stress and defense protein synthesis." In: *Proceedings of the National Academy of Sciences of the United States of America* 111.39, pp. 14181–6.

Sawasaki, T., M. Nishihara, and Y. Endo (2008). "RIP and RALyase cleave the sarcin/ricin domain, a critical domain for ribosome function, during senescence of wheat coleoptiles". In: *Biochemical and Biophysical Research Communications* 370.4, pp. 561–565.

Scholthof, K.-B. G. et al. (2011). "Top 10 plant viruses in molecular plant pathology". In: *Molecular Plant Pathology* 12.9, pp. 938–954.

Schrodinger LLC (2010). *The PyMOL Molecular Graphics System*.

Schrot, J., A. Weng, and M. F. Melzig (2015). "Ribosome-inactivating and related proteins." In: *Toxins* 7.5, pp. 1556–615.

Selin, C. et al. (2016). "Elucidating the role of effectors in plant-fungal interactions: Progress and challenges". In: *Frontiers in Microbiology* 7.4, p. 600.

SenGupta, D. J. et al. (1996). "A three-hybrid system to detect RNA-protein interactions in vivo." In: *Proceedings of the National Academy of Sciences of the United States of America* 93.16, pp. 8496–501.

Shang, C., W. J. Peumans, and E. J. M. Van Damme (2014). "Occurrence and Taxonomical Distribution of Ribosome-inactivating Proteins Belonging to the Ricin/Shiga Toxin Superfamily". In: *Ribosome-inactivating Proteins*. Oxford: John Wiley & Sons, Ltd., pp. 11–27.

Shatters, R. G. et al. (2006). "Phylogenetic and Structural Relationships of the PR5 Gene Family Reveal an Ancient Multigene Family Conserved in Plants and Select Animal Taxa". In: *Journal of Molecular Evolution* 63.1, pp. 12–29.

Sheard, L. B. et al. (2010). "Jasmonate perception by inositol-phosphate-potentiated COI1-JAZ co-receptor". In: *Nature* 468.7322, pp. 400–405.

Sheinerman, F. B., R. Norel, and B. Honig (2000). "Electrostatic aspects of protein-protein interactions". In: *Current Opinion in Structural Biology* 10.2, pp. 153–159.

Shewry, P. R. (2009). "Wheat". In: *Journal of Experimental Botany* 60.6, pp. 1537–1553.

Shi, W.-W. et al. (2016). "Structures and Ribosomal Interaction of Ribosome-Inactivating Proteins". In: *Molecules* 21.11, p. 1588.

Shiu, S. H. and A. B. Bleecker (2001). "Plant receptor-like kinase gene family: diversity, function, and signaling." In: *Science's STKE : signal transduction knowledge environment* 2001.113, re22.

Spanu, P. D. (2017). "Cereal immunity against powdery mildews targets RNase-Like Proteins associated with Haustoria (RALPH) effectors evolved from a common ancestral gene". In: *New Phytologist* 213.3, pp. 969–971.

Spanu, P. D. and R. Panstruga (2017). "Editorial: Biotrophic Plant-Microbe Interactions." In: *Frontiers in plant science* 8, p. 192.

Spanu, P. D. et al. (2010). "Genome Expansion and Gene Loss in Powdery Mildew Fungi Reveal Tradeoffs in Extreme Parasitism". In: *Science* 330.6010, pp. 1543–1546.

Spoel, S. H. and X. Dong (2012). "How do plants achieve immunity? Defence without specialized immune cells". In: *Nature Reviews Immunology* 12.2, pp. 89–100.

Spoel, S. H., J. S. Johnson, and X. Dong (2007). "Regulation of tradeoffs between plant defenses against pathogens with different lifestyles." In: *Proceedings of the National Academy of Sciences of the United States of America* 104.47, pp. 18842–7.

Spoel, S. H. et al. (2003). "NPR1 modulates cross-talk between salicylate- and jasmonate-dependent defense pathways through a novel function in the cytosol." In: *The Plant cell* 15.3, pp. 760–70.

Springer, A. et al. (2015). "Differences in gene expression between natural and artificially induced leaf senescence in barley". In: *Journal of Plant Physiology* 176, pp. 180–191.

Srivatsan, S. G., N. J. Greco, and Y. Tor (2008). "A Highly Emissive Fluorescent Nucleoside that Signals the Activity of Toxic Ribosome-Inactivating Proteins". In: *Angewandte Chemie International Edition* 47.35, pp. 6661–6665.

Stael, S. et al. (2015). "Plant innate immunity - sunny side up?" In: *Trends in Plant Science* 20.1, pp. 3–11.

Staskawicz, B. J. et al. (2001). "Common and Contrasting Themes of Plant and Animal Diseases". In: *Science* 292.5525, pp. 2285–2289.

Stirpe, F. (2013). "Ribosome-inactivating proteins: From toxins to useful proteins". In: *Toxicon* 67, pp. 12–16.

Stirpe, F. et al. (1992). "Ribosome-Inactivating Proteins from Plants: Present Status and Future Prospects". In: *Bio/Technology* 10.4, pp. 405–412.

Sullivan, P., E. Arendt, and E. Gallagher (2013). "The increasing use of barley and barley by-products in the production of healthier baked goods". In: *Trends in Food Science & Technology* 29.2, pp. 124–134.

Surico, G. (2013). "The concepts of plant pathogenicity, virulence/avirulence and effector proteins by a teacher of plant pathology". In: *Phytopathologia Mediterranea* 52.3, pp. 399–417.

Swords, W. E. (2003). "Chemical Transformation of E. coli". In: *E. coli Plasmid Vectors*. New Jersey: Humana Press, pp. 49–54.

Szabo, L. J. and W. R. Bushnell (2001). "Hidden robbers: The role of fungal haustoria in parasitism of plants". In: *Proceedings of the National Academy of Sciences* 98.14, pp. 7654–7655.

Tang, D., G. Wang, and J.-M. Zhou (2017). "Receptor Kinases in Plant-Pathogen Interactions: More Than Pattern Recognition". In: *The Plant Cell* 29.4, pp. 618–637.

Tao, Y. et al. (2003). "Quantitative nature of Arabidopsis responses during compatible and incompatible interactions with the bacterial pathogen Pseudomonas syringae." In: *The Plant cell* 15.2, pp. 317–30.

The Scotch Whisky Association (2015). "The Economic Impact of Scotch Whisky Production in the UK". In:

Thordal-Christensen, H. et al. (2018). "Why did filamentous plant pathogens evolve the potential to secrete hundreds of effectors to enable disease?" In: *Molecular Plant Pathology* 19.4, pp. 781–785.

Tilman, D. et al. (2001). "Forecasting agriculturally driven global environmental change." In: *Science (New York, N.Y.)* 292.5515, pp. 281–4.

Todd, A. E., C. A. Orengo, and J. M. Thornton (2002). "Sequence and Structural Differences between Enzyme and Nonenzyme Homologs". In: *Structure* 10.10, pp. 1435–1451.

Troch, V. et al. (2014). "Formae speciales of cereal powdery mildew: Close or distant relatives?" In: *Molecular Plant Pathology* 15.3, pp. 304–314.

Tsai, C.-J. et al. (1997). "Studies of protein-protein interfaces: A statistical analysis of the hydrophobic effect". In: *Protein Science* 6.1, pp. 53–64.

Tsuda, K. and F. Katagiri (2010). "Comparing signaling mechanisms engaged in pattern-triggered and effector-triggered immunity". In: *Current Opinion in Plant Biology* 13.4, pp. 459–465.

Tsuda, K. and I. E. Somssich (2015). "Transcriptional networks in plant immunity". In: *New Phytologist* 206.3, pp. 932–947.

Tsuda, K. et al. (2013). "Dual regulation of gene expression mediated by extended MAPK activation and salicylic acid contributes to robust innate immunity in Arabidopsis thaliana." In: *PLoS genetics* 9.12, e1004015.

Ullrich, S. E. (2010). *Barley*. Ed. by S. E. Ullrich. Oxford, UK: Wiley-Blackwell, p. 637.

Van der Does, D. et al. (2013). "Salicylic acid suppresses jasmonic acid signaling downstream of SCFCOI1-JAZ by targeting GCC promoter motifs via transcription factor ORA59." In: *The Plant cell* 25.2, pp. 744–61.

Varden, F. A. et al. (2017). "Taking the stage: effectors in the spotlight". In: *Current Opinion in Plant Biology* 38, pp. 25–33.

Verhage, A., S. C. M. van Wees, and C. M. J. Pieterse (2010). "Plant Immunity: It's the Hormones Talking, But What Do They Say?" In: *Plant Physiology* 154.2, pp. 536–540.

Vigers, A. J. (1991). "A New Family of Plant Antifungal Proteins". In: *Molecular Plant-Microbe Interactions* 4.4, p. 315.

Virgilio, M. de et al. (2010). "Ribosome-inactivating proteins: from plant defense to tumor attack." In: *Toxins* 2.11, pp. 2699–737.

Voinnet, O. et al. (2003). "An enhanced transient expression system in plants based on suppression of gene silencing by the p19 protein of tomato bushy stunt virus." In: *The Plant journal : for cell and molecular biology* 33.5, pp. 949–56.

Voros, K. et al. (1998). "Characterization of a methyljasmonate-inducible lipoxygenase from barley (*Hordeum vulgare* cv. Salome) leaves". In: *European Journal of Biochemistry* 251.1-2, pp. 36–44.

Walsh, T. A., A. E. Morgan, and T. D. Hey (1991). "Characterization and molecular cloning of a proenzyme form of a ribosome-inactivating protein from maize. Novel mechanism of proenzyme activation by proteolytic removal of a 2.8-kilodalton internal peptide segment." In: *The Journal of biological chemistry* 266.34, pp. 23422–7.

Wasternack, C. (2007). "Jasmonates: An update on biosynthesis, signal transduction and action in plant stress response, growth and development". In: *Annals of Botany* 100.4, pp. 681–697.

Waterschoot, J. et al. (2015). "Production, structure, physicochemical and functional properties of maize, cassava, wheat, potato and rice starches". In: *Starch/Staerke* 67.1-2, pp. 14–29.

Wawra, S. et al. (2017). "The RxLR Motif of the Host Targeting Effector AVR3a of Phytophthora infestans Is Cleaved before Secretion". In: *The Plant Cell* 29.6, pp. 1184–1195.

Wheeler, T. and J. von Braun (2013). "Climate change impacts on global food security". In: *Science* 341.6145, pp. 508–513.

Whigham, E. et al. (2015). "Broadly Conserved Fungal Effector BEC1019 Suppresses Host Cell Death and Enhances Pathogen Virulence in Powdery Mildew of Barley (Hordeum vulgare L.)" In: *Molecular Plant-Microbe Interactions* 28.9, pp. 968–983.

Wicker, T. et al. (2013). "The wheat powdery mildew genome shows the unique evolution of an obligate biotroph." In: *Nature genetics* 45.9, pp. 1092–1096.

Wiermer, M., B. J. Feys, and J. E. Parker (2005). "Plant immunity: the EDS1 regulatory node". In: *Current Opinion in Plant Biology* 8.4, pp. 383–389.

Williamson, M. P. (2013). "Using chemical shift perturbation to characterise ligand binding". In: *Progress in Nuclear Magnetic Resonance Spectroscopy* 73, pp. 1–16.

Wise, A. A., Z. Liu, and A. N. Binns (2006). "Three Methods for the Introduction of Foreign DNA into Agrobacterium". In: *Agrobacterium Protocols*. New Jersey: Humana Press, pp. 43–54.

Wong, K.-B. et al. (1994). "Structure/function relationship study of Gln156, Glu160 and Glu189 in the active site of trichosanthin". In: *European Journal of Biochemistry* 221.2, pp. 787–791.

Wong, Y.-T. et al. (2012). "Maize ribosome-inactivating protein uses Lys158-lys161 to interact with ribosomal protein P2 and the strength of interaction is correlated to the biological activities." In: *PloS one* 7.12, e49608.

Wu, J. and I. T. Baldwin (2010). "New Insights into Plant Responses to the Attack from Insect Herbivores". In: *Annual Review of Genetics* 44.1, pp. 1–24.

Yang, G. (2018). *MSc thesis:* Blumeria *effector BEC1054 increase susceptibility of Nicotiana benthamiana to Peronospora tabacina*. Tech. rep. Imperial College London.

Yang, Y. et al. (2010). "Solution Structure of an Active Mutant of Maize Ribosome-Inactivating Protein (MOD) and Its Interaction with the Ribosomal Stalk Protein P2". In: *Journal of Molecular Biology* 395.5, pp. 897–907.

Yaron, A., F. Naider, and S. Scharpe (1993). "Proline-Dependent Structural and Biological Properties of Peptides and Proteins". In: *Critical Reviews in Biochemistry and Molecular Biology* 28.1, pp. 31–81.

Yoshida, K. et al. (2009). "Association genetics reveals three novel avirulence genes from the rice blast fungal pathogen Magnaporthe oryzae." In: *The Plant cell* 21.5, pp. 1573–91.

Young, L., R. Jernigan, and D. Covell (2008). "A role for surface hydrophobicity in protein-protein recognition". In: *Protein Science* 3.5, pp. 717–729.

Young, T. E. and D. R. Gallie (2000). "Programmed Cell Death in Higher Plants". In: *Programmed cell death in higher plants*. Ed. by E. Lam, H. Fukuda, and J. Greenberg. Dordrecht: Springer Netherlands, pp. 39–57.

Yu, X. et al. (2017). "From Chaos to Harmony: Responses and Signaling upon Microbial Pattern Recognition". In: *Annual Review of Phytopathology* 55.1, pp. 109–137.

Zaeytijd, J. D. and E. J. M. V. Damme (2017). "Extensive Evolution of Cereal Ribosome-Inactivating Proteins Translates into Unique Structural Features, Activation Mechanisms, and Physiological Roles". In: *Toxins* 9.4, p. 123.

Zamioudis, C. and C. M. J. Pieterse (2012). "Modulation of Host Immunity by Beneficial Microbes". In: *Molecular Plant-Microbe Interactions* 25.2, pp. 139–150.

Zhou, M. X. (2009). "Barley Production and Consumption". In: *Barley*. Springer, Berlin, Heidelberg, pp. 1–17.

Zipfel, C. and G. Felix (2005). "Plants and animals: A different taste for microbes?" In: *Current Opinion in Plant Biology* 8.4, pp. 353–360.